SPECTROSCOPIC STUDY OF SUNSPOT FIELDS

by

K.D. GANESH

A thesis submitted to the
Karnatak University
for the degree of
Doctor of Philosophy

Kodaikanal Observatory
Kodaikanal
November, 1966.

CERTIFICATE AND THE BY SUPERVISOR

I certify that the thesis entitled "A SPECTROSCOPIC STUDY OF WOLF-RAYET STARS" by K.S. Ganesh is a record of the research carried out by him at the Kodaikanal Observatory. The candidate has worked on this thesis under my supervision since October 1961. I declare that the thesis has not previously formed the basis for the award of any Degree, Diploma, Associateship, Fellowship or similar title. The thesis contains a detailed study of Mount Wilson spectrograms as well as spectra obtained at Kodaikanal by the candidate. These observations have been employed by him to study the masses and other features of Wolf-Rayet binary systems as well as the temperatures and spectral characteristics of the Wolf-Rayet stars.

M K Vainu Bappu

(M.K. Vainu Bappu)
Director
Kodaikanal Observatory

ACKNOWLEDGEMENTS

This work was carried out during my stay at Kodaikanal as a Senior Research Scholar, supported by the fellowship provided by the Ministry of Education, Government of India. I thank the Ministry of Education for the financial support.

I feel greatly indebted to Dr. N.K. Vainu Appu for the ever helpful inspiration and guidance he provided me during the preparation of this thesis. He has been extremely kind to me and I acknowledge with respect his help to put this study in a presentable form.

I am very grateful to my friend and well wisher Dr. V. Natarajan whose contribution to the out come of this thesis is Himalayan in both size and magnitude.

The preparation of the art and manuscript of this thesis is greatly aided by the efforts of Messrs. A.M. Satchu, Ramaswamy V, P.Shamul Hameed, A.M. Ghouse, S.G. Veeraraghavan, Vellaichamy and others and I thank them for the help.

I will be failing in my duty if I do not thank Mrs. Vasuma Rajam for the constant encouragement and interest she showed in my welfare and I take this opportunity to thank her for that.

My special thanks go to Messrs. J.C. Bhattacharyya, U.V. Gopala Rao, P. Viswanadham, A.T. Das, S. Gopal, K. Rajagopalan, L.M. Puneetha and Dr. Bhatnagar for the keen interest they displayed in my progress.

It will not be out of the way if I ~~owe to~~ thank Mrs. Gopala Rao and Mrs. P. Viswanadham who made my stay at Kodaikanal all the more congenial.

Finally, I would like to record my sincere thanks to the staff of this Observatory, who provided me all the help during my stay at Kodaikanal.

It is a pleasure to thank the Director General of Observatories for having kindly granted permission to work at the Kodaikanal Observatory.

TABLE OF CONTENTS

Table of CONTENTS

TABLE OF CONTENTS

SUMMARY

In this thesis I have presented a detailed study of Wolf-Rayet stars, both single and the Wolf-Rayet binaries. The observational material is derived partly from the Mount Wilson plates which were kindly lent to me by Dr. T.K. Vainu Ba[illegible]u and partly from Kodaikanal plates taken by me with the 20-inch Kodaikanal reflector.

In Chapter I, I have discussed briefly, present information available in the literature regarding the Wolf-Rayet stars. I have discussed the features of the different hypotheses, put forward by various investigators in this field of research. The location of these stars in the evolutionary picture is also discussed.

Chapter II deals mainly with the techniques used for obtaining the spectra and their subsequent reduction and analysis. I have discussed the processing of the different spectra obtained with the different instruments and have elaborated on the measurement of radial velocities and the technique of photographic spectrophotometry.

In Chapter III, I have discussed the problem of line identifications in the WR stars. The discussion

centres on the need for high dispersion in some of these studies. The displaced violet absorptions are measured for HD 192163 and arguments are given to indicate the prevalence of a positive excitation gradient. I have given a list of emission lines in the near infra-red region on the basis of the spectra obtained at 111A/mm and 250A/mm dispersion of five stars of the WN sequence and two of the WC sequence. This identification list is a very exhaustive one and is based on recent laboratory investigations of the different ionization stages of carbon and nitrogen. I have also given a list of equivalent widths of prominent lines in some of the northern Wolf-Rayet stars for which low dispersion spectra have been available.

In Chapter IV, I have made an attempt to derive the temperatures of both the carbon and nitrogen sequences. The hydrogenic transitions of CIV are utilized to derive the temperatures of the WC sequence. This method, first utilized by Empey, has the advantage that one can safely utilize the calculated Einstein A_{mn}, coefficent for hydrogen. On the basis of the line intensity ratios of these hydrogenic transitions, temperatures of 56911° for HD 165763,

31563° for HD 192641, 37318° for HD 192103 and 23967° for HD 184738 have been derived.

The temperatures of the nitrogen sequence are derived mainly from the helium (4-n) series of emission lines. I have used the line intensity ratios of 4686/5411, 4542/5411, 4340/5411, 4200/5411 etc. to derive the temperature of a typical WN star, HD 192163. The contribution to the Pickering series by the Balmer series is shown to exist. I have indicated the difficulties one faces at-present if one were to use the 5-n series of helium to derive the temperatures of the Wolf-Rayet atmosphere.

In Chapter V, I have discussed the radial velocities of five binaries that have Wolf-Rayet components. The observations reported herein are the first detailed studies made of the Wolf-Rayet system γ_2-Velorum. A period of 78.5 days has been derived for this star. The velocity curves of both components permit the derivation of $a_{\gamma 7}\sin^3 i$ and $a_{WC7}\sin^3 i$ for this system. Detailed velocity curves are presented for the systems HD 193576, HD 193928, HD 186943 and HD 211853. I have given an improved mass determination for HD 193576. Orbital elements

with least squares corrections have been obtained for all systems except HD 211853.

I have shown the variations with phase for line contours of the several emission and absorption features of HD 193576, HD 193928, HD 186943 and HD 211853. With the aid of high dispersion spectra obtained at primary and secondary minima of HD 193576, I have shown the effect on the higher members of the Balmer series of the WR electron scattering envelope. I have discussed finally the contributions that studies of the binary systems can make towards the elucidation of the Wolf-Rayet phenomena.

In Chapter VI, I have made an estimate of the number of atoms above $1cm^2$ of the photosphere of the Of star Zeta Puppis. I have also made a similar calculation for the case of ionized helium using the 4-n and 5-n series. The electron density calculated with the aid of the Inglis-Teller formula agrees with the determinations of Mic for other Of stars.

CHAPTER I

THE WOLF-RAYET PHENOMENON

1.1. Introduction.

The Wolf-Rayet stars are among the most peculiar objects available in the sky. They are characterised by broad emission lines of different stages of ionisation of helium, carbon, nitrogen and oxygen. If the large emission band-widths are interpreted as due to velocity effects in the Wolf-Rayet atmosphere, then the velocities represented by the line widths range from 500 to 2000 Km/sec.

The Wolf-Rayet stars are essentially a rare stellar phenomenon. A recent survey, carried out by Roberts (1962) of the Wolf-Rayet stars in our galaxy, lists 123 Wolf-Rayet stars within 2 kiloparsecs of the Sun. These stars are confined to the galactic plane and are distributed in the Cygnus - Carina arm, the Sagittarius arm, the Vela spur and to some extent in the Perseus region. It is surprising that no Wolf-Rayet star appears in the direction of the Orion spur. In fact, the entire quadrant about the anticenter of the galaxy is devoid of Wolf-Rayet stars. About 50 of these objects have been detected in the Magellanic clouds. This result originates from the

objective prism survey carried out mainly at Mount Stromlo Observatory by Westerlund. This survey, particularly in the Large Magellanic Cloud, is complete to magnitude 17, which corresponds to an absolute magnitude of -1.7 if a distance modulus of 18.7 magnitudes is assumed for the Large Cloud. The most luminous of the Wolf-Rayet stars in the Large Cloud are seen in the 30 Doradus complex. One can conclude with a certain degree of certainty that the Wolf-Rayet stars are essentially Population I objects.

1.2. Spectral Characterization.

Much is known today about the spectral characterization of the Wolf-Rayet stars, as a result of the pioneering investigations of Beals and Miss Payne. This information has been supplemented considerably by the laboratory investigations of Edlen. It is apparent that from such a survey, the Wolf-Rayet stars can be roughly classified into two categories, one that is carbon rich and the other which is nitrogen rich. Such a classification originates from the appearance of the spectra and we are still not sure whether it is caused by anomalous abundances or by selective excitation.

In recent years, the identifications of lines in the spectra of the Wolf-Rayet carbon sequence

(WC sequence) have been greatly aided by the investigations of Beetaston (1955, 1956) and Allen (1956). Smith (1955) has carried through a detailed survey with a low dispersion spectrograph of all Wolf-Rayet stars in the southern hemisphere that are brighter than magnitude 11.0. The investigations of Beals (1930, 1936), Rappa (1951, 1957) and Smith provide a reasonable information on the spectroscopic characteristics of most of these objects in the northern and southern hemispheres.

A good deal of similarity exists between the spectra of Wolf-Rayet stars and that of the nuclei of planetary nebulae. The planetary nuclei also have emission bands of appreciable widths that originate from different stages of ionization of carbon, nitrogen, oxygen and helium. However, when examined in greater detail, certain differences between the two categories of spectra can be noticed. The planetary nuclei have simultaneously the intense emission lines of both carbon and nitrogen. In the Wolf-Rayet stars, such a simultaneous appearence of emission of both carbon and nitrogen with the same degree of completeness, is not seen. The present state of line identifications seems to suggest that the strong lines of carbon are absent in WN stars, except for a few lines which may

be selectively excited, by fluorescence processes in the stellar atmospheres. Similarly the WC sequence is devoid of the strong lines that originate from any of the stages of ionization of the nitrogen atom.

Two other characteristics of Wolf-Rayet stars, which are rather important in any speculation on their origin, are the fact that the spectra are essentially invariant over a period of half a century or more, and also that no forbidden lines are seen in any of the spectra.

1.3. Temperatures.

Numerous investigators have attempted over the years, to derive the temperatures of the Wolf-Rayet stars. If we confine our attention to the effective temperatures derived from continuum intensities, we find, that the first systematic attempt was made by Petrie (1947) who obtained a value of the order of 18000°. Several uncertainties existed in these measurements that originated not only from the techniques of photographic photometry but also from the corrections necessitated by interstellar reddening. Miss Underhill (1959) has shown that the continuum of Wolf-Rayet spectra in the neighbourhood of 3500A, simulated the intensity gradient as seen

in the late O or early B type stars. She argued that it is most likely that the effective temperatures of the Wolf-Rayet stars fall in the neighbourhood of 25000° to 35000°. Kuhi (1966) has recently carried through photo-electric scans of the energy distribution in several Wolf-Rayet stars in the northern hemisphere. Avoiding the locations of strong emission lines, Kuhi detected the rather peculiar behaviour that the colour temperature decreases with increasing wavelength. The values of the WN and WC stars resemble those of the O and early B stars in the blue and ultra-violet regions but become considerably lower as one proceeds to the red and near infrared regions.

The emission spectra have been utilized for estimating the ionization and excitation temperatures. Making use of the Zanstra-Menzel mechanism of photo-ionization and subsequent recombination, Beals (1934) obtained a range in ionization temperatures for the Wolf-Rayet stars from 60000 to 110000°. An extension of these studies by Vorontsov-Velyaminov (1946) modified these values down to the range 25000° to 84000°. These temperatures depend on the ion used for the determination and this led Beals to postulate the hypothesis that the Wolf-Rayet atmosphere is stratified, with the higher

ionization stages originating closer to the surface of the star. Aller (1943) derived excitation temperatures by comparing intensities of pairs of lines of different ionization levels on the assumption of thermodynamic equilibrium. These excitation temperatures ranged from 20000° to 120000°. Weenen (1950) in a rediscussion of Aller's data found that the excitation temperatures have little or no significance. Beppu (1958) employed the hydrogenic transitions of CIV to derive excitation temperatures of WC_7 and WC_8 stars. The values for these two types were 49000° and 27000° respectively. The argument employed by Beppu has been that the CIV hydrogenic transitions originate from the higher levels of the atom and as such, abnormal populations of the various levels caused by deviations from thermodynamic equilibrium would be non-existent.

Excitation temperatures derived from transitions that originate from such levels would, therefore, be a very representative excitation parameter. Several recent investigators have tended to show that the excitation gradient in the Wolf-Rayet atmosphere varies in a fashion similar to that in the solar corona, i.e., the higher excitation lines originate at greater distances from the stellar surface with the lower excitation lines prevalent

close to the surface. These aspects are mostly speculated on theoretically and are derived indirectly from the spectrophotometry of the binary systems. It is not known with any degree of certainty whether a stratification does exist in the Wolf-Rayet emission envelope.

1.4. Wolf-Rayet Binaries.

Much of our present information regarding Wolf-Rayet characteristics originate from the intensive studies carried out in the last two decades on one or two Wolf-Rayet binary systems. The first of these, HD 193576, was discovered by Wilson (1943) and it is perhaps this particular system that has provided a maximum of information about the Wolf-Rayet phenomenon. Several stars since then, have been found to be binaries. Spectroscopic orbits exist for about seven of them. There are several stars in which the spectrum of the companion is distinctly seen, even though the radial velocities, signifying orbital motions, are absent, possibly due to an unfavourable inclination of the orbital plane. And there are several systems yet to be studied in great detail.

The masses of the Wolf-Rayet stars seem to be of the order of 3 to 10 solar masses. These are derived from one or two binary orbits. Most of the companions

of the Wolf-Rayet stars in binary systems are early O or B type stars. This fact is particularly significant in ascribing population characteristics to the Wolf-Rayet stars. The single stars are usually seen in stellar associations and stellar complexes that are of relatively recent origin. It is also, therefore, of significance to note that the companions of the binary systems are also young, signifying that Wolf-Rayet stars are essentially young objects.

Some of these binary systems are also eclipsing systems by virtue of a favourable inclination of their orbital plane. HD 193576 (V_{444} Cygni) has provided considerable information on the nature of the envelopes of the Wolf-Rayet stars. Kopal and Mrs. Shapley (1946) have shown that the unequal widths of minima can be explained by assuming an electron-scattering envelope around the Wolf-Rayet star. In a picture of this system due to Kron and Gordon (1950), we notice that the light curve can be suitably obtained by assuming, that in addition to a luminous core, there are distinct regions of the envelope of different opacity and luminosity which are responsible for the different values of light dimming seen at different phases of the binary system. Another well-studied eclipsing binary is HD 214419 (CQ Cephei) which has a period of 1.64 days.

However, this small period necessarily implies that the two stars are close together and hence tidal deformations add complexities to an already difficult problem. One of the very significant features of the system of CQ Cephei, first pointed out for the emission line HeII 4686 by Miltner (1950), and later extended to other emission lines by Beppu and Sinvhal (1955, 1959), is that when the continuum experiences an eclipse consequent to the Wolf-Rayet star being occulted by its companion, the emission lines tend to increase in intensity. This is so at both primary and secondary minima, and a minimum of intensity in the emission lines is observed at elongations. Any conjecture regarding the Wolf-Rayet phenomenon has to explain this striking behaviour of CQ Cephei.

1.5. Kinematical features.

The earliest kinematical picture of the Wolf-Rayet stars was given by Beals (1929, 1930) and Mensel (1929) in which the broad emission lines are supposed to originate from a single expanding shell. The first to question the validity of the single expanding shell hypothesis was Wilson (1942) who postulated the need for observing "the transit time effect" in a binary system like V_{444} Cygni on the basis of the expanding shell

concept, and failed to find it in an observational study. While the expanding shell theory has stayed on, it is being increasingly recognized that this simple picture is by no means coincident with actual reality in the Wolf-Rayet atmosphere. There have been several conjectures on the various mechanisms that may be responsible for the broad emissions. Munch (1950) showed that electron scattering could increase the widths of these lines considerably. Several authors have modified the expanding shell hypothesis to include varying velocity fields and density gradients. Chandrasekhar (1934) showed that occultation effects are to be expected from the expanding envelope. Beyer and Menzel (1954) have discussed the expanding shell and included the variation of emission intensity with latitude. Sobolev (1947) and Rottenberg (1952) considered radiation transfer in moving atmospheres. In general, most of these theories suffer from several drawbacks. They have more parameters for solution than can be inferred from the observations.

It is difficult to infer directly from the empirical line contours themselves whether the acceleration in the emission envelope is positive or negative. It seems more likely that this inference will be made from considerations of excitation rather than the study of emission line

profiles.

Limber (1964) has recently made the suggestion that forced rotational instability, consequent to continual gravitational contraction in a post main-sequence stage, is responsible for the Wolf-Rayet phenomenon. Limber, in an extension of these arguments, finds considerable support for this theory from the observations, both spectroscopic and photometric, obtained for the systems V_{444} Cygni and CQ Cephei. Further studies on the other binaries may be necessary to examine this aspect of the problem in greater detail.

1.6. Wolf-Rayet stars and the Hertzsprung-Russell diagram.

It is a difficult problem to specify the absolute magnitude of a Wolf-Rayet star. The experimental problem is one of satisfactorily eliminating the contribution of the emission lines to the radiation that is being measured. The determination of absolute magnitudes also needs some idea about the distances of the stars. This is possible in some cases wherein the Wolf-Rayet star is a member of either a cluster or an association or is present in a cloudy galaxy. Examples of this kind are the clusters NGC 6231, the Cygnus association and the Large Magellanic Cloud. A few stars are also seen in the Eta-Carina complex.

Graham (1965) has recently determined the absolute magnitudes of the galactic Wolf-Rayet stars on the basis of their association with well defined agregates and with photoelectric V magnitudes. However, these absolute magnitudes need to be corrected for the contribution of the emission lines through the V filter. He gets a mean absolute magnitude of -6.4 for these stars. Studies by Westerlund and Smith (1964) of Wolf-Rayet stars in the Large Magellanic Cloud with the aid of filters that isolate the continuum region free of emission bands shows that in general the field WN stars have an absolute magnitude of -3.8. However, the mean absolute magnitude of WN stars of the 30 Doradus complex is -5.8. It is likely that this difference signifies mass loss to be an important factor in the evolution of the Wolf-Rayet stars. The 30 Doradus complex may be having single WN stars that are extremely young when compared to the field WN stars.

It should be pointed out that any consideration of the Wolf-Rayet phenomenon should also explain the similarities between the spectrum of the Wolf-Rayet star and the spectrum of the planetary nuclei, which are of course recognized objects of an older population and are also small in mass. It seems, therefore, that the Wolf-

Rayet phenomenon is essentially one that is rare and not a necessary stage of evolution experienced by every star in the mass range one to sixty solar masses. It is likely, that in the process of evolution, there is some feature of rare occurrence that triggers off the course of evolution towards a Wolf-Rayet star. Also it seems rather surprising that the anti-centre region should be devoid of Wolf-Rayet stars, specially when we have ample evidence of star formation in Orion and Taurus. Some investigators tend to believe that the Wolf-Rayet stars, since many of these are not in clusters, are essentially older objects in a young population.

The data relating to the existence of WN and WC sequences have to be considered in the evolutionary context. If these spectral differences originate by virtue of peculiar abundances then these abundance differences have to find a natural explanation in nuclear transformations in the interior, coupled with good mixing. This necessarily implies a certain age for the star's Wolf-Rayet formation. On the other hand, it is possible that selective excitation may be the cause for the spectroscopic peculiarities. It seems, therefore, that the present state of knowledge pertaining to the Wolf-Rayet stars indicates that while these are essentially young objects, we are still far from a

satisfactory explanation for the sequence of events that lead to the formation of such a star.

I have outlined above the status of information available today on the Wolf-Rayet phenomenon. In this thesis, I hope to provide additional information on the characteristics of the Wolf-Rayet stars, by studies of the single systems as well as the binary systems. A study of the binary system γ Velorum furnishes information on the masses of the WC star and an O7 star. Spectrophotometry of several binary systems studied in this thesis indicate the complexities of gas streaming that one can see in these star systems.

I have used available high dispersion spectra for making precise line identifications, after separation of the various blends. The intensities of selected lines are then used to determine excitation temperatures of some of these objects. Many important questions have been treated inadequately or omitted entirely. However, an attempt is made in this thesis to explore the main characteristics of these stars with observation material that have the characteristics of high dispersion and homogeneity.

CHAPTER II

THE OBSERVATIONS

2.1. General.

A detailed description of the present status of information concerning the Wolf-Rayet stars has been given in the previous chapter. I now describe the objects studied in this thesis and the techniques utilized in collecting the information. The basic procedure has been photographic spectrophotometry by conventional methods, utilizing high and low dispersion spectra. These have been used for wavelength measurements and corresponding identifications, line profile studies and equivalent width measurements, as well as radial velocity measures.

2.2. High Dispersion Spectra.

Most of the Wolf-Rayet stars in the northern hemisphere are relatively faint for easy access for high dispersion spectroscopy. The brightest of those stars that form part of the Cygnus association are close to 7.0 mag. High dispersion spectra ranging from 3350A to 6750 have been obtained for the stars listed in Table II-1, with the 100-inch telescope and associated Coude Spectrograph. The 32-inch Schmidt camera, in conjunction with a 6-inch collimator of the coude spectrograph, provided spectra of

Table II-1a

HD	Spectral Class	RA 1900	Declination 1900	Magnitude.	Average Exposure time (in minutes for Mount Wilson 100-inch Telescope 10Å/m		20Å/m
					IIa-O baked	103a-D	103a-E.
50896	M6	$06^h50^m.0$	-23° 48'	6.4			
165763	M6	18 02 .5	-21° 16'	7.7	60	108	61
191765	M7	20 06 .5	+35° 55'	7.8	98	72	121
192103	M7	20 08 .1	+35° 54'	7.9	127	81	68
192163	M6	20 08 .4	+38° 03'	7.4	90		
192641	M7	20 10 .8	+36° 21'	7.9	135	116	156
193077	M6	20 13 .3	+37° 07'	8.0	106		105
193576	M5	20 15.4	+38° 25'	8.5	125		
193793	M6	20 17.1	+43° 30'	6.8	56		36

dispersion 10A/mm in the blue and 20A/mm in the visual and red regions.

The emulsion used for photography in the blue was Eastman IIa-O. The visual region spectra were obtained on 103a-E, 103a-E and 103a-F plates. The comparison sources, as wavelength standards, are the iron arc for the blue and a combination of the iron arc and Neon lamp for the visual and red regions of the spectrum. The spectra were widened to 130 microns on the photographic plate, and all spectra were obtained with a projected slit-width of 20 microns in focal plane.

A single spectrogram of the bright southern Wolf-Rayet star γ_2-Velorum was obtained at Kodaikanal with a Littrow Spectrograph attached to the 90cm reflector. This spectrograph utilizes a 120cm collimator-camera arrangement with a 300 lines/mm grating, blazed in the first order at 1.5 microns. This grating was used in the third order to yield a dispersion of 9A/mm. This was used to study the region from 3900A to 4900A.

The coude spectrograph at Mount Stromlo, in Australia, was also used to provide high dispersion spectra of γ_2-Velorum in the ultraviolet and of the Of star Zeta Puppis from 3500A to 6800A. The Mount Stromlo coude

spectrograph was used in the third order of a 600 lines/mm grating with a 32-inch camera that yielded a dispersion in the blue of 6.7A/mm. The dispersion in the red when used in the second order of the grating was 10A/mm.

The Struve plate of γ_2-Velorum was utilized for a determination of the spectral class of the B companion.

2.3. Low Dispersion Spectra in the Visual and Photographic Regions.

At the Mount Wilson Observatory, spectra were obtained of several stars in the northern hemisphere brighter than magnitude 10.0, with the aid of a one prism spectrograph attached to the 60-inch reflector. This spectrograph has a collimator of focal length 36 inches and was used with a camera of 8-inch focus which provided a dispersion at H γ of 75A/mm. This camera was utilized exclusively for obtaining spectra of all the stars in the blue region. It was also used for obtaining the numerous spectra required of the Wolf-Rayet binary systems for studies of radial velocity variations, line profile changes and equivalent width determinations of the various lines. Exposure times on IIa-O baked plates were of the order of 30 minutes for a star of magnitude 8.5 and a spectrum width of 500 microns.

At least one spectrum in the 5000A-6800A region was obtained of each star in the programme with the one prism combination, to provide material for a detailed spectral classification of these objects. These spectra were obtained with a 10-inch camera and with Eastman 103a-F emulsion.

Low dispersion spectra were obtained at Kodaikanal of γ_2-Velorum in both the 1964-65 and 1965-66 observing seasons. These were obtained with a grating spectrograph at the cassegrain focus of the 50cm reflector. The focal lengths of the collimator and camera are 300cm and 50cm respectively. A 1200 lines/mm grating was used in the first order during the 1964-65 season. This gave a dispersion of 125A/mm. For the 1965-66 series of plates, a 600 lines/mm grating blazed in the first order at 7900A was used and spectra of γ_2-Velorum were obtained in the second order blue region, on high contrast Ilford G-40 process plates. The 1965-66 series on γ_2-Velorum have a width of spectrum of 300 microns. The extreme speed of the spectrograph coupled with the brightness of the object enabled well-exposed spectra to be obtained with exposure times of the order of 10 to 15 minutes. The slit-width used was such as to provide a projected slit-width in the camera focal plane of 15 microns. A comparison spectrum

of Argon was impressed on the blue series of plates as wavelength reference.

Table II-2 gives a list of the stars observed that have low dispersion spectra.

The Mount Wilson and Mount Stromlo high and low dispersion spectra were obtained by Dr. M.K.V. Bappu and kindly turned over to the author of this thesis for study.

2.4. The Spectra in the Near Infra-red.

The stars HD 192103, HD 192163 and HD 165763, were bright enough to be within the reach of the 60-inch telescope at Mount Wilson in combination with a grating spectrograph and a 10-inch camera. Exposures of the order of 4 hours were necessary to obtain spectra of these three stars with a spectrum width of 110 microns at a dispersion of 111A/mm. Kodak I-N plates, hypersensitized with ammonia, were used for this purpose. The programme was extended further at Kodaikanal, using the Cassegrain spectrograph in the first order of the Bausch and Lomb grating. With a dispersion of 250A/mm, it is possible to obtain spectra of Wolf-Rayet stars of magnitude 7.0 in a little under two hours.

Table II-2

HD	Spectral Class	RA 1900	Declination 1900	Magnitude.	Average Exposure time (in minutes)		
					60-inch One Prism 7-inch Camera 75A/mm at H_γ IIa-O baked	60-inch, 10-inch Camera	
						103a-O	103a-F
4004	M5	$0^h 38^m.0$	+64° 14'	10.2			
16523	M6	02 34 .0	+56° 18'	10.0			
50896	M6	06 50 .0	-23° 48'	6.4			
63275	M7	08 07 .0	-47° 03'	2.2			
169668	M6	18 02 .1	-19° 25'	9.6			
165763	M6	18 02 .5	-21° 16'	7.7	60	103	61
168206	M7	18 13 .5	-11° 59'	8.9			
186943	M6	19 42.2	+28° 01'	10.0	88		
191765	M7	20 06.5	+35° 53'	7.8	58	72	121
192103	M7	20 08.1	+35° 54'	7.9	127	87	
192163	M6	20 08 .4	+38° 03'	7.4	90		
192641	M7	20 10 .8	+36° 21'	7.9	135	116	156
193077	M6	20 13.3	+37° 07'	8.0	106		105
193576	M5	20 15 .4	+38° 25'	8.5	125		
193793	M6	20 17 .1	+43° 32'	6.8	56		
193928	M6	20 17.8	+36° 36'	9.4	75		
211853	M6	22 15. 0	+55° 37'	9.4	90		

Table II-3

HD	Spectral Class	R.A. 1900	Declination 1900	Magnitude	Dispersion	Exposure time	Remarks
192103	WC7	$20^h08^m.1$	+ 35° 54'	7.9	111A/mm	272 mins.	60-inch Cassegrain grating spectrograph 1st order.
192163	WN6	20 08 .4	+ 39° 05'	7.4	111A/mm	209 mins.	
165763	WC6	18 02 .5	- 21° 16'	7.7	111A/mm	133 mins.	
50896	WN6	36 50 .0	- 23° 48'	6.4	250A/mm	175 mins.	
93131	WN7	10 40 .1	- 59° 36'	6.7	250A/mm	80 mins.	Kodaikanal 20-inch Cassegrain spectrograph 1st order grating.
92740	WN7	10 57 .4	- 59° 09'	6.5	250A/mm	89 mins.	
151932	WN7	16 45 .3	- 41° 41'	6.6	250A/mm	40 mins.	
68273	WC7	08 06 .5	- 47° 03'	2.2	250A/mm	30 mins.	
66811 (ζ Puppis)	O5	08 00 .1	- 39° 43'	2.2	250A/mm	30 mins	

The Kodaikanal infra-red spectra were obtained on Eastman I-N emulsion hypersensitized in an ice bath for 4 minutes. Ammonia hypersensitization was not employed, in order to avoid chemical fog. The spectra at Mount Wilson were obtained with a projected slit width of 40 microns and those at Kodaikanal with a projected slit width of 32 microns and a width of spectrum of 110 microns. Table II-3 gives the list of stars for which infra-red spectra are available.

All the spectra obtained at the three observatories were developed in D-19 for 5 minutes and at 68°F. Adequate care was taken in rocking the plates to avoid complications due to Eberhard effects.

2.3. Photometric calibrations.

Every plate, soon after exposure, was provided with a calibration prior to development. At the Mount Wilson 100-inch coude spectrograph, the calibration was effected by a series of sixteen spectra on either side of the star exposure that were photographed with the same optics as those used for obtaining the star spectrum. These sixteen spectra have different intensities depending upon the widths of the step-slits used for providing the spectra.

The intensities of these calibration strips were frequently checked, particularly at the beginning of each months observing run. A check on the uniformity of illumination was made to ensure that the calibration remained valid during the observing period. In addition to these an auxiliary calibration unit in the dome of the 100-inch telescope provided a continuous wedge calibration which was useful for subsequent reduction of these spectra using the Babcock direct-intensity microphotometer. These wedge spectra were obtained with a triangular slit wherein the intensities at distances from a fiducial mark were proportional to the linear distance between the point and the fiducial mark. All the Mount Wilson coude spectra had an additional provision of this wedge calibration, and both wedge exposure and star exposures were developed simultaneously. The spectra obtained at the 60-inch telescope were calibrated in two ways. Firstly, most of them were impressed with calibration marks from a spot-sensitometer that has 10 spots covering a range in intensity. Four sets of these were impressed on each plate thus providing an adequate range of calibration. In addition a wedge calibration with the wedge-slit spectrograph in the 100-inch dome was also made available and all plates were developed simultaneously. It was, therefore, possible to

utilize the Babcock microphotometer to obtain direct intensity tracings of even the 60-inch spectra.

The calibration at the Mount Stromlo observatory on the 72-inch coude was essentially similar to that used at the Mount Wilson Observatory, except for the fact, that in place of the step-slit, triangular slits were used on either side of the star exposure to provide wedge calibration.

At Kodaikanal, the calibration was effected by a Hilger step-wedge combined with a Hilger medium quartz spectrograph. Two exposures of the step-wedge spectra, slightly differing in intensity, were obtained and these were developed simultaneously with the star exposure.

2.6. The Measurement of Radial Velocity.

Several plates obtained of the Wolf-Rayet spectroscopic binaries were used for radial velocity measurements to derive the spectroscopic orbits. The Mount Wilson spectrograph has been in use for radial velocity measurements for nearly half a century and has been an instrument that has provided the bulk of radial velocity data that are available to the astronomers of today. The velocity measurements of emission and absorption lines on the Mount Wilson spectra were made with a

Hilger single screw measuring engine as well as a Zeiss Abbe Comparator.

Radial velocity measures of Wolf-Rayet spectra are usually more difficult than measurements of the absorption lines in normal star spectra, essentially because of the diffuseness of many of the lines and their very large widths. Multiple settings on each line help reduce the scatter in the measures. The reduction of the prism spectra were followed by using a pre-calculated set of computed positions of the wavelengths of lines on the basis of a mean Hartmann dispersion formula. The comparison lines of the iron are on each plate are used to determine the correction curve required for the particular plate measured and from these the radial velocities of selected emission and absorption lines were determined. For the Wolf-Rayet binaries of the Nitrogen sequence most measures were on HeII 4686A and NIV 4058A. If absorption lines could be easily measured, as in the case of HD 193576, the radial velocities were determined from the lines H_β , H_γ and in some cases H_δ . In one or two binaries NV 4603A was also measured. The Kodaikanal spectrograph was first tested out on selected radial velocity standards of the Wilson General catalogue. The velocities obtained at

different telescope positions indicated that the spectrograph was free of flexure and that it could be utilized for radial velocity determinations with an accuracy commensurate with the dispersion used. On a reasonably narrow lined spectrum one could have a radial velocity value, at 125Å/mm, with a standard error of 5 to 6 km/sec. Since an error of this magnitude is much less than the likely error caused in the measurement of the broad emission lines of the Wolf-Rayet spectra, the spectrograph was used with confidence for a radial velocity study of the binary system γ_2-Velorum.

2.7. The Spectrophotometric Reductions.

Most of the Mount Wilson spectra were traced with the Babcock direct intensity microphotometer. This was possible because of the availability of wedge calibrations for these spectra. The Babcock instrument is a very convenient one for obtaining a large number of intensity tracings compared to the conventional procedure, which would be a very painstaking process. The instrument was set as carefully as possible with the zero of the intensity scale coinciding with the fiducial mark on the wedge. However, since the instrument is least sensitive in the vicinity of zero intensity, a subsequent determination

for each spectrum tracing, of this zero correction, was effected by tracing the step-slit calibration and determining the location of the zero, from the known intensities of the step-slits.

In most cases the zero corrections were of the order of 2 to 3%. Some of the Mount Wilson spectra had conventional density tracings only. I reduced these to intensities with the aid of the calibration curve in the following way. Perpendicular to the line of zero transparency, the intensity marks were registered on the tracings. With the aid of the calibration curve these intensity marks were registered at selected intervals in such a way that the final intensity tracing had a convenient array of points in order to trace out the whole spectrum. These intensity marks were made on either side of the tracings. On a separate sheet of paper the direct intensity scale is plotted as ordinate and the microphotometer tracing was placed on this paper in such a way that the intensity mark on the tracing, corresponded to the intensity value on the paper placed below. The intersection of these intensity marks along the density tracing was then transferred onto the paper below. The microphotometer chart was then moved over to the next intensity step

and a similar series of intersection points determined. When a set of such transfers is effected for all the intensity points, the density trace is removed. The points on the intensity tracing are connected in a way as to provide an exact intensity tracing of the spectrum. This was found to be a convenient method which also has the virtue of speed for spectrophotometric reductions.

For plates which were taken at Kodaikanal, the new semi-automatic intensitometer developed at Kodaikanal (Bappu 1966) was used for this purpose. A density tracing of the spectrum is first made with the conventional microphotometer. The density trace is obtained by a Brown recorder operating in the ratio mode with a comparison voltage originating from a photomultiplier that monitors the light source of the microphotometer. This eliminates possible intensity fluctuations of the lamp due to line voltage fluctuation. This tracing was obtained on one half of the Brown recorder chart and the other half is used for obtaining the intensity tracing.

The calibration curve is drawn on a perspex sheet and held against a reference line on the Brown recorder obtained by means of a taut wire. The microphotometer tracing is fed back to the first spool of the Brown

recorder and made to unroll a second time. The point of intersection of the tracing with the wire is the point where the calibration curve is made to intersect and the observer manupulates the calibration curve vertically up and down in such a way that the calibration curve always passes through the intersection of the reference wire and the tracing. The up-and-down movement of the calibration curve is directly coupled to a helical potentiometer, the output of which is fed back to the recorder. The recorder thus traces out the direct intensity. This process of intensity reduction is exceedingly quick and convenient and greatly facilitated several of the reductions necessary for the spectra obtained at Kodaikanal. It also has the advantage of providing an accurate location of the zero of intensity.

CHAPTER III

THE SPECTRA OF WOLF-RAYET STARS

3.1. Introduction.

Most studies of Wolf-Rayet spectra during the present century have made efforts to identify the various emissions seen in the spectrum. Developments in this field have gone hand-in-hand with laboratory studies of the emission lines of the various stages of ionization of carbon, nitrogen, oxygen and silicon. Most of these laboratory studies have originated in Edlen's laboratory and one might even say that the physical researches by the group directed by Edlen seem to have oriented their efforts towards unraveling the spectra of the Wolf-Rayet stars.

The descriptions of Wolf-Rayet spectra are numerous. Some of the earliest of these have been from Victoria by Plaskett and Beals. Miss Payne surveyed with a prismatic camera most of the WR spectra brighter than mag 10.0 in both the northern and southern hemispheres. Smith (1955) made the first systematic studies from slit spectra, of the southern Wolf-Rayet stars. Underhill (1959) has studied the spectra of HD 192103 and HD 192163 with higher dispersion than used earlier. Swings and

Jose (1950) surveyed the infra-red spectra of seven WR stars at the low dispersion of 345A/mm with the aid of the nebular spectrograph on the McDonald 82-inch telescope. Andrillat (1957) extended these studies to 7 stars of the WC sequence and 16 stars of the WN sequence. This study was made at the very low dispersion of 636A/mm at 8000A, and hence gives only an idea of the prominent contributors to the emission spectrum in this region.

In what follows we shall describe the salient features of some high dispersion spectrograms of selected stars of both sequences, the infra-red spectra of both WC and WN stars obtained with dispersion higher than that used by previous investigators and equivalent widths of some emission lines obtained from low dispersion spectra for purposes of spectral classification.

3.2. The high dispersion spectra.

When one examines high dispersion spectra of the WR stars in the blue region, the technique to be used is to confine oneself to the tracings at a magnification of 10 or 20 for both the study of wavelengths and intensities. For identifications in these objects, one also needs spectra of differing spectral types that can be examined

simultaneously, so that the excitation differences will show up the development of the spectrum of each ion from star to star.

The investigations of the past have catalogued the various lines seen in the different stars at relatively low dispersion. Low dispersion is useful when it involves the ob... of the broad spectra characteristics alone. When use has to be made of the data for quantitative analysis, low dispersion spectra are unsuitable for the purpose. In fact for some stars even high dispersion is unsuitable, since an emission feature is a composite of different emission lines that are blended effectively in the stars atmosphere by Doppler motions and hence, cannot be separated by any amount of spectral resolution.

In Figs. III-1, III-2, III-3, III-4, III-5 and III-6, I give the intensity tracings of selected spectra of WC and WN stars in the regions 3950-4650A and 5400-6000A.

Figs. III-1 to III-3 show the intensities in the spectrum of WC8, WC7 and WC6 stars in the region 3950-4650A. All the spectra have an original dispersion of 10A/mm and were obtained with the 100-inch coude spectrograph. The

WC8 star is the nucleus of Campbell's hydrogen envelope star. While it cannot be considered as typical of a WC8 star, its spectral characteristics are remarkably similar to that of a WC8 star and in fact has been used as a standard for a long time. The WC8 spectrum has narrow emission lines and shows a well developed spectrum of CII and CIII. Almost every prominent feature described in the laboratory study of CII by Glad (1953) and of CIII by Bockhasten (1956) has been identified in the blue, visual and red regions of HD 104738 by Rappu and Wilson. These ions must be contributing effectively in HD 192103 and also, along with CIV, OIII, OIV, NV in HD 165763. But when it comes to a study of the emission complexes in such a WC6 star, all we can do is to be aware that it is built up by several different contributing ions. There is thus little point in even attempting to measure the equivalent width of the whole feature unless it be as some measure for spectral classification.

With this in mind one sees in Figs. III-1 to III-3 the development of the spectral sequence from WC8 to WC6. Except for certain features like HeII 4542, HeII 4340, CIV 4229, which can be isolated easily from a blend, many of the other lines are blended hopelessly.

FIGURE III-1

Intensity traces of HD 165763, HD 192103
and HD 184738 in the region 3850 - 4150A

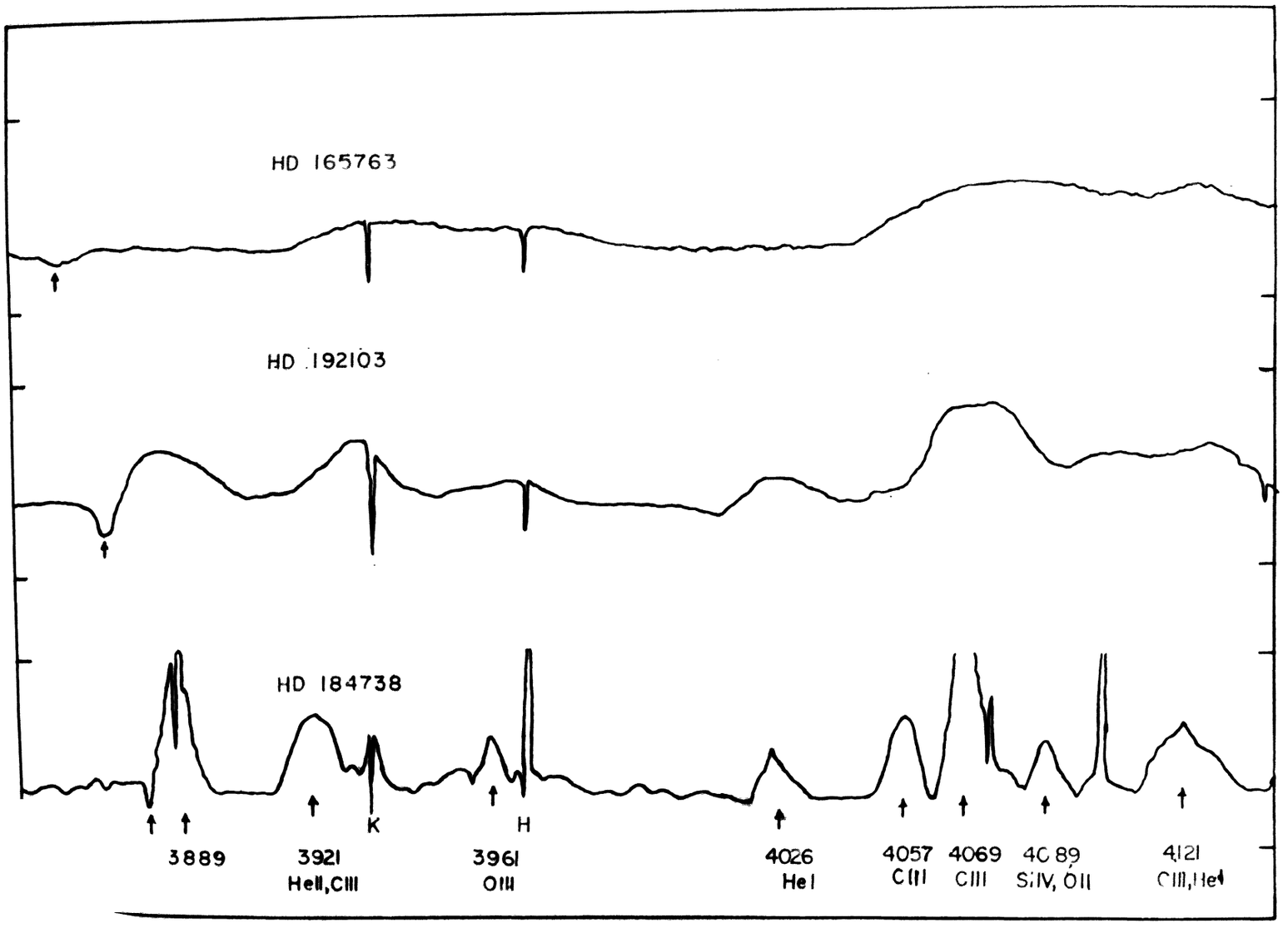
HD 165763
HD 192103
HD 184738
K
H
3889
3921
HeII,CIII
3961
OIII
4026
HeI
4057
CIII
4069
CIII
4089
SiIV, OII
4121
CIII,HeI

FIGURE III-2

Intensity traces of HD 166763, HD 192103 and HD 194739 in the region 4100 - 4300A

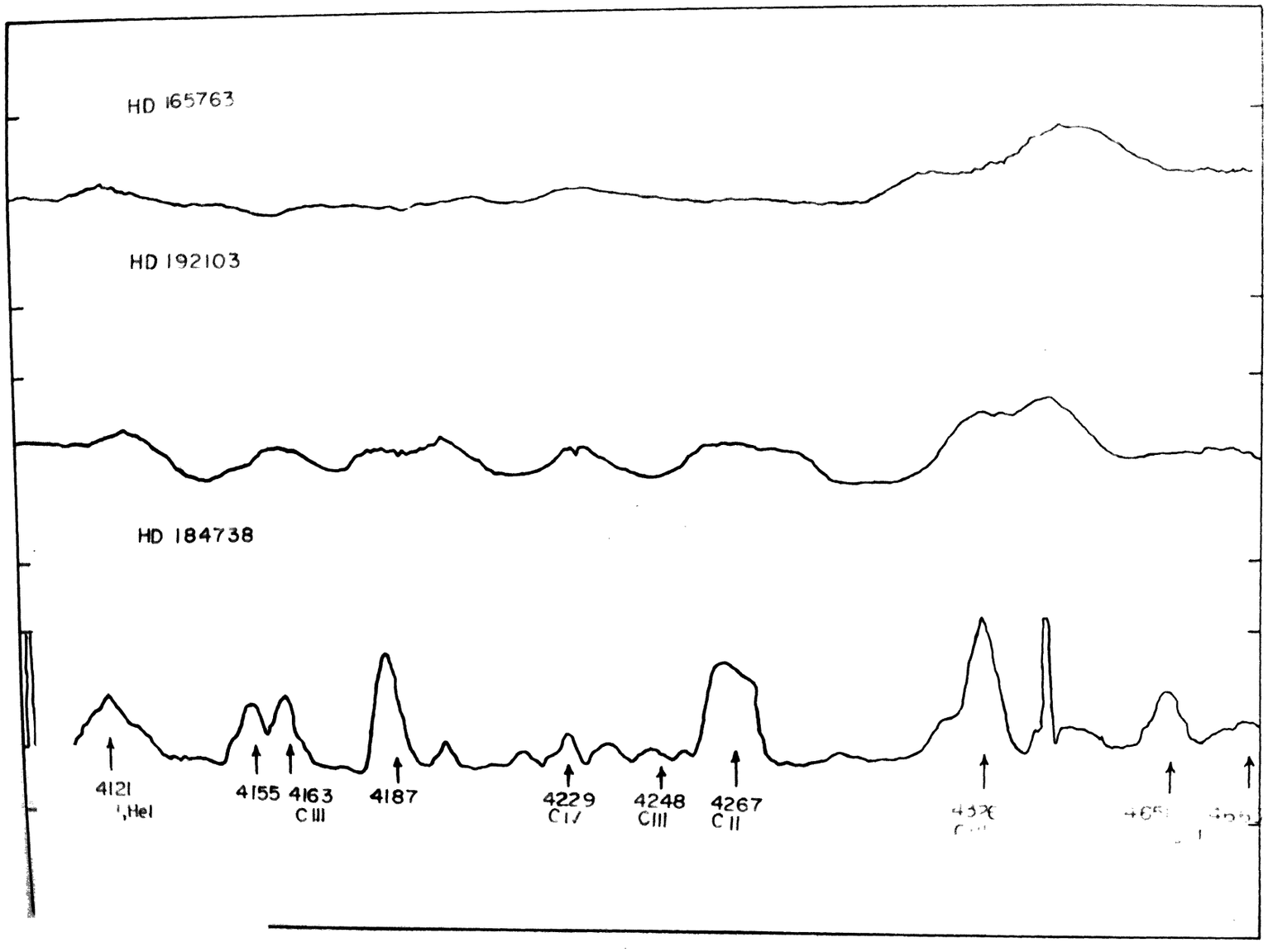
HD 165763
HD 192103
HD 184738
4121
He I
4155
4163
C III
4187
4229
C IV
4248
C III
4267
C II

FIGURE III-3

Intensity traces of HD 165763, HD 192103 and HD 184738 in the region 4300A - 4670A

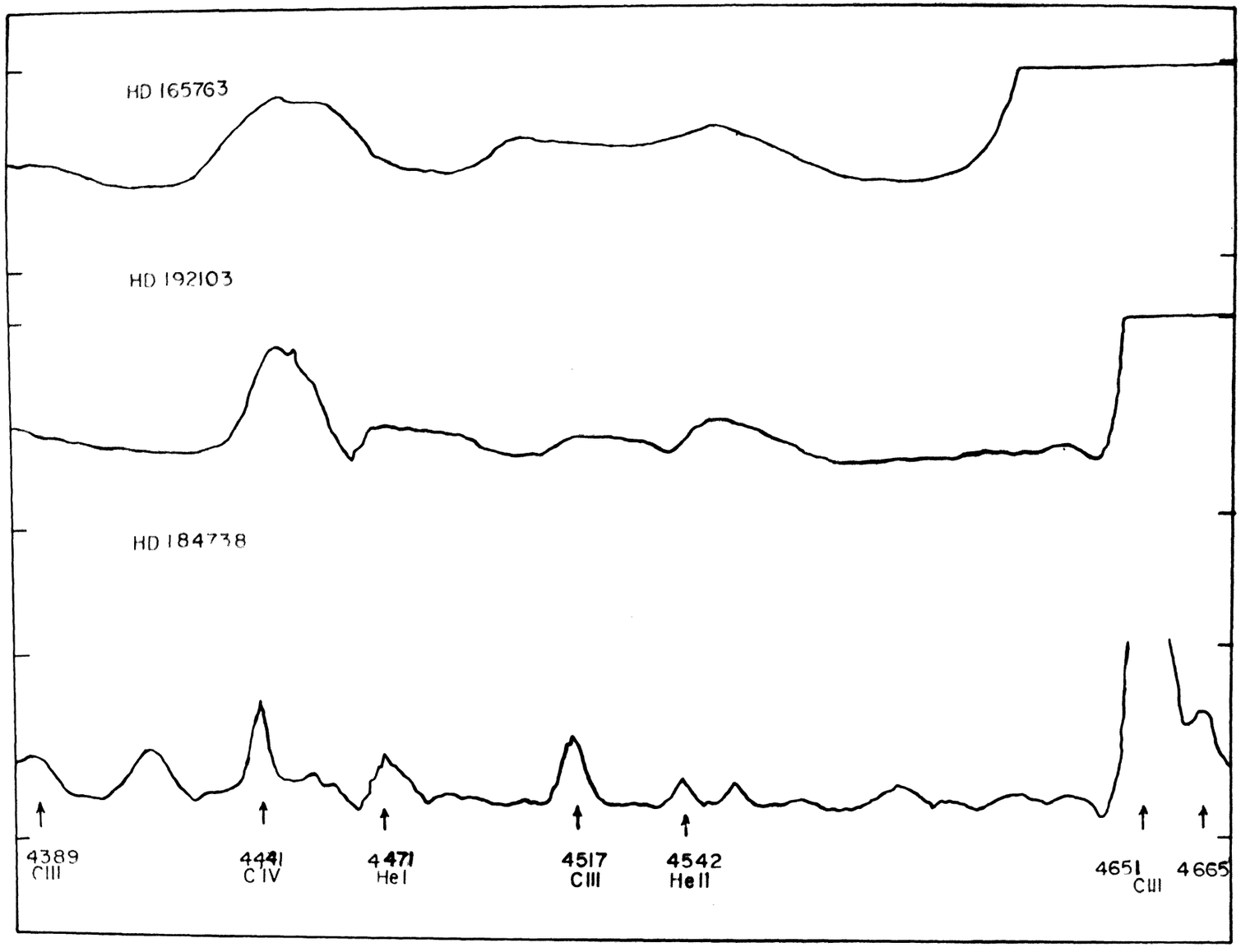
HD 165763
HD 192103
HD 184738
4389
CIII
4441
CIV
4471
HeI
4517
CIII
4542
HeII
4651
CIII
4665

In the spectrum of HD 184738, Mayall and Wilson, Swings and Struve (1940) report on several CIII features that have violet edges. We lose many of these details in HD 165763 and HD 192103. However, the CIII complex at 4650A has a definite violet edge and violet edges are present for the HeI lines. In the blue spectrum of HD 165763, we see such displaced violet absorption weakly for 4471A and one of moderate intensity for 3889A, HeI. The displacement of the absorption at 3889A is -1850 Km/sec. In the spectrum of HD 192103, the displaced violet edge of 4650A is appreciable in intensity and one sees such violet edges for the HeI lines 4471A, 4026A and most strikingly, 3889A. The displacement of the violet edge of 3889A is only -1220 Km/sec. This may be contrasted with the violet edge of 3889A in HD 184738 which has a displacement of only -530 Km/sec. The variation of mass motion, along the temperature sequence illustrated, is obvious.

In the yellow region of the spectrum, the prominent lines are of HeII, HeI, CIV, CIII and OV. Fig. III-4 shows the tracings of HD 165763 and HD 192103 in the wavelength regions 5400 to 6000A. Also shown on this figure for comparison is an intensity tracing of HD 192163, a star of the WN sequence. We shall compare the WC and WN

FIGURE III-4

Intensity traces of HD 165763 WC6, HD 192103 WC7, and HD 192163 WN6, in the region 5400A-5900A

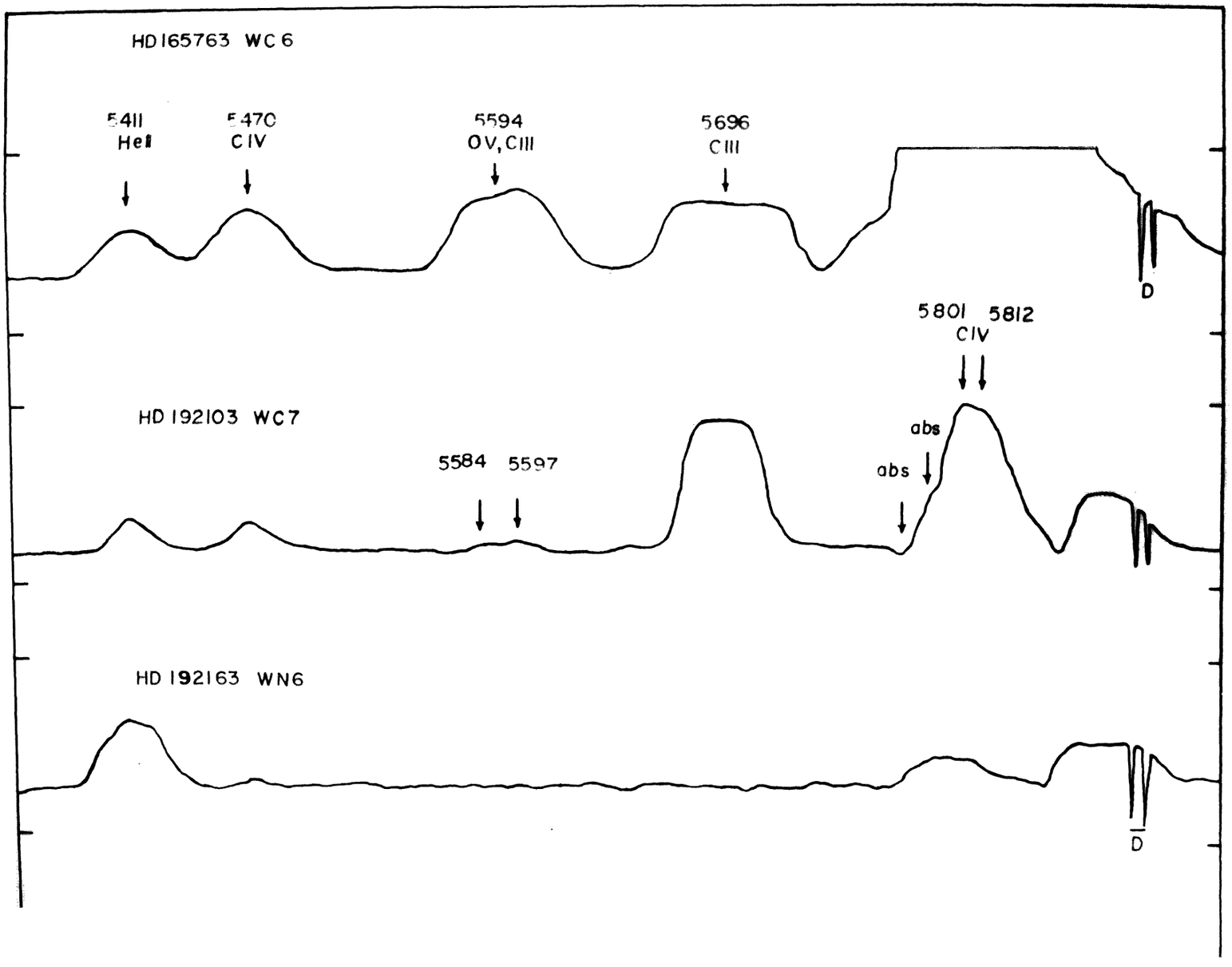
HD165763 WC6
5411
HeII
5470
CIV
5594
OV, CIII
5696
CIII
D
5801 5812
CIV
HD192103 WC7
abs
abs
5584 5597
HD192163 WN6
D

sequence, later. For the present, the salient characteristics of HD 165763 in this region are the intense 5801-5812A CIV emission, and intense OV at 5590A, so much so that both the contributors 5580A and 5590A seen resolved in HD 192103 merge together. CIV 5470 has increased in intensity considerably when compared to its performance in HD 192103, while 5696A with a typical flat-topped profile has decreased in intensity. In HD 192103, the violet absorption of HeI 5876 is strong. This part of the wavelength region goes off-scale in the tracing of HD 165763. For HD 192103 we see displaced violet absorption of both the CIV lines 5801A and 5812A. In the tracing of HD 165763 we see the displaced absorption of CIV 5801 at 5764A or a displacement of -1900 Km/sec.

The CIII 5696 poses an enigma in studies of line contours of WC stars. It is nearly flat-topped and was used by Beals as a good illustration of the consequences of the simple expanding shell. Its profile looks very unlike the profile of any other line in the spectrum. Also its width at half intensity is greater than it should be on the basis of similar measures for lines of comparable intensity and excitation. It is difficult to explain

FIGURE III-5

Intensity traces of HD 192163 WN6 AND HD 193077
WN5 in the region 3650 - 4200A

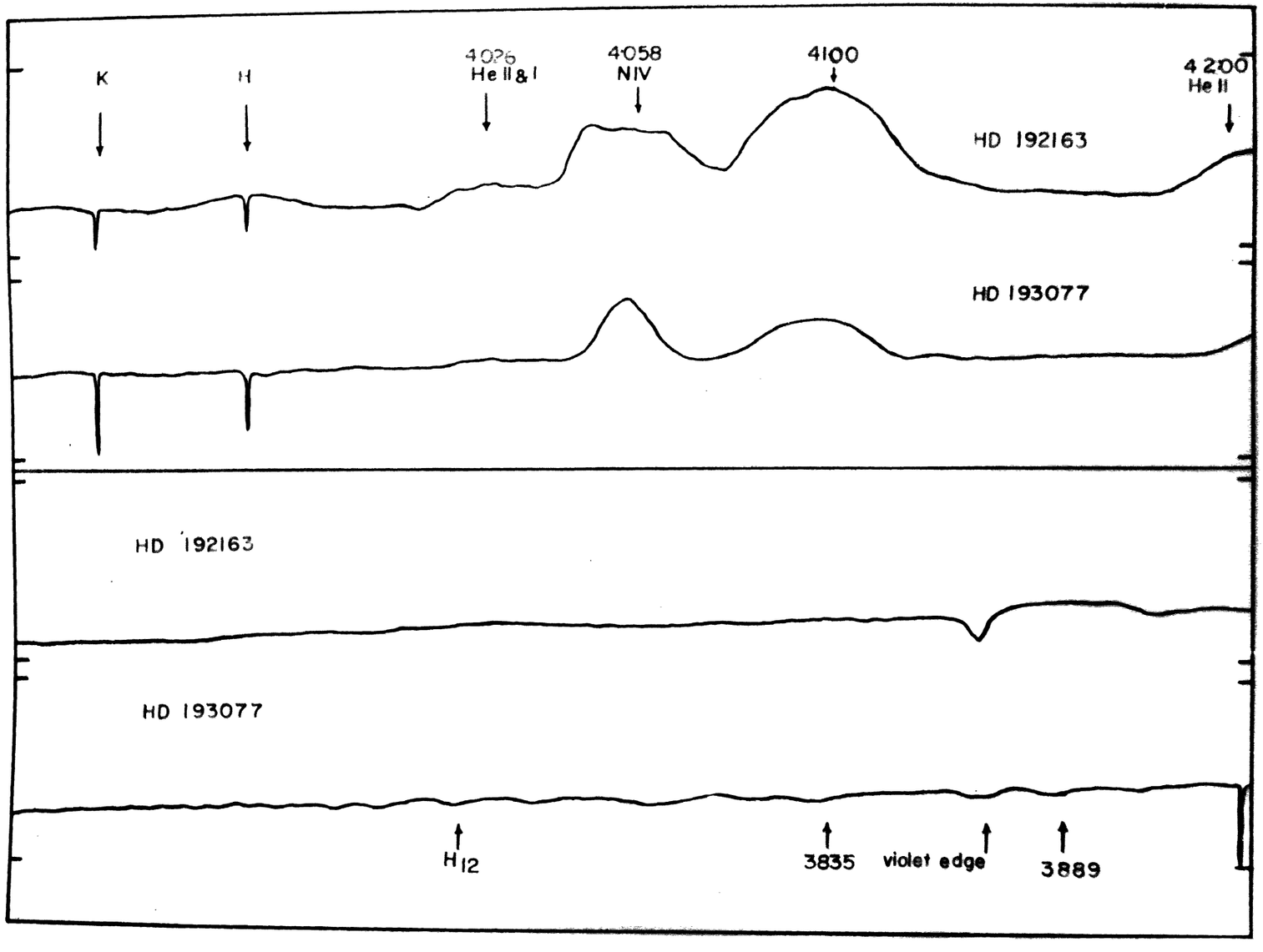
K
H
4026
He II & I
4058
NIV
4100
4200
He II
HD 192163
HD 193077
HD 192163
HD 193077
H12
3835
violet edge
3889

FIGURE III-6

Intensity tracces of HD 192163 W6, and HD 193077

W5 in the region 4200 - 4700A

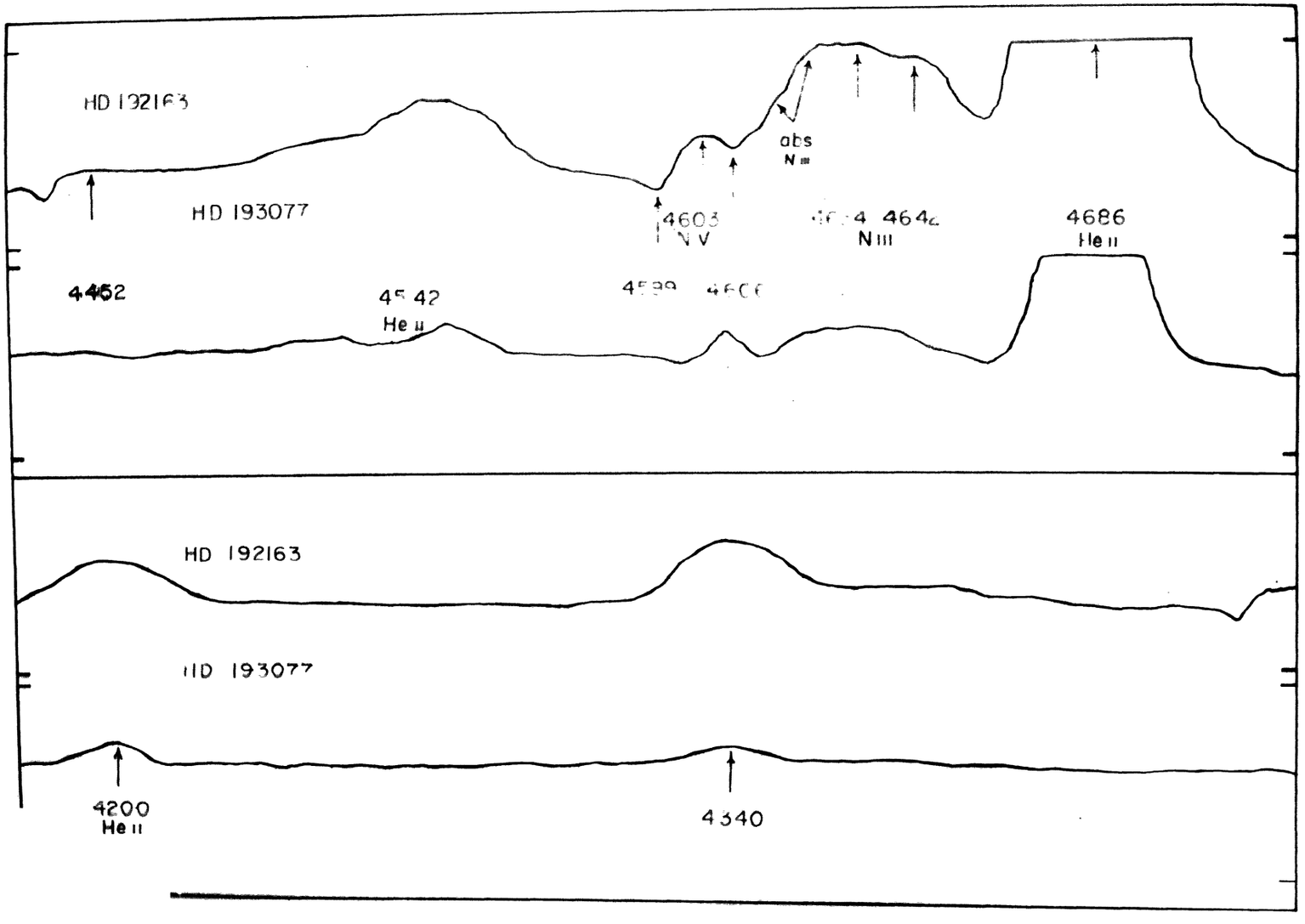
HD 192163
HD 193077
abs
N III
4603
N V
4640 4642
N III
4686
He II
4462
4542
He II
HD 192163
HD 193077
4200
He II
4340

these features satisfactorily. The flat-topped profile could be the result of a summation of two blended features. If the two features are of comparable excitation characteristics they could be excited, more or less depending on the excitation source, and still maintain the flat topped profile. Or it could be due to self reversal, which however, does not look a satisfactory explanation. It could also be due to the summation of CIII 5696 originating from two component sources, one, the conventionally excited one and the other component by virtue of fluorescence. The fluorescence components would flank the conventional emission line on both sides, by virtue of the upward and downward motions of the gas that gives rise to the emitting radiation.

The spectrum tracing (Figs. III-5, III-6) of HD 192163 shows the main characteristics of stars of the WN sequence. The prominent lines in the blue are HeII 4686 and members of the Pickering series, NIII 4630-40 and NIV 4058. Many of the remaining NIII transitions are blended, leaving little hope of separating them, unless we examine a WN8 star with high dispersion. The displaced violet absorptions in this star are the most striking among the stars for which spectra at high

dispersion are available. This star shows the displaced absorptions of HeI 5876, CIV 5801-5812, NV 4619, NV 4603, HeI 4472, HeI 4026 and HeI 3889. Displaced weak absorption can also be seen at 4617A and 4623A presumably originating from NIII 4634 and NIII 4640. If this is so, their displacement is -1100 Km/sec in agreement with the displacement expected for their excitation. Listed below are the displacements of these absorption features arranged in order of excitation potential. One sees the dependence of the displacement on the state of excitation, in the sense, that the largest displacements are for the lines of lower excitation.

		E.P. upper level	E.P. lower level	Vel. Km/sec.
HeI	3888.6	22.91	19.73	-1412
HeI	5875.6	22.97	20.87	-1383
HeI	4471.6	23.63	20.87	-1313
HeI	4026.3	23.94	20.87	-1280
CIV	5801.5	39.51	37.39	-1100
CIV	5812.1	39.51	37.39	-1083
NV	4603.2	98.99	56.31	- 884
NV	4619.4	98.99	56.31	- 842

The most intense of the displaced absorptions of HeI is of λ3889A. However, the intensity of this absorption is only a little greater than those of the other triplets listed above. Hence dilution effects are very small and the HeI λ3889 absorption must be originating close to the 'surface' of the star on the basis of our concepts of phenomena in a shell. Hence the lower excitation lines originate close to the "luminous core" envisaged by Kron and Gordon (1950) for a Wolf-Rayet star. If so the absorbing ions are decelerated in the atmosphere, for the higher excitation NV absorption velocities are only about 0.6 of the velocities of the HeI absorption. Such a positive excitation gradient cannot be explained on simple ionization and recombination phenomena. I believe that this points to the effective role played by collisional excitation.

One other aspect of the nitrogen stars needs attention. The emission complex at 4640 displays much structure and extends well out to 4662A. It is not possible to explain this feature unless we invoke the presence of a few CIII, CIV transitions of low intensity. We shall discuss in a subsequent paragraph the identification of CIV λ3201-12. For the present we assume that the presence

FIGURE III-7

High dispersion Wolf-Rayet spectra in the region 5680 - 5900Å

a) HD 50896 WN5

b) HD 192163 WN6

c) HD 191765 WN6

d) HD 184738 WC8

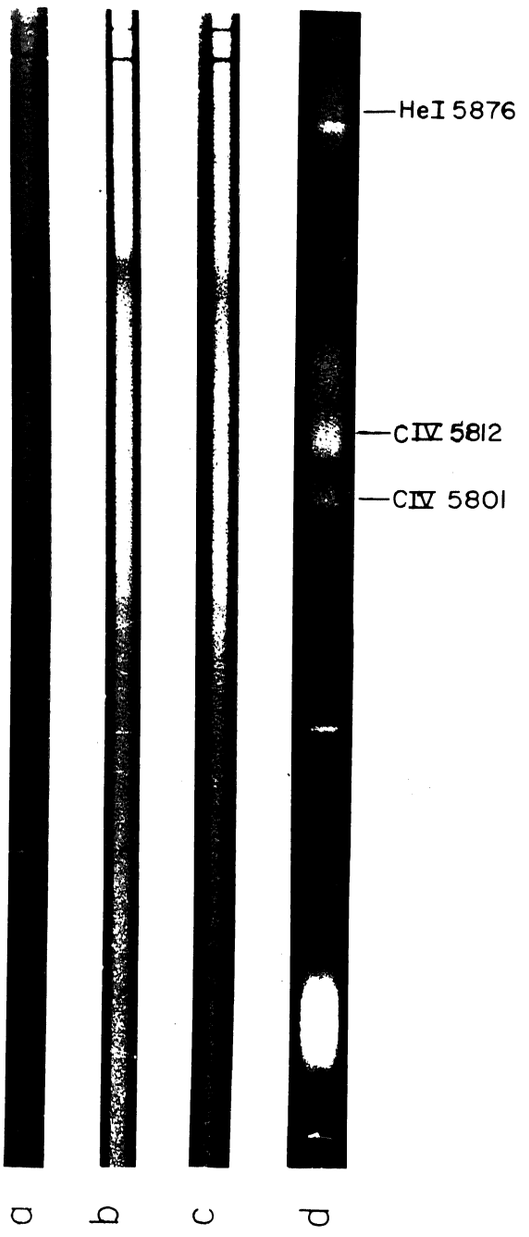
HeI 5876
CIV 5812
CIV 5801
a
b
c
d

FIGURE XXI-1

High dispersion Wolf-Rayet spectra in the region 5680 - 5970A

a) HD 193793 WC6
b) HD 165763 WC6
c) HD 192641 WC7
d) HD 192103 WC7
e) HD 184738 WC8

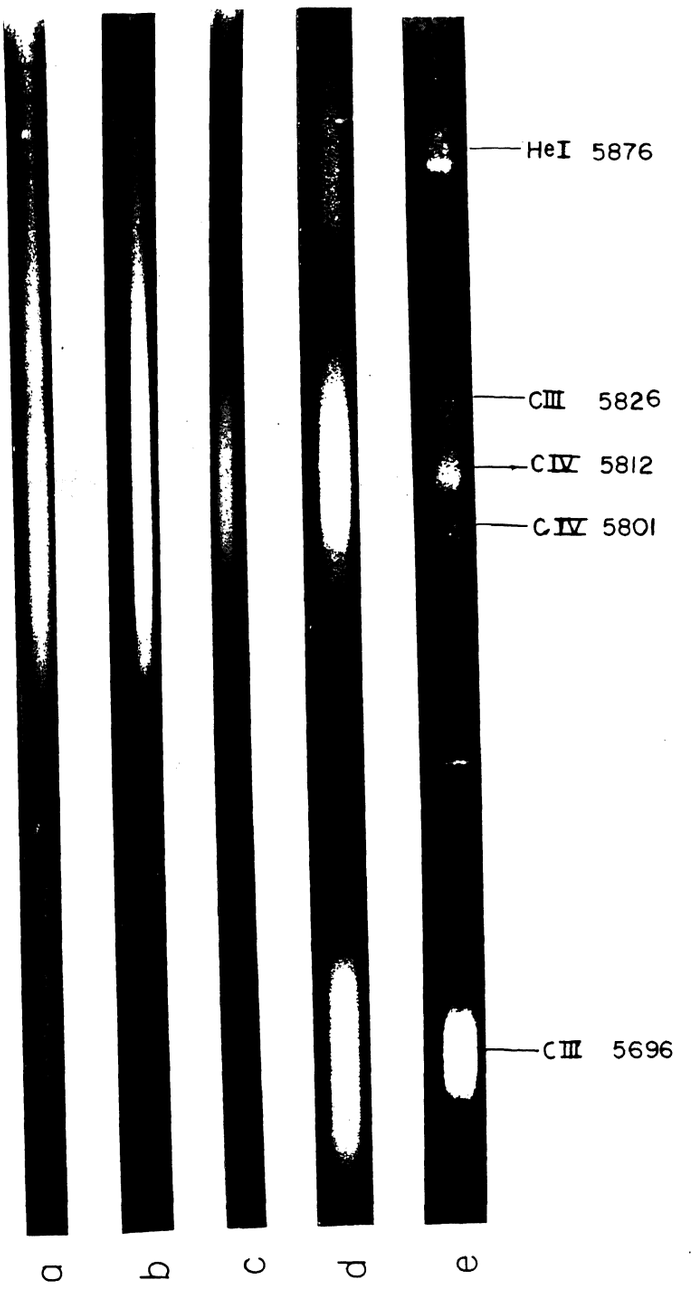
HeI 5876
CIII 5826
CIV 5812
CIV 5801
CIII 5696
a
b
c
d
e

of the CIV ion is sufficient justification that the CIII, CIV transitions in the neighbourhood can be operative. The intensity anomaly and the absence of CIII 5696 must be attributed to the absence of the particular selective excitation mechanism.

In Fig. III-4, we see that the identification of CIV 5801-12 is a firm one. In HD 192163 one can even see the distortion on the violet side caused by the displaced CIV absorption. This can be seen on Fig.III-7 where the spectra in this wavelength region of some of the WN stars is shown. Along with these spectra, I have also shown the spectrum of HD 184738, WC8 where the CIV 5801, CIV 5812 and CIII 5826 lines are seen. It is quite conclusive that from the intensity gradient of the profile in the WN stars the maximum of emission is in the vicinity of 5812A, as is to be expected if the origin of the emission is CIV. One other argument is the result of Hallin's (1966 laboratory study of NIV which fails to list any emission lines between 5800Å and 5830 as due to NIV. We then conclude that the CIV identification of the 5801-12 emission is correct.

3.3. The infra-red spectra.

I have listed in Tables III-1 and III-2 the lines measured from tracings of the WN and WC stars ~~respectively for which infra-red stars respectively~~ for which infra-red spectra are available. The spectra of HD 192163 WN6, HD 192103 WC7 and HD 165763 WC6 have a dispersion of 111A/mm and were obtained with the Mount Wilson 60-inch. The spectra of HD 50896 WN5, HD 92740 WN7, HD 93131 WN7, HD 151932 WN7.5 were obtained at Kodaikanal with a dispersion of 250 A/mm. The identifications have been made after marking on the tracing, with an accuracy of 1A, the transitions of NII, NIII, NIV, NV, HeII, HeI, SiIV, CII, CIII, CIV, OII, OIII, OIV, OV. Identifications became a simple task since one could easily compare the excitation aspects for the different stars.

The spectra of NII, NIII, NIV and NV are all fully developed in the stars of the WN sequence, in the near infra-red. The A-band affects the identification of NV, though its presence can be seen in the profile of the A-band. The stars HD 92740 and HD 93131 are near Eta Carina and hence are only about 20° above the horizon when on the meridian. The air mass effects have been,

FIGURE III-9

The infra-red spectrum of HD 50896 WN5,
obtained at Kodaikanal.

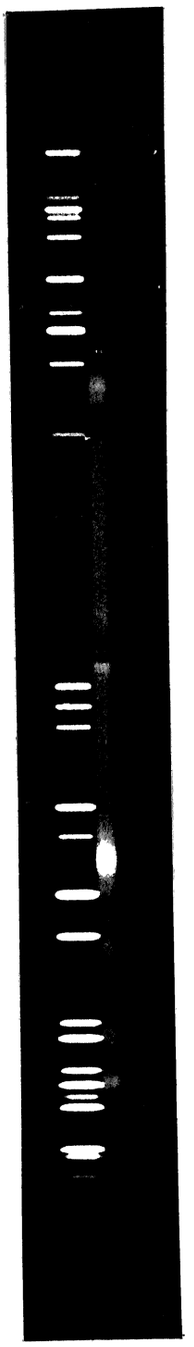

Table III-1

INTENSITY

A.	Origin	HD 90806 vB5	HD 192163 vB6	HD 93131 vB7	HD 92740 vB7	HD 151932 vB7.5
1.	2.	3.	4.	5.	6.	7.
6560	HeII		10			
6596	SII		3			
6610	SII		0-1			
6630 | 6635 |	SII		0			
6643	NIII		0-1			
6668	SiIV	1-2	0-1			
6678	HeI	4	5	2	2-3	2-3
6683	HeII	3-4	4	-	3	2
6701	SiIV	1	0-1		2-3	
6706	SiIV 6701 | NV 6719 |			1-2		
6719	NV	1	0-1		2	
6737	NIII		1			
6767	SiII	0-1				
6810	NII		0-1		0-1	
6820	NII 6810 | NII 6834 |					

Table III-1 ... Contd.

1.	2.	3.	4.	5.	6.	7.
6822	NII 6810 NII 6834	1-2				
6834	NII		0			
6838	NII 6810 6834 6847 6857					2
6847	NII		0			
6855	NII 6847 6857			1-2	3	
6957	NII	1				
6870	NII		1			
6888	NII	0-1	1-2			
6891	HeII	4	3	1		
6942	NII		1			
6945	NII 6942				1	
6965	NIII 6965 NII 6967				1	
6967	NIII 6965 NII 6967 NIII 6976			1		
6970	NIII 6965 NII 6967 NIII 6976	1-2				

Table III-1 ... Contd.

1.	2.	3.	4.	5.	6.	7.
6976	SIII 6965 SII 6967 SII 6976 SIIV 6998 (Weak)		2			
6998	SIIV 6998 SII 7015	2				
7010	SIIV 6998 SII 7015			1		
7015	SII 7014 7015		0-1		1	2-3
7048	SIIV		1-2	2		
7055	SIIV	2				
7065	HeI 7065 SIIV 7068	3	4		1-2	
7066	HeI 7065 SIIV 7068			3		2-3
7109	SIV 7103 7109 7111			5	5	3-4
7116	SIV 7103 7109 7111 7123 7127 SII 7139		10			

Table III-1 ... Contd.

1.	2.		3.	4.	5.	6.	7.
7117	NIV	7103 7109 7111 7123 7127	10				
	NIV	7139					
7123	NIV	7125 7127			4-5		
7127	NIV	7125 7127				5	
7139	NII				1		
7175	HeII	7178			1-2		
7178	HeII	7178	4	5		1	1-2
	NII	7189					
7215	NII		1-2	1	2-3	2	1
7257	NII		1-2	0-1			
7281	HeI		2-3	1		1-2	
7321	NV			0-1			
7350	NIII	7355			2		
7355	NIII		1		1-2		
7360	NIII		7355				1-2
7411	NIII	7404 7411 7418		1-2	2	2	

1	2						
1.	2.		3.	4.	5.	6.	7.
7412	HII	7404 7411 7418					1-2
7418	HII	7404 7411 7418	1				
7582	HIV		3	4	2	1	3
7593	HeII		4	6			1
7618	HV	7616 7619	3	4	1-2		1
7655	SiIV			0-1			1
7667	SiIV				3		
7679	SiIV		1-2	0-1			1
7686	HIII			0-1	2		
7705	HIV		2-3	0-1	2		
7720	SiIV	7719 7724		1		1	1-2
7721	SiIV	7719 7724			2		
7762	HII					0-1	
7815	HeI	7816	1				
7816	HeI			1			

Table 11-1 *** Contd.

Table III-1 ... contd.

1.	2.	3.	4.	5.	6.	7.
7821	SaI 7815			1		
7858	SII	1	1		1-2	
7970	SII 7967 SII 7979	0-1	1			
7985	SIII 7985 7990				0-1	
7990	SIII 7985 7990			1-2		
7994	SIII 8000 8005		1			
8005	SIII 7985 7990 8000 8005 8006	1-2				
8015	SIII 8006 8022 8026			2		
8026	SIII 8022 8026		1-2			
8055	SIII 8022 8026 8040				1	

Table III-1 ... Contd.

1.	2.	3.	4.	5.	6.	7.
8349	HeII 8322 8326 8340 8363	1-2	1			
8348	HeII 8349 8363			1		
8363	HeII		1		1	
8257	HeII	6	4	1	3-4	1-2
8256	HeI	1	1			1
8336	HeII				0-1	
8359	HeI 8362	2				
8362	HeI 8336		1-2			
8443	HeI	2-3				

Table III-2

λ	Origin	HD 165763	HD 192103
6565	HeII	7	10
6583	CII 6578 6582	6	4
6592	CIV	4	5
6609		3-4	2
6640	OII	1	0-1
6678	HeI	2-3	6
6683	HeII 6683 O.5 6685	4	4
6729	CII,CIII 6727 CIII 6731	9	7
6747	CII,CIII 6742 CIII 6744 CII 6751	10	7
6764	CIII 6762	9	
6790	CII 6780 6783 6787 OV 6790 SiIV 6791 6801	5	4
6818	CII 6812 OV 6819 6830	2-3	1
6857	OII 6847 6857 CIII 6863	2-3	2-3
6891	OV 6878 CIII 6881 OII 6885 HeII 6891 OII 6895 CIII 6900 CII 6908 OV 6909	1-2	3

Table III-2 ... Contd.

λ	Origin		HD 165763	HD 192103
6965			1	1
7012	OII	7004	4-5	3
7035	OIV	7032		5
7053	CIII	7037	8	3-4
	CII	7055		
		7046		
		7053		
		7064		
7065	CIV	7062	7	6
	CII	7064		
	HeI	7065		
7120	CII	7112	2	2
		7113		
		7116		
		7119		
		7126		
		7132		
		7134		
7177	CV	7177	2-3	
	HeII	7177		
7178	CV	7177		2-3
	HeII	7178		
7210	CIII	7210	3	4
		7212		
7235	CII	7231	3	3
		7236		
		7237		
7248	OIII	7243	1-2	3
		7250		
7282	HeI	7281	1	1
	OIII	7281		
7295	OIII	7294	0-1	1-2
7322	OIII	7319		1-2
7354	CIII		1-2	1

Table III-2 ... Contd.

λ	Origin		HD 165763	HD 192103
7367	OIII	7366	1-2	1
		7369		
7379	CIV		2-3	4-5
7418	OIV	7419	1-2	2
	OV	7422		
7488	OV	7485	0-1	3
	CIII	7487		
7510	CII	7505		2-3
	OII	7504		
	CII	7509		
	OIV	7511		
	CIII	7514		
	CII	7520		
7586	CIII	7577	4	4
		7578		
		7586		
		7592		
	MgII	7592		
	CIII	7595		
7615	CIII	7613	3-4	4
		7626		
7707	CIII	7707	7-8	4-5
	SV	7708		
7729	CIV	7726	8-9	6-7
		7737		
7785 7800	CIII	7780	1-2	3-4
		7796		
7808	HeI	7816		1-2
7862	CIV	7862	1-2	3-4
		7876		
	CIII	7873		
7951	CIV	7938	1	2
	CIII	7963		
8029	CIII	8021	1-2	2
	CII	8029		
		8038		
		8039		

Table III-2 ... Contd.

A	Origin		HD 165763	HD 192103
8062	CII	8062	1	1-2
		8063		
8165	CIII	8196		3-4
	OV	8205		
8240	CIV	8236		3
	HeII	8237		
8260	CIII	8256		1-2
		8272		
8300	CIII	8297		1-2
	OV	8311		
8341	CIII	8333		2-3
		8342		
		8348		
8360	CIII	8358		2
		8359		
	HeI	8362		

Swings - J. Opt. Soc. America 41, 155, 195?

" A few strong emission features unexplained, especially 7862, 8250, and 8330 A in WC stars; 8005, 8035 A and a complex group near 8240 A in WN stars. A strong emission near 7600 A, which appears common to the hot sequences is not convincingly identified."

FIGURE III-12

HIV 7109-7123 in HD 93206 W5, HD 192163 W6

HD 92740 W7 and HD 151932 W7.5

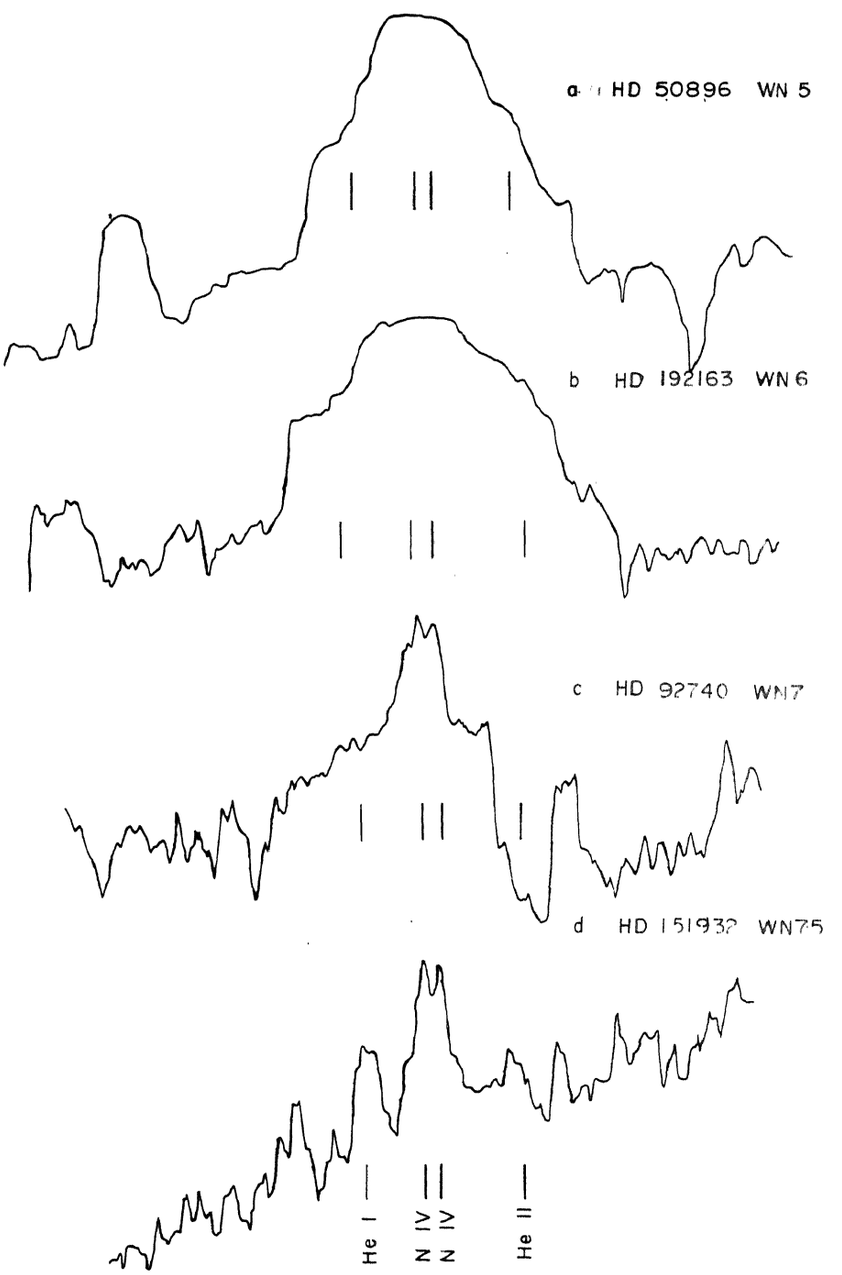
a HD 50896 WN 5
b HD 192163 WN 6
c HD 92740 WN7
d HD 151932 WN7.5
He I
N IV
N IV
He II

Table III -3

WC Sequence

Wave-length	Ion	V in A Units		
		HD 192103 WC7	HD 192641 WC7	HD 165763 WC6
3450		3.6		
3567		7.0	1.5	
3608	CIII	8.3		
3685	CIV	10.7	3.4	
3760	CIII	9.0		
3809	OVI	1.2		
3836	OVI	1.8		
3891	HeI, CIII	11.8		
3929	CIV	13.1	2.5	
3964	HeII, OIII	5.2		
4026	HeI, HeII	4.8		
4068	CII	14.4	1.9	7.7
4100	HeII	7.0	0.7	7.3
4122	CIII, OV	7.9	1.1	6.3
4198	CIII	9.5		

Table III-3 ... Contd.

WC Sequence.

Wave-length	Ion	W in A Units. HD 192103 WC7	HD 192641 WC7	HD 165763 WC6	HD 16523 WC6
4177	CIII	3.9			
4200	HeII	9.8	1.6	4.8	
4229	CIV	7.8	1.4	6.4	
4266	CII	4.4			
4334	HeII, CIV	21.0	6.0	26.2	
4375	CIII	3.6			5.8
4441	CIV	24.3	13.8	27.0	44.9
4471	HeI	3.5			
4511	CIII	2.5			14.8
4545	HeII, CIV	9.4	8.6	14.8	23.5
4606	HeII		21.0	62.6	
4726	CIV, OIV	26.8	11.2	18.3	25.9
4860	H HeII		1.3	13.4	27.5
4933	HeI, OV			14.2	16.9
5696	CIII		41.6	79.1	
5812	CIV		9.4		
6560			20.1	67.7	
6732	CIV, CII		6.0		

Table III - 4

WR Sequence

Wave-length	Ion	W in A Units					
		HD 192163 WN6	HD 193077 WN6	HD 191765 WN7	HD 50896 WN5	HD 165688	HD 4004 WN5
4026	HeI,HeII	5.7		5.4			7.0
4058	NIV	35.2	27.3	27.5		49.1	33.4
4100	NIII,HeII	58.0	11.1	41.7			66.9
4200	HeII,NIII	17.1	4.0	16.0			24.5
4340	HeII,NIII	16.8		11.2	43.4	20.0	37.0
4603	NV	10.4	4.5	6.5		10.4	11.8
4634	NIII	112.5	3.8	50.3	20.5	108.2	98.8
4686	HeII	43.0	13.7	29.0	27.5	46.8	75.1
5406	HeII		4.3	57.2			
5800	CIV			33.4			
5870	HeI			27.1			
6556	HeII		3.2	31.7			

therefore, considerable. In particular this is likely to affect the intensity of HeII 8237. However, these stars were placed on the observing programme because they are of spectral class WN7 and hence their spectra would be of great interest. This has proved to be so for one sees in these spectra the double structure of the $3p^3P - 3d^3D$ multiplet of NIV at 7109A and 7123A. Fig.III-10 shows the changes in overall profile as one goes along the spectral sequence from WN 5 to WN 7.5.

The WC stars show the complete spectrum of CII, CIII, CIV in this region. Also seen are lines due to OII, OIII, OIV and OV. The ionized helium lines are presumably blended but one may be able to say more on this aspect only on the basis of spectra of 20-30 A/mm dispersion.

3.4. Equivalent widths from low dispersion spectra.

These equivalent widths listed in Tables III-3 and III-4 have been measured in order to facilitate an analysis of CIV and HeII, detailed in Chapter IV, for stars for which high dispersion spectra were not available. However, the analysis of Chapter IV finds high dispersion as a necessary pre-requisite. The equivalent widths are therefore of limited utility for temperature studies, but could be used for quantitative spectral classification.

CHAPTER IV

TEMPERATURES OF THE WOLF-RAYET STARS

4.1. Introduction.

We have reviewed briefly in Chapter I, the efforts made by several investigators to derive a representative temperature for the emission characteristics of a Wolf-Rayet star. Numerous uncertainties make such an estimate difficult and hence we are far from a realistic point of view concerning the WR phenomenon. The salient facts we are more or less definite about are the following:

1) The Kinematic state of the atmosphere implies considerable mass motion.

2) An extended atmosphere exists with emission lines formed in the lower levels of the atmosphere. However, the term "lower levels" implies only a relative state with respect to the considerably extended WR atmosphere ($16R_\odot$ for V444 Cygni) and hence the characteristics of non-local thermodynamic equilibrium would necessarily apply.

3) There is increasing evidence that the higher layers of the atmosphere are responsible for the higher

excitation lines. As seen in Chapter III, the velocities would then decrease with height.

4) Selective processes have to be invoked to explain the presence of certain lines when others of the same ion cannot be easily seen.

The original Beals postulate of the Zanstra-Menzel mechanism of photoionization with subsequent recombination is an over simplified case of the actual situation. The Wolf-Rayet stars are high temperature objects and necessarily may have an intense UV spectrum. However, the first rocket evaluations of the UV region of γ Velorum show that while there seems an increased intensity at 1600A compared to that at 2000A, the flux measured, falls short of the flux expected of a model atmosphere of Te = 28470 and log g = 3.8. Hence, the Wolf-Rayet star may not necessarily be as rich in shortwave radiation as we had expected it to be earlier.

In view of the extreme predominance of mass motions, it is also obvious that collision effects will play a significant role. We are still not clear about the nature of the atmospheric support. If as Thomas (1949) pointed out, microscopic motion alone exists in the form

of a Te > Tr, where Te and Tr are the Kinetic and radiation temperatures respectively, then a positive excitation gradient follows as a direct consequence similar to the solar chromosphere and corona. We have increasing evidence to show that the higher excitation lines originate further from the star's "photosphere". As such the picture of pure ionization and subsequent recombination alone, by virtue of radiation from an ultrahot core is obviously over simplified.

The derivation of temperatures representative of the populations of the excited levels, has the characteristic of being non-committal regarding the nature of the excitation. Aller (1943) pioneered in this approach. But his selection of emission lines was confined to every single feature for which line strengths could be computed and which could have an intensity measure from the low dispersion slitless spectra. It is increasingly obvious as has been seen in Chapter III that the profile of a Wolf-Rayet emission line is inevitably a summation of blends, and that great care is necessary to select the lines for study in any attempt to infer temperatures from line ratios. In fact, judging from the high dispersion spectra that I have studied, I consider that there are very few lines, actually,

that can come under such a classification of being free of blends.

A second difficulty that is apparent in Aller's study is that his results have been affected by the absence of thermodynamic equilibrium in the atmosphere. Thomas has shown (1949) that Aller's variation of Ni He with ionization may not indicate stratification in the WR atmosphere, but could also be due to departures from thermodynamic equilibrium. Hence, in choosing any technique of excitation temperature determination in the WR atmosphere, one needs to be careful to avoid abnormal population effects of the levels caused by deviations from thermodynamic equilibrium.

Such an approach was first employed by Beppu (1950) with high dispersion spectra. Beppu's work was greatly facilitated by the identification by Edlen (1936) of the hydrogenic transitions of CIV. The use of these CIV transitions in a determination of the state of excitation of the CIV ions had two attractive aspects. Firstly one could employ the Einstein $A_{n'n}$ coefficients calculated already for hydrogen. Secondly the CIV transitions identified in the WR stars originate from transitions between

the higher levels. Rappu used the (7-n) series, more especially the transitions 4229A (7-12), 3567A (7-15) and 3451A (7-16). In discussions of deviations from thermodynamic equilibrium, one considers the ratio b_n between the actual population of the n^{th} level of an ion and the population under conditions of thermodynamic equilibrium. In studies of the excitation temperatures, these b_n parameters necessarily play a role and if we are to derive any values that represent a situation close to reality, we have to account for them satisfactorily. This is the main feature of Rappu's analysis that was confined to just two stars. We follow a similar line of reasoning and extend these results considerably in this chapter.

4.2. The method of temperature determination.

Let us consider two emission lines that are the result of transitions $n' \rightarrow n$ and $n'' \rightarrow n$. We then have

$$\frac{I_{n'n}}{I_{n''n}} = \frac{N_{n'} A_{n'n} h\nu_{n'n}}{N_{n''} A_{n''n} h\nu_{n''n}}$$

where $N_{n'}$ and $N_{n''}$ are the populations of levels n' and n'' respectively and $A_{n'n}$ the Einstein coefficient for spontaneous transition $n' \rightarrow n$.

Since,

$$N_n = b_n N_i N_e \frac{h^3}{(2\pi m k T_e)^{3/2}} \frac{\omega_n}{2\omega_i} \exp\left(\frac{x_n - x_i}{kT}\right)$$

we have

$$T = \frac{(\nu_{n'} - \nu_{n''})\frac{h}{k}}{\ln\left(\frac{I_{n'n}}{I_{n''n}}\right) - \ln\left(\frac{A_{n'n}\,\nu_{n'}\,\omega_{n'}}{A_{n''n}\,\nu_{n''}\,\omega_{n''}}\right) - \ln\left(\frac{b_{n'}}{b_{n''}}\right)}$$

We identify T, the excitation temperature, with the kinetic temperature T_e in the limiting case. The temperature determinations call for a knowledge of the b_n ratios. However, the advantage of using the hydrogenic transitions of CIV is that the b_n ratio can be taken as 1. Thomas (1949b) and Chamberlain (1953) have shown that for large values of n, $b_n \to 1$. Also, b_n for any n, decreases rapidly with large nuclear charge. Hence, if we consider any transitions involving n greater than 5 and for an ion with larger nuclear charge than hydrogen, the ratio $\frac{b_{n'}}{b_{n''}}$ is obviously 1. We can then derive safely by simple astrophysical formulae the temperature parameter just by a judicious choice of lines.

One measures the intensity of the emission line conventionally in terms of the intensity of the continuum.

This has a physical significance in measures of the equivalent widths of absorption lines. However, in the case of emission lines one can compare the differences between the energies radiated in two emission lines only after one can normalize the two continua against which the emission intensity is measured. Rappu's analysis of the CIV hydrogenic transitions needs refinement in this specific aspect. Rappu could not make these corrections with certainty because until early this year, accurate spectrophotometry of the continuum of the WR stars did not exist in the literature. Recently a significant contribution to this problem has been the painstaking work of Kuhi (1966) who measured the intensities photoelectrically at selected locations in the spectra that were free of emission lines. A factor that has to be compensated for, is the correction to interstellar reddening. Kuhi has done this on the basis of our knowledge of this feature today.

4.3. The Temperatures of stars of the WC sequence.

In Table IV-1, I give the measured equivalent widths of those CIV hydrogenic transitions in the WR carbon sequence stars that are relatively free of blends. Kuhi has given unreddened fluxes for HD 165763, HD 192641 and

Table IV-1

The emission line intensities in the WC sequence.

		HD 165763 WC5			HD 192641 WC7			HD 192103 WC7			HD 184738 WC8		
	Transition	W(A)	Kuhi factor	I	W(A)	Kuhi factor	I	W(A)	Kuhi factor	I	W(A)	Combin. corrn. 15000°	I
5470	7 - 10	33.78	1.0	33.78	10.57	1.0	10.57	19.5	1.0	19.5	-	1.0	-
4229	7 - 12	7.00	1.368	9.58	2.49	1.368	3.409	9.72	1.459	14.18	3.84	1.192	4.58
3889	6 - 9	18.35	1.528	28.00	6.204	1.614	10.013	16.43	1.614	26.52			
3567	7 - 15	3.52	1.614	5.68	1.32	1.592	2.10	5.6	1.542	8.64	2.61	1.253	3.27
3450	7 - 16	-	-	-	-	-	-	4.57	1.644	7.51	2.25	1.256	2.83

HD 192103. The intensities I of the emission lines are the rectified ones after applying the Kuhi correction factors for each star. These are also given for each star and represent interpolated values from a plot of the continuum fluxes measured by him. Kuhi has no determination of the energy distribution in HD 184738, the nucleus of Campbell's hydrogen envelope star, presumably because of its faintness. I have, therefore, used correction factors appropriate to black-body radiation at 15000°K. The basis of this choice is to some extent arbitrary. Firstly, the colour temperatures of Wolf-Rayet stars, as determined in the 4000-5000A region are much lower than their excitation temperatures, almost by a factor two. Beppu's earlier estimate of temperature for this star was 28000°. Also the stars HD 192103 and HD 192641 have estimates of the colour temperatures by Kuhi of the order of 20,000° in the 5000A region. Hence my estimate of 15000° for HD 184738 is likely to represent an upper limit of colour temperature.

The atomic parameters utilized are given below:

	n-n'	$A_{nn'}$ for hydrogen	ν
5470	7-10	30.8×10^3	$.5481 \times 10^{15}$
4229	7-12	12.4×10^3	$.7089 \times 10^{15}$
3889	6-9	70.3×10^3	$.8125 \times 10^{15}$
3567	7-15	3.512×10^3	$.8405 \times 10^{15}$
3450	7-16	2.463×10^3	$.8690 \times 10^{15}$

Table IV-2 gives the temperatures obtained for the different line ratios. The mean values together with the probable errors are also given. A few features need discussion. In HD 192103, the values of temperature given by line ratios involving 3687A are conspicuously low. This is because, the intensity of 3687A is very low. The value measured from the spectrum is low by a factor of 1.4, the value of intensity of 3687A needs to be 36.2 instead of 26.5 which is the measured value. An error of this magnitude cannot be made in the photometry. Clearly the cause is elsewhere and the immediate suspicion is of weak Balmer line-absorption that suppresses the true intensity. The profile of this line in HD 192103 is distinctly different from that seen in the other carbon stars, thus strengthening the argument. 3687A has a line

TABLE IV-2

Temperatures of the WC stars

Line Ratio	Temperatures			
	HD 165763	HD 192641	HD 192103	HD 184738
4229/5470			38298° *	
3687/5470			14280°	
3267/5470			40157° *	
3450/5470			38354° *	
3687/4229	61154°	62497°	20391°	
3267/4229	51847°	39518°	42583° *	20543°
3450/4229			38104° *	21683°
3267/3687	57733°	52664°	24363°	
3450/3687			24355°	
3450/3267			26409° *	29675°
Mean	56911° ± 2600	51560° ± 6500	37318° ± 3400	23967° ± 4100

The mean temperature derived for HD 192103 is from the values denoted by an asterisk.

intensity that yields satisfactory temperatures in the other two stars in which it can be measured.

The intensity of 5470Å also calls for comment. This line has been measured on the spectra of HD 165763, HD 192641 and HD 192103. Only in the case of HD 192103 does it give physically significant temperatures. In both the other stars its intensity is larger than need be to give a temperature in agreement with the other line ratios. I believe, that this may be due to blending with OV 5474. This problem would exist only in the high temperature stars and hence we find it absent in HD 192103.

Our study of the four stars shows a temperature variation with spectral class as is to be expected. The temperature of HD 184738 may be raised by a thousand degrees or two when its continuum fluxes are better determined.

4.d. The temperatures of stars of the WN sequence.

We are not as fortunately placed in the case of the nitrogen sequence Wolf-Rayet stars as we have been for the WC sequence. The use of the CIV hydrogenic transitions eliminated the need of new determinations of transition probabilities. It also eliminated the problem of lack of

thermodynamic equilibrium, because, the transitions used, originated from the higher levels. An approach of this type could be used for the WN stars by employing hydrogenic transitions of NV. Edlen (1956) has listed the ones that may be expected to be present in the region of the spectrum accessible to ground-based telescopes. However, these are two weak to be identified with certainty and also fall in regions where they are likely to be heavily blended with the lines of the other ions.

We, therefore, have to depend on the helium series of emission lines for any information on these stars using the reasoning that we applied earlier. Two series are available; the (4-n) and (5-n) series are seen on the spectra that one usually gets in the range 4000-9000A. The difficulties that we are likely to face are twofold. First there can be possible minor line contribution to the alternate members of the Pickering series. Secondly, we have no means of determining the b_n ratio.

In the following discussion, I shall use intensity data only of HD 192163, since among the high dispersion spectra available for this study, it has the strongest lines that not only improve photometric accuracy but also

minimize blending possibilities by virtue of a narrower line-width. Intensity measures made of the 4-n series have been confined to 6560A (4-6), 5411A (4-7), 4860A (4-8), 4542A (4-9), 4340A (4-10) and 4200A (4-11). These are listed below along with the Kuhi continuum corrections.

	Transition.	V(A)	Kuhi factor	I
6560	4 - 6	161.3	0.624	100.6
5411	4 - 7	75.0	0.822	61.6
4860	4 - 8	46.9	1.000	46.9
4542	4 - 9	32.0	1.086	34.7
4340	4 -10	23.4	1.148	26.9
4200	4 -11	17.2	1.225	21.1

On the assumption that the b_n ratios of the transitions are unity we get for the different line ratios the following values of temperature.

HD 192163	
Line ratio.	Temperature
$\frac{4861}{5411}$	27200
$\frac{4542}{5411}$	33036
$\frac{4340}{5411}$	31157
$\frac{4200}{5411}$	30639
$\frac{4542}{4861}$	48067
$\frac{4340}{4861}$	35397
$\frac{4200}{4861}$	33335
$\frac{4340}{4542}$	25958
$\frac{4200}{4542}$	26805
Mean = 32397 ± 4200°	

A temperature cannot be obtained from the $\frac{5411}{6560}$ ratio. Values of temperature obtained from the $\frac{4861}{6560}$, $\frac{4342}{6560}$, $\frac{4200}{6560}$ ratios are 161000°, 75600° and 66000° on the assumption of a b_n ratio of unit. If we assume on the basis of the value obtained from any

$\frac{4542}{5411}$ or $\frac{4340}{5411}$ that the temperature is 33000° we can reverse the argument and get at the b_n ratios. These turnout to be the following:

6560/5411	6560/4860	6560/4542	6560/4340
b_6/b_7	b_6/b_8	b_6/b_9	b_6/b_{10}
1.226	1.203	1.227	1.212
	5411/4860	5411/4542	5411/4340
	b_7/b_8	b_7/b_9	b_7/b_{10}
	0.9804	1.0000	0.9881
		4860/4542	4860/4340
		b_8/b_9	b_8/b_{10}
		1.020	1.007
			4542/4340
			b_9/b_{10}
			.9872

The b_n ratios obtained for 6563A are all larger than unity. If the b_n ratio were unity and the temperature is 33000° then the intensity of the 6560A emission line needs to be 82.7 instead of 100.6. An error of 18 per cent cannot be admitted in the photometry, even if it is by a photographic technique. Hence, we either accept the deviation from unity of the b_n ratio or explain the

enhanced intensity of 6560A by other means.

If the b_n ratio is not unity then we should have $\frac{b_6}{b_n}$ $_{n>7}$ increase as n takes on larger values. Instead, we see that the b_6/b_n ratio is almost constant with b_6/b_7 and b_6/b_9 having larger values than b_6/b_8 and b_6/b_{10}. This indicates a contamination in the intensity affecting 6560A, 4860A and 4340A. The conclusion seems to be that we have here a case of Balmer contribution affecting the intensities of these lines. In other words the intensities of 6560A, 4860A, 4340A are higher than would be expected if they were purely of the helium flickering series. The b_n ratios b_7/b_8, b_7/b_9, b_7/b_{10} indicate that this reasoning has validity since b_7/b_8 and b_7/b_{10} are less than unity while b_7/b_9 is unity. Clearly the hydrogen contribution is obvious but the amount of hydrogen emission present is little. Perhaps, these objects are really hydrogen deficient.

We have seen that in HD 192163, the b_7/b_9 ratio of 4542A (4-9) is unity. Hence, if we can use the (5-9) series we should be more justified in assuming the b_n ratio to be unity. The lines identified with certainty of this

Table IV - 3

Intensity ratio $I_{5-n'}/I_{6406A}$ for different temperatures

n-n'	(A)	Temperature				
		20000°K	30000°K	40000°K	50000°K	60000°K
5-16	6310	0.8364	0.8318	0.8292	0.8279	0.8269
5-15 (Unit)	6406	1.0000	1.0000	1.0000	1.0000	1.0000
5-14	6527	1.1852	1.1941	1.1981	1.2005	1.2024
5-13	6683	1.4508	1.4733	1.4836	1.4906	1.4951
5-12	6931	1.7606	1.8073	1.8312	1.8457	1.8556
5-11	7177	2.1896	2.2784	2.3249	2.3524	2.3714
5- 9	8236	3.4916	3.7936	3.9557	4.0552	4.1237

series are 6519A (5-16), 6406A (5-15), 6527A (5-14), 6683A (5-13), 6891A (5-12), 7177A (5-11) and 8236A (5-9). Many of these lines are blended, though from the results of Chapter III, it is seen that 8236A, 7177A and 6406A can be extricated free of the blends. The temperature evaluation needs photometry on higher dispersion spectra than what I had available in the infra-red. I have, therefore, computed the line ratios necessary for different temperatures, in terms of the intensity of 6406A, and for a b_n ratio unity. These are in Table IV-3. It is obvious that to determine a temperature with an accuracy of 5000° in the range 25000°-35000°, the photometry will have to be done to better than one per cent, if one uses high dispersion material available with the spectral sensitivity of the 103a-F emulsion. However, if one uses the line ratio 8236A/6406A, this comes well within the accuracy of photographic photometry. It will be well worthwhile to attempt the spectrophotometry of HD 192163 at a dispersion of 20A/mm. The utility of the (5-n) series cannot be exploited today by observations shortward of 6800A.

CHAPTER V

WOLF-RAYET BINARIES

5.1. Introduction.

Most of the present day information that we have regarding the fundamental parameters of the stars originate from comprehensive investigations of the binary systems. The masses and the radii of stars are the basic data determined by prolonged and systematic investigations of visual and eclipsing binaries. Perhaps, the only physical parameter pertaining to the density distribution of matter in the stellar interior can be studied by an investigation of the phenomenon of apsidal motion in binary systems.

The Wolf-Rayet binary systems are no exception. Most of our information pertaining to the Wolf-Rayet atmosphere has originated from studies made on one or two binary systems with a Wolf-Rayet component. At the top of any list which indicates the contribution of binary systems to an understanding of the Wolf-Rayet phenomenon comes HD 193576 which has been the most exhaustively studied binary system. This system was discovered to be a spectroscopic binary by Wilson (1939). Gaposchkin (1941) subsequently showed that the star is also an eclipsing variable

and precise light curves for this system have been obtained photoelectrically by the Krons and Hiltner. The discovery of HD 193576 as a spectroscopic binary prompted an exhaustive search of other Wolf-Rayet stars for binary properties. Pioneering in these efforts have been Wilson at Mount Wilson and Hiltner at the McDonald Observatory and most of the binary systems that we know today with Wolf-Rayet components have been discovered by these two individuals. Many of these binary systems have spectroscopic orbits available as a result of measurement of HeII 4686 or any of the other emission lines. The system of CQ Cephei is another Wolf-Rayet binary system which has admirably supplemented the information supplied by HD 193576. This system was discovered by Hiltner and a preliminary orbit was calculated as early as 1944. Later Hiltner (1950) carried through a remarkable photoelectric experiment whereby he isolated the emission band 4686A and compared its intensity over the entire orbital cycle with that of the neighbouring continuum. Hiltner came to the amazing conclusion that HeII 4686 increased in intensity at primary and secondary minima and had a minimum of intensities at elongations. There is as yet no satisfactory explanation available for this behaviour. In the last decade spectrophotometric measures on both

V_{444} Cygni and CX Cephei have been made by a few investigators. Sanyu and Sinvhal (1959) have photoelectrically measured the variation of HeII 5411 and established that the variation is similar to that observed for HeII 4686 by Wiltner. The choice of HeII 5411 was made in an effort to search for anomalous excitation possibilities of HeII 4686. The fact that the member of the Pickering series also shows the same behaviour indicates that all the helium lines essentially have an enhanced intensity at primary and secondary minima.

Sanyu and Sinvhal have also shown that 4861A of HeII has a peculiar light variation when compared to 5411A of HeII. They explain this in terms of the fact that the emission line at 4861A is seriously affected by superposed absorption and hence 4861A does not really indicate a pattern of variation of the ionized helium lines.

Wilson (1940) had shown that the 4686A line in V_{444} Cygni did not suffer much of an eclipse when occulted by the O companion. Sanyu and Sinvhal (1955) studied this phenomenon photographically by plotting the equivalent widths against phase for some of the observed emission

lines. They have shown that the lines HeII 4686 and NIV 4058 have negligible eclipse effects at primary minimum. However, HeII 4860 and NV 4603 have minimum intensities at primary minimum and this is correlated with the presence of violet absorption edges or the effect of the companion's hydrogen absorption spectrum. More recently Kuhi (1965) has scanned the spectrum of V_{444} Cygni photoelectrically from 3400A to 11000A with a spectrum scanner used as a narrow band photometer. He finds that in the process of the eclipse of the Wolf-Rayet component by the O star, the lines of ionised He, NIII and NIV do not share in the eclipse but actually undergo a brightening. This behaviour is most conspicuously seen in 4686A. On the other hand, the line identified as CIV 5808 decreases in intensity as the Wolf-Rayet star is eclipsed by the O star. Apparently a similar behaviour is indicated in the case of the HeI line at 10830A. The interesting feature is that the CIV line goes into eclipse two hours before the neutral helium line does.

Most of the other binary systems with a Wolf-Rayet star as one of the components have shown a wide range of line profile and intensity variations. The Wolf-Rayet atmosphere has such kinematical activity present in

it and it is natural to expect that a reproducibility of these features would perhaps be not easily possible. In the case of CQ Cephei, Hiltner has shown that the intensities of HeII 4686 apart from the change experienced during a cycle, undergo violent fluctuations from day to day. This has been pointed out by several authors who have studied Wolf-Rayet spectra. Struve (1944) showed that the intensities changed from night to night in HD 151932, a star which is a member of the cluster NGC 6231. Bappu (1951) showed that some of these spectral variations are present in HD 191765, a Wolf-Rayet star in Cygnus. It is, therefore, necessary to study in detail, line profile changes and line intensity changes along with systematic efforts to determine the orbital parameters of most of the binary systems.

The Wolf-Rayet binary with the shortest period happens to be CQ Cephei. V_{444} Cygni has a period of 4.21233 days. Considering the fact that the emission lines originate in an extended atmosphere, it is likely that tidal distortions in a close binary system may seriously upset any possible conjecture of the exact nature of the kinematical conditions in the Wolf-Rayet atmosphere. It is, therefore, necessary to extend the studies of

of these system to those that have a good separation of the components and hence larger periods of orbital revolution. While it is generally recognized that a substantial number of Wolf-Rayet stars have early type companions, nevertheless, we do suffer from a rarity of this species. HD 168206 (CV Serpentis) has a period of 29 days. HD 190918 has a period of 35 days but unfortunately the smallness in the amplitude and the mass function indicates that it is unlikely to be an eclipsing system. Until the discovery of γ_2-Velorum, HD 168206 seemed to be the only system with a long enough period and value of inclination. γ_2-Velorum, of which we shall have more to say later, was assumed to have a period of 16 days (Sapozhnikov 1959). However, our studies show that this values needs a five-fold enhancement. Other than HD 190918, γ_2-Velorum has the largest value of period in a Wolf-Rayet binary system known today. However, the parameters derived for it, indicate that the orbital inclination is such as to make it a possible eclipsing binary. Besides, Sapozhnikov has earlier noticed a light variation in this system which could be easily associated with the eclipsing properties of the star. Here is a system that is a very promising candidate for a detailed photoelectric study by every possible technique because its brightness is such that it

is easily accessible even for a small telescope.

A very interesting feature of the spectroscopic orbital parameters of the Wolf-Rayet binary systems is the shift to positive velocities of the γ-axis. In the Wolf-Rayet stars, this was first detected by Wilson in V_{444} Cygni and subsequent studies by both Miltner and Wilson have shown that the HeII 4686 line in all cases has a red shift of the order of about 150 Km. when compared to a similar γ-axis value for the system derived from the other lines. Table (V-1) lists the spectroscopic binaries found so far, and along with other data, it gives the values of γ-axis as obtained from the other lines. This summary strikingly shows the red shift of 4686A with respect to the values obtained from other lines. It is interesting to consider that a similar characteristic is seen in some of the more massive star systems. 29 Canis Majoris, for instance, the components of which are O stars, shows this feature. The longer wavelength of 4686A seems to be a general characteristic of not only the Wolf-Rayet stars, but also of some of the nucleus of the planetary nebulae. Campbell's hydrogen envelope star has a wavelength of 4686.55 which corresponds to a red shift of +55.66 Km/sec. In general, the wavelength of 4686A as measured in Wolf-Rayet spectra has

Table V-1

Wolf-Rayet Binaries

HD	Spectral Class	K Km/sec.	Period days	γ axis of 4686	γ axis of emission/absorption
[illegible][1]	[illegible]5	550	2.13		
+40°4220	[illegible]	135	6.60		
152270	[illegible]7	160	8.82	+130 −x	x absorption − 44
168206[2]	[illegible]7	165	29.6	+200	+ 45
186943	[illegible]5	235	9.5534	+115	+ 15
192918	[illegible]5	38	55	+ 80	− 21.8
193576[3]	[illegible]6	308	4.21	+ 70	− 40
193928	[illegible]6	130	21.6	+ 59	−130
214419[4]	[illegible]6	295	1.64	+137	− 75

1 Eclipsing binary CX Cephei
2 Eclipsing binary CV Serpentis
3 Eclipsing binary V444 Cygni
4 Eclipsing binary CQ Cephei

a systematic difference from a corresponding laboratory measurement. This may be a vital clue to the kinematics of the Wolf-Rayet envelope.

The red-shift has been interpreted by Struve, Miltner and others as indicative of violet absorption that effectively changes the center of gravity of emission lines. In some cases where strong violet absorption existed such an explanation is correct. But, in the case of 4686A no violet absorption is usually detected with certainty and it is rather difficult to put forward the same explanation for the red-shift of 4686A.

It will be seen that the field of study pertaining to binary systems with Wolf-Rayet components is likely to be a very profitable one. The measurement of radial velocities, detailed spectrophotometry of precision in the light of different lines of all Wolf-Rayet binary systems and of selected eclipsing systems that have different orbital periods, are essentially observational data that will furnish many a clue to the nature of the Wolf-Rayet atmosphere. It is this approach that prompted my study of five Wolf-Rayet binaries, the results of which are reported in this chapter.

PLATE I

The spectrum of γ_2-Velorum

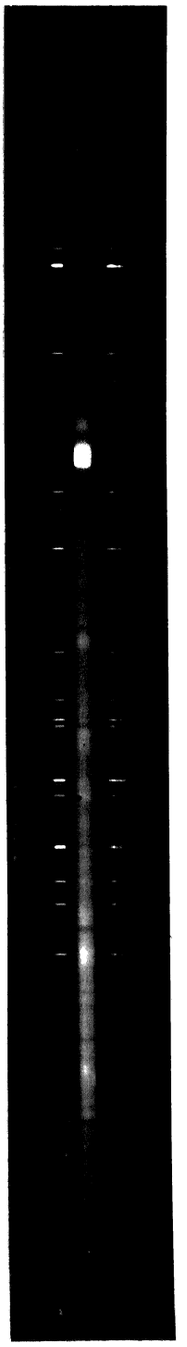

PLATE II

The spectra of (a) HD 193576 (b) 193928

(c) HD 211853


a
b
c

5.2. The Wolf-Rayet binary γ^2-Velorum.

The spectrum of γ^2-Velorum has long been known to be composite and variable. The spectrum has been described by Cannon (1901) and Wormsell (1916) from objective prism spectra obtained at Arequipa and the Cape respectively. Perrine (1918) first announced the striking spectral variations of both emission and absorption lines. These have been confirmed in a recent study by Smith (1955) who found that the variations were both short-lived and infrequent. Smith also gives a list of wavelengths of both emission and absorption lines as seen on high contrast low dispersion slit spectra obtained by him with the 60-inch reflector at Boyden station. Sahade (1955) announced that radial velocities measured indicated the star to be a binary that exhibits the spectra of two components, with most of the absorption lines associated with a companion of spectral type B. From the few measures that Sahade had at his disposal a period of the order of 24 days was indicated. Gaposchkin (1959) estimated from radial velocities obtained at Mount Stromlo that a tentative period of 16.2 days could be assigned for the orbital motion. His visual estimates indicated light variability with a small range thus

holding out promise of the system being an eclipsing binary.

The brightness of γ_2-Velorum enables the examination of its spectrum in the far ultraviolet by the techniques of rocket spectroscopy. Stecher and Milligan (1962) from objective grating spectra find the energy distribution from 1600A to 3000A to depart substantially from that of a black body at 30000°K. Aller and Faulkner (1964) have determined photoelectrically the energy distribution in the domain 3400 - 5900A. On the basis of measures of monochromatic magnitudes made at Mount Stromlo on five nights they estimate a colour temperature of 32000°K. One needs to recognise in such continuum flux measurements, the role played by the continuum of the O star.

γ_2-Velorum is the brighter star of the optical double γ-Velorum. The fainter component is of WC type 8:IV and is 2.4 mag. fainter than γ_2-Velorum. The absolute magnitude of the Wolf-Rayet star is M_V= -5.6, if a value of M_V = -3.3 is ascribed to γ_1-Velorum on the basis of the MK classification type assigned. One assumes also, following Schleisinger and Jenkins (1940)

that both γ_1, γ_2-Velorum form a proper motion system. This Wolf-Rayet star along with Zeta Puppis probably excites the Gum nebula, which is the largest HII region known in our galaxy.

The number of Wolf-Rayet binary systems that exhibit the spectra of both components is very small. Of these, the best studied is V_{444} Cygni which has a Wolf-Rayet star of the nitrogen sequence along with an early type star. Sahade has shown that the absorption lines indicative of an early type star are seen on the spectra of γ_2-Velorum. Since γ_2-Velorum contains a WC7 star with an early type companion, presumably an O star, it furnishes the possibility of determination of a reliable mass for the WC7 star and an O star, if the orbital parameters can be derived in detail and also if the orbital plane is favourably inclined for detection of an eclipse. Only one other system HD 168206 (WC7+O) has a preliminary spectroscopic orbit available for both the components. It, therefore, is of great interest to study the system of γ_2-Velorum in detail and increase our information of masses of these early stars.

Spectra of this star were obtained at Kodaikanal over the period February-April, 1965 and November-April,

1966. A total of 147 spectrograms obtained with the cassegrain grating spectrograph attached to the 50cm Kodaikanal reflector have been utilized in this study. The velocity measures of the emission lines were confined to those of HeII 4686, CIV 4441 and the band at 4652A originating essentially from CIII. The velocity curves defined by these measures yield the orbital parameters of the Wolf-Rayet star. The velocity measures of the O component depend entirely on the measures of 4340 H$_\gamma$, 4100 H$_\delta$, with occasional measures on HeII 4200 and HeI 4471. All these measures are listed in Table V-2. The previous investigators of this system have reported an appreciable scatter in the velocity measures. We find this to be prevalent even in our measures. The emission band 4652A was, therefore measured, more to establish the trend of radial velocity variation, by the use of an easily measurable line, than to utilize it for a study of the physical characteristics of the system.

The long series of observations from November 1965 to April 1966 gave a period of 78.5 days. Fig.(V-1) is a plot of the velocities of 4652A covering the period of observation of this system at Kodaikanal. In

$\overline{V}$-2

Table ~~III-1~~

Veloci[illegible] [illegible] 68273

Plate	JD of observation (2438000.0)	Phase (in period)	Velocities in Km/Sec. 4686e	4652e	4441e	4340a	4200a	4101a
1.	2.	3.	4.	5.	6.	7.	8.	9.
27	2438817.20	0.04	+ 97.9	+ 57.4	—	− 31.1	—	—
33a	818.17	0.05	+154.2	+ 73.5	—	− 65.6	− 15.7	− 21.9
33b	818.18	0.05	+ 41.6	+ 09.0	−150.5	− 13.8	−104.9	− 58.5
40	820.12	0.07	+149.7	+ 49.0	—	+ 4.1	− 46.4	− 90.6
45	820.27	0.08	+ 88.9	+ 16.8	−108.7	− 22.8	—	+ 32.9
49	821.25	0.09	+121.6	− 7.7	—	—	—	− 31.4
54	822.28	0.09	+ 65.3	0.0	−108.7	− 40.1	− 34.3	− 59.2
55	824.25	0.09	− 70.4	—	−150.5	—	—	—
58	825.29	0.14	+ 40.3	+ 8.4	−142.4	+ 03.5	—	+ 32.9
65	827.22	0.17	+ 09.0	− 32.2	—	− 57.3	—	− 03.7
66	827.27	0.17	− 39.7	− 56.8	−201.8	+ 38.0	—	− 22.7
69	828.25	0.18	+ 9.0	− 36.7	−134.3	+ 38.0	+ 47.0	—
73	830.12	0.20	− 41.0	0.0	—	+ 29.0	+ 02.1	−132.3
76	831.24	0.22	+ 56.9	− 07.7	− 49.3	+ 72.5	—	− 22.7
80	834.18	0.25	−105.7	− 57.4	− 219.4	− 05.5	—	+ 05.1
82	834.24	0.25	+ 15.4	+ 89.0	−236.3	− 40.1	+ 20.0	− 13.2
87	837.13	0.29	− 31.4	−129.6	− 58.1	+ 72.5	+ 2.1	+ 69.4
92a	843.10	0.37	+ 01.0	+ 33.0	+ 35.0	+ 11.7	—	− 99.2
92b	843.13	0.37	+ 09.0	+ 08.4	−253.0	− 57.3	—	− 22.7
95	851.22	0.47	+ 56.9	+ 97.4	−108.7	− 22.8	+ 28.6	− 29.2
99	858.19	0.56	+121.6	+ 40.0	− 41.2	+ 03.4	—	− 77.5
100	859.17	0.57	+ 72.9	+ 40.6	+ 27.0	− 22.8	—	− 49.7

V-2

Table ~~III~~-1 - continued.

1.	2.	3.	4.	5.	6.	7.	8.	9.
150	2439083.34	0.43	- 47.4	- 15.5	+168.1	+ 03.5	+ 47.1	- 31.4
151	083.38	0.43	+ 17.3	+ 16.8	-133.7	- 13.8	—	-141.1
152	083.41	0.43	- 25.0	+ 09.0	-218.7	- 57.3	+ 47.1	- 68.0
153	084.40	0.44	+165.9	+ 60.6	- 06.7	+ 64.2	—	+ 51.9
156	085.37	0.45	- 47.3	+ 32.9	-201.8	—	+ 95.7	—
158	086.31	0.47	+121.6	- 56.1	—	- 57.3	—	- 95.8
159	086.35	0.47	+ 09.0	0.0	-168.1	- 57.3	+109.9	- 95.8
161	086.44	0.47	- 23.0	- 47.7	- 08.0	- 04.8	+127.8	- 21.9
165	087.36	0.48	+ 25.6	+ 09.0	- 66.2	+ 03.5	+101.4	- 31.4
167	108.29	0.75	+121.5	+146.5	+120.2	+ 11.7	—	- 77.5
168	108.29	0.75	+177.9	+194.8	+ 94.5	+ 11.7	—	-141.8
169	108.34	0.75	+153.6	+178.6	+ 18.2	- 40.0	+ 38.6	- 87.0
171	111.35	0.78	+105.6	+146.4	+ 69.5	—	—	-114.0
176	112.24	0.80	+225.9	+178.6	- 24.5	+ 11.7	+ 10.7	- 59.2
177	112.27	0.80	+193.9	+146.4	—	- 22.8	+ 2.1	-151.3
181	112.32	0.80	+145.2	+130.3	+171.5	-109.8	+ 15.0	-132.3
185	119.25	0.89	+202.2	+187.0	+120.9	- 82.9	—	+ 5.9
186	119.26	0.89	+154.2	+219.3	+171.5	- 4.6	+ 29.3	- 98.5
187	119.28	0.89	+129.9	+154.8	+180.8	- 82.9	+ 42.1	-114.3
193	120.26	0.90	+238.8	+211.5	+138.9	- 40.1	+ 29.3	-114.0

V-2

Table ~~III-1~~ - continued.

1.	2.	3.	4.	5.	6.	7.	8.	9.
194a	2439 120.29	0.90	+242.5	+195.4	+154.6	-118.1	—	-178.3
194b	120.31	0.90	+213.5	+179.3	—	- 22.1	+ 20.7	- 68.0
197	124.27	0.95	+113.9	+ 81.9	- 31.7	- 48.4	—	—
198a	124.30	0.95	+121.6	+ 49.0	- 57.4	- 57.4	+ 82.1	-205.4
198b	124.32	0.95	—	+ 57.4	+104.0	- 57.3	—	-168.8
198c	124.33	0.95	—	+154.8	-184.9	- 31.1	—	-196.6
202	125.28	0.96	+226.5	+138.7	- 66.2	-126.4	- 60.0	-150.6
203a	125.34	0.96	—	+130.3	+ 61.4	- 31.1	+ 20.7	+ 42.4
208	134.26	0.08	- 71.0	-153.5	-185.0	- 65.6	—	-104.5
213a	135.33	0.09	- 47.4	- 96.7	-235.0	+ 29.7	+227.0	- 22.0
213b	135.39	0.09	- 55.0	- 96.7	-303.8	- 31.1	—	- 32.9
214	136.24	0.10	- 79.3	-104.5	-235.6	- 48.4	+ 97.1	- 40.2
215a	136.28	0.10	- 07.0	- 88.3	-150.5	- 13.8	—	+ 24.1
215b	136.30	0.10	+ 01.3	- 64.5	-116.8	+ 12.4	+272.0	+ 42.4
218a	137.19	0.11	- 71.0	- 40.0	- 83.0	+ 29.7	+137.1	- 68.0
218b	137.21	0.11	- 47.4	-104.5	-125.6	- 22.1	—	+ 24.1
221	140.31	0.15	- 95.3	- 88.4	-261.2	- 13.8	—	- 58.5
223	143.28	0.19	- 79.3	- 96.7	-133.7	- 65.6	+ 20.7	-187.1
228	145.30	0.22	- 23.0	-104.5	- 14.9	- 57.3	—	-214.9
231b	146.16	0.23	—	- 80.6	- 66.2	- 23.5	+ 11.4	- 49.7

1.	2.	3.	4.	5.	6.	7.	8.	9.
236a	2459 147.20	0.24	- 86.8	-121.2	- 57.4	- 49.4	+ 83.5	+155.0
236b	147.21	0.24	- 25.2	- 72.2	+ 10.1	+ 58.7	+177.7	+ 42.4
241	151.32	0.29	-130.9	- 40.0	-116.8	- 4.8	+101.4	- 24.1
247	155.37	0.35	-104.3	- 72.2	-185.0	- 4.8	+ 11.4	- 12.4
249	159.22	0.39	-194.5	+ 32.9	- 99.9	+ 29.7	+ 65.0	- 40.2
249	159.22	0.39	+198.2	+ 36.6	- 96.2	+ 26.0	—	- 36.5
252a	160.36	0.41	—	+ 25.3	- 21.2	+ 57.5	—	+ 34.7
252d	160.37	0.41	—	+ 21.0	- 32.9	+ 19.4	—	+ 32.1
254	161.19	0.42	+ 95.1	+ 20.3	- 68.7	- 38.3	—	- 16.4
255	163.18	0.44	+103.5	+ 30.7	- 68.7	- 18.0	—	—
259a	164.14	0.46	—	- 26.4	- 90.3	—	—	- 76.5
262a	165.14	0.47	+ 19.3	+ 35.5	- 46.7	—	—	-122.0
262b	165.15	0.47	- 14.3	+ 24.2	- 23.5	—	—	- 97.4
267a	167.26	0.50	+ 66.0	+ 98.0	- 64.0	+ 40.5	—	- 20.5
267b	167.27	0.50	+ 56.7	+ 51.5	- 62.5	- 04.8	—	-130.0
267c	167.28	0.50	+ 61.1	+ 69.3	- 24.8	—	—	-156.6
269	168.18	0.51	+ 69.3	+ 61.4	- 03.0	—	—	- 44.2
274	170.09	0.53	+ 62.5	+ 95.1	- 08.3	—	—	-137.5
275	170.12	0.53	+ 35.7	+ 67.4	- 45.8	+ 28.7	—	-105.8
276	170.15	0.53	+ 40.0	+ 72.5	- 56.9	+ 12.0	—	- 79.6
284a	173.10	0.57	+140.8	+100.5	+103.6	- 34.2	—	- 47.7
284c	173.11	0.57	+136.6	+104.7	+ 45.8	- 38.4	—	- 89.1
288a	174.13	0.58	+112.4	+104.8	+ 98.3	- 15.3	—	- 93.4
288c	174.16	0.58	+105.2	+105.3	+ 55.3	- 17.3	—	—
291a	175.12	0.59	+141.5	+113.3	+ 81.6	- 22.4	—	-143.0

1.	2.	3.	4.	5.	6.	7.	8.	9.
291a	2439 175.16	0.60	+150.3	+126.3	+81.4	- 44.3	—	-198.4
293b	176.13	0.61	+143.8	+127.4	+ 91.3	- 85.7	—	+ 27.4
293c	176.14	0.61	+126.0	+110.1	+100.5	—	—	+ 10.2
296a	177.12	0.62	+143.9	+135.9	+100.7	+ 17.7	—	+163.2
302a	181.09	0.67	+203.9	+185.6	+135.9	—	—	-187.7
302b	181.10	0.67	+185.2	+178.1	+112.2	- 36.1	—	-179.9
305	181.27	0.68	+166.7	+200.1	+110.8	- 49.3	—	-104.4
306	181.37	0.68	+211.5	+155.6	+101.2	- 61.1	—	-159.6
307a	182.15	0.69	+158.0	+ 77.3	+115.8	—	—	—
307b	182.16	0.69	+125.2	+182.8	+ 55.5	—	—	-136.1
311a	183.12	0.70	+165.8	+174.7	+ 55.8	- 63.2	—	-238.8
311b	183.13	0.70	+197.0	+189.4	+ 87.4	- 74.6	—	—
315a	185.31	0.73	+189.6	+197.6	+147.6	- 90.3	—	-278.1
315b	185.32	0.73	+182.0	+191.0	+166.7	-116.4	—	-249.2
318a	186.83	0.75	+240.6	+217.2	+119.0	—	—	- 98.6
318b	186.84	0.75	+169.6	+194.7	+ 85.0	- 41.6	—	-171.7
321a	187.60	0.76	+222.5	+191.3	+109.3	- 70.9	—	-227.3
321c	187.61	0.76	+238.3	+191.1	+109.2	- 70.7	—	-209.0
327a	191.67	0.81	+238.3	+207.2	+137.3	- 55.4	—	-128.2
328c	191.72	0.81	+240.7	+217.5	+137.9	- 57.1	—	-132.9
329b	191.75	0.81	+245.3	+222.1	+159.8	- 32.2	—	- 55.6
330c	191.80	0.81	+253.8	+239.0	+168.4	- 60.6	—	- 93.2
336a	193.78	0.83	+202.8	+205.7	+150.3	- 77.3	—	- 48.8
336b	193.79	0.83	+252.2	+245.7	+131.7	- 49.9	—	+129.9
338a	194.70	0.85	+247.9	+232.9	+149.1	- 41.1	—	+180.8

1.	2.	3.	4.	5.	6.	7.	8.	9.
338b	2439 194.75	0.85	+265.8	+217.8	+162.9	- 41.1	—	+190.8
344	202.50	0.92	+191.2	+183.7	+ 73.5	- 78.3	—	—
345b	202.62	0.92	+178.7	+171.8	+ 80.3	- 64.5	—	-185.8
345c	202.62	0.92	+162.2	+154.5	—	- 53.0	—	-204.1
349	207.66	0.01	+100.6	+ 44.1	+ 22.0	—	—	+ [illegible].8
350	207.68	0.01	+ 79.5	+ 22.8	+ 14.6	- 78.0	—	+ 30.5
351	207.72	0.01	+ 85.3	+ 36.9	+ 16.0	- 71.9	—	+ [illegible].4
352	207.74	0.01	+ 95.5	+ 31.3	+ 18.2	- 68.8	—	- 06.2
353a	207.77	0.01	+100.3	+ 59.7	+ 3.0	- 64.3	—	- 11.2
354	215.65	0.11	- 12.7	-102.3	—	+ 06.4	—	- 27.6

Figure X-1

Velocity variation of HD 68273
November 1965 - March 1966.

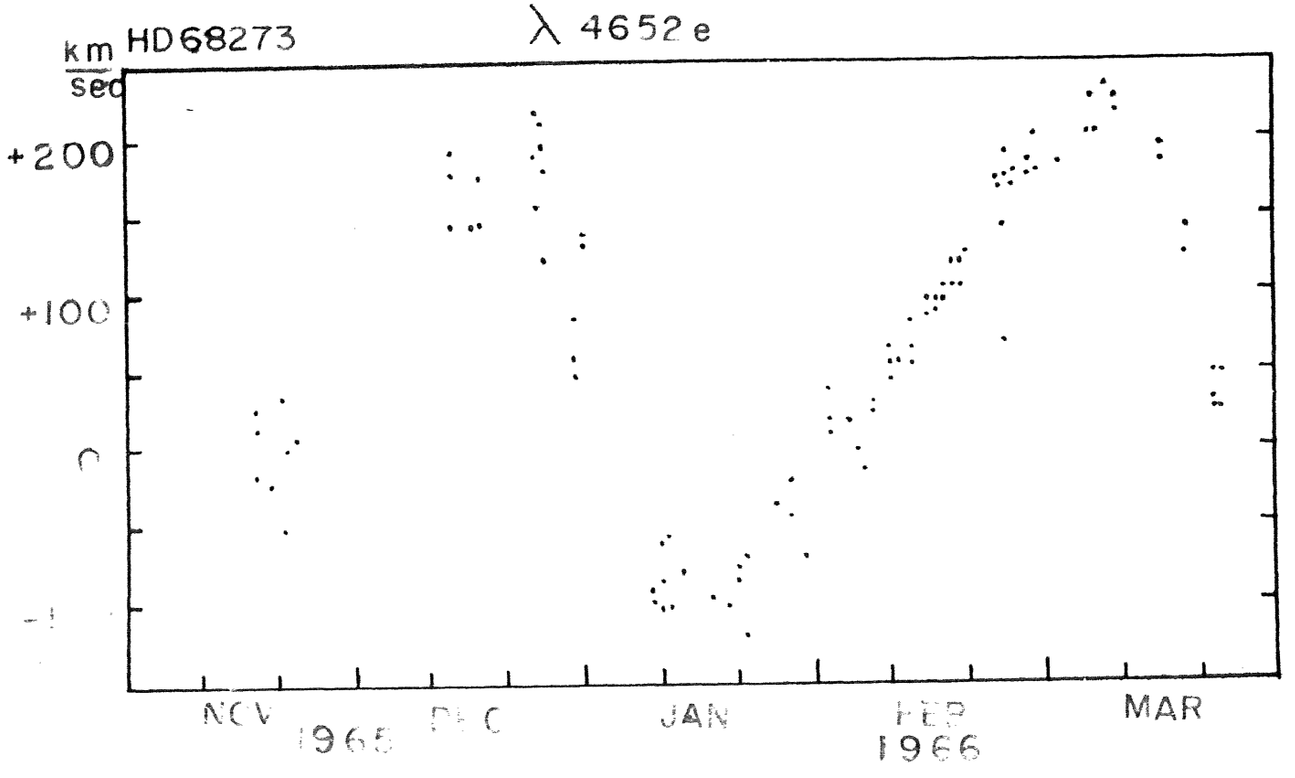
HD68273
λ 4652 e
km/sec
+200
+100
0
-1
NOV
1965
DEC
JAN
FEB
1966
MAR

combination with our velocity measures, we used a few values of velocities obtained by the Lick observers from Chile, to derive a more reliable period which works out to be 78.5 days. The zero phase is assumed to be JD 2439128.25. The observations on two nights seem to rule out the possibility of a period close to a day. It is difficult at this stage to derive a more exact period of this system. Extended observations for some years would be necessary for a more exact spectroscopic determination. However, if the system is an eclipsing binary, then the efforts of a single season should be capable of furnishing a reliable estimate of the period.

The velocity curves of HeII 4686 and CIV 4441 were first drawn to enable the derivation of the systemic velocity as indicated by these emission lines. The preliminary orbit obtained for 4686A has a γ-axis value of +62.5 Km/sec. while that obtained for CIV 4441 is -20 Km/sec. It is difficult to explain the difference of 80 Km between the two γ-axes as due entirely to red-shift in the HeII 4686 line, because it seems likely that the 4441A emission line is affected by absorption on its longward side. This would naturally shift the γ-axis in the negative direction.

Table V-3

No.	Mean phase	Mean Velocities			
		4686	4652	4441	4340
1	0.02	+101.20	+ 45.90	+ 19.10	- 64.00
2	0.10	- 39.80	- 88.60	-181.03	- 10.65
3	0.12	- 61.30	- 72.09	-163.90	+ 13.63
4	0.17	- 77.16	- 38.92	-162.99	+ 39.92
5	0.24	-109.80	- 80.20	-217.26	- 31.90
6	0.29	- 83.09	- 89.62	-114.46	+ 33.96
7	0.34	- 38.25	- 76.75	-173.80	+ 9.36
8	0.44	- 25.00	+ 27.35	- 88.90	+ 21.03
9	0.46	- 8.07	+ 31.33	-130.45	+ 30.65
10	0.48	+ 23.64	+ 39.21	- 47.99	+ 40.47
11	0.53	+ 51.86	+ 74.11	- 27.99	+ 20.35
12	0.57	+114.35	+ 107.04	+ 71.37	- 27.23
13	0.62	+157.90	+139.75	+108.27	+ 17.65
14	0.68	+179.02	+180.45	+115.17	- 48.05
15	0.71	+183.34	+188.18	+133.56	- 86.12
16	0.75	+217.82	+190.61	+105.63	- 61.07
17	0.80	+214.40	+197.45	+143.51	- 56.43
18	0.87	+206.09	+208.46	+152.74	- 59.81
19	0.91	+201.70	+187.30	+114.30	- 40.96
20	0.95	+180.52	+123.61	+94.25	- 34.53

The observations were grouped into 20 normal points given in Table V-3, wherein the phases, velocities, weights and final O-C values are all listed. The initial plots of radial velocities showed that the orbits are circular and hence, it was decided to solve for the elements using Sterne's method. This method is particularly well suited for orbits of low eccentricity. One starts with elements describing circular orbits and the final least squares solution yields quantities that are the most probable values of the elliptic orbits. Sterne's method was applied separately for the three emission line HeII 4686, CIV 4441, CIII 4652 as well as the H line at 4340.

From the following observational equations for 4686A

1.0000x	+0.1253y	-0.9686z	+0.2487u	+0.9921v	+20.1200 = 0
1.0000x	-0.3681y	-0.7290z	-0.6845u	+0.9298v	-48.7400 = 0
1.0000	-0.4818	-0.5358	-0.8443	+0.8763	-53.6500 = 0
1.0000	-0.7290	+0.0628	-0.9980	+0.6845	-33.3000 = 0
1.0000	-0.9298	+0.7290	-0.6845	+0.3681	-36.5800 = 0
1.0000	-1.0000	+1.0000	0.0000	0.0000	-00.9200 = 0
1.0000	-0.9511	+0.8090	+0.5878	-0.3090	+38.0900 = 0
1.0000	-0.5878	-0.3090	+0.9511	-0.8090	-01.7900 = 0
1.0000	-0.4818	-0.5358	+0.8443	-0.5763	-00.3700 = 0
1.0000	-0.3681	-0.7290	+0.6845	-0.9298	+14.7100 = 0
1.0000	-0.0628	-0.9921	+0.1253	-0.9980	-01.7200 = 0
1.0000	+0.1874	-0.9298	-0.3681	-0.9823	+24.1600 = 0
1.0000	+0.6374	-0.1874	-0.9823	-0.7705	-18.0800 = 0
1.0000	+0.7705	+0.1874	-0.8443	-0.6374	-00.4300 = 0
1.0000	+0.8763	+0.5358	-0.8443	-0.4818	-07.5800 = 0
1.0000	+0.9686	+0.8763	-0.4818	-0.2487	+13.4000 = 0
1.0000	+0.9980	+0.9921	+0.1253	+0.0628	+05.6800 = 0
1.0000	+0.8763	+0.5358	+0.8443	+0.4818	+15.1700 = 0
1.0000	+0.7290	+0.0628	+0.9980	+0.6845	+32.3200 = 0
1.0000	+0.5358	-0.4258	+0.9048	+0.8443	+39.4000 = 0

where $x = \delta V_o$

$y = \delta K$

$z = K e \cos\omega$

$u = K e \sin\omega$

$v = K (t - T_o)$

the following normal equations were obtained

$$
\begin{aligned}
20.0000x + 0.7443y - 0.5513z - 0.4180u - 1.1186v + 000.0900 &= 0 \\
+0.7246 + 1.1288 - 0.2058 - 0.2780 - 127.8480 &= 0 \\
+9.2912 - 0.9976 + 0.8066 - 25.1902 &= 0 \\
+10.4564 - 0.4722 - 262.7440 &= 0 \\
+10.2754 + 76.7250 &= 0
\end{aligned}
$$

which when solved gave the following values of corrections to the preliminary elements:

$\delta V_o = -0.18$ Km/sec

$\delta K = +13.01$ Km/sec

$e = 0.1744$

$\omega = 80° 21'$

$T_o = 0.783$

$T = 0.905$

The observational equations for 4652A are the following

FIGURE V-2

Velocity curves of HD 68273. Upper HeII 4686, lower CIV 4441. The sizes of the filled circles correspond to the weights of the normal points

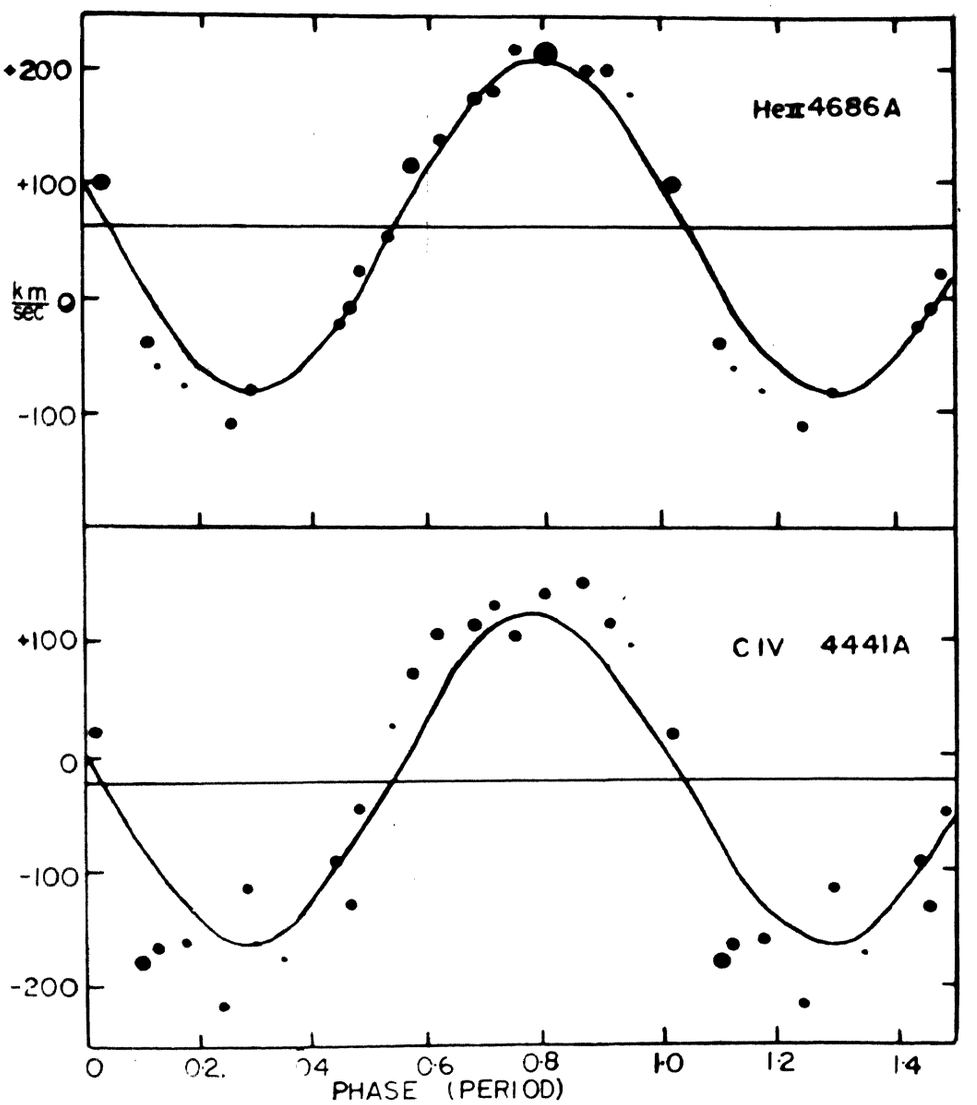
+200
+100
km/sec
0
-100
HeII 4686A
+100
0
-100
-200
CIV 4441A
0
02.
04
06
08
1·0
1·2
1·4
PHASE (PERIOD)

FIGURE V-3

Velocity curves of HD 93373. Upper diagram CTIO-CIV 4052. Lower diagram H absorption -434 km/s. The sizes of the filled circles correspond to the weights of the normal points.

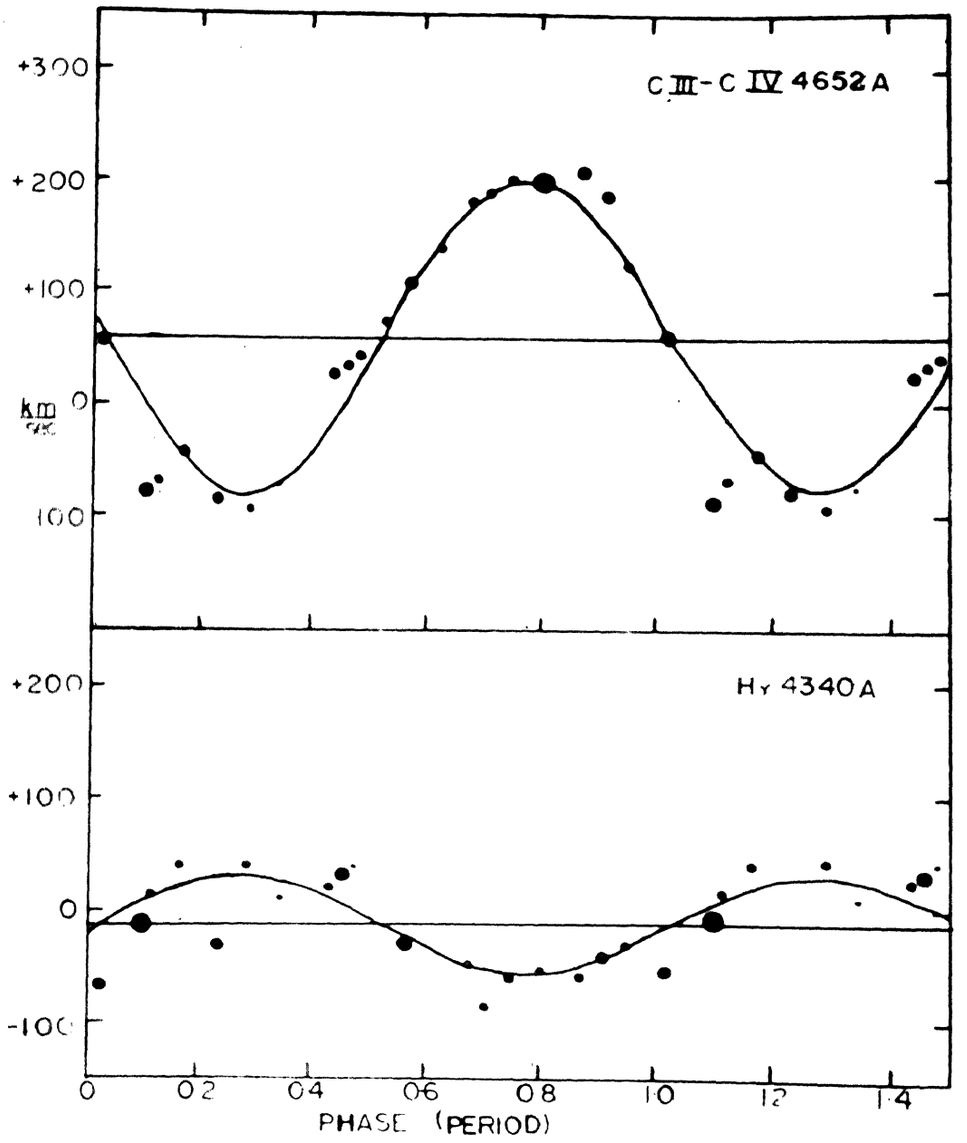
+300
+200
+100
km/sec
0
100
C III - C IV 4652 A
+200
+100
0
-100
Hγ 4340 A
0
0·2
0·4
0·6
0·8
1·0
1·2
1·4
PHASE (PERIOD)

FIGURE V-4

Velocity curves of AX 602/3. Upper diagram
H&K absorption 4200A. Lower diagram K
absorption 4170A. The sizes of the filled
circles correspond to the weights of the
normal points.

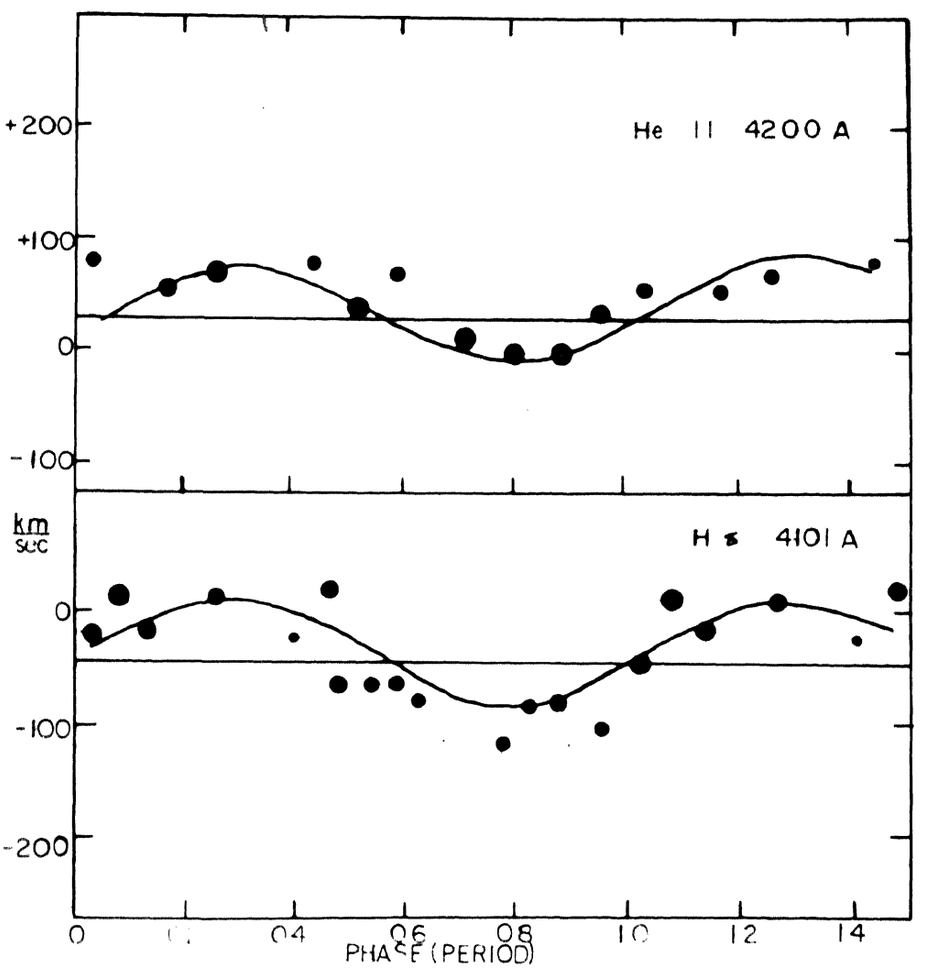
+200
+100
0
-100
He II 4200 A
km
sec
H δ 4101 A
0
-100
-200
0
04
06
08
10
12
14
PHASE (PERIOD)

1.0000x	+0.0628y	-0.9921z	+0.1253u	+0.9980v	-22.3200 = 0
1.0000	-0.4258	-0.6374	+0.7705	+0.9048	-89.0400 = 0
1.0000	-0.5358	-0.4258	+0.9048	+0.8443	-57.2700 = 0
1.0000	-0.7705	+0.1874	-0.9823	+0.6374	+ 8.4700 = 0
1.0000	-0.9511	+0.8090	-0.5878	+0.3090	- 7.7500 = 0
1.0000	-0.9980	+0.9921	+0.1253	-0.0628	-10.6700 = 0
1.0000	-0.9298	+0.7290	+0.6845	-0.3681	- 7.2600 = 0
1.0000	- 0.5358	-0.4258	+0.9048	-0.8443	+42.1700 = 0
1.0000	-0.4258	-0.6374	+0.7705	-0.9048	+30.8900 = 0
1.0000	-0.3090	-0.8090	+0.5878	-0.9511	+22.5600 = 0
1.0000	0.0000	0.0000	+1.0000	-1.0000	+14.5900 = 0
1.0000	+0.2487	-0.8763	-0.4818	-0.9686	+13.6100 = 0
1.0000	+0.6845	-0.0628	-0.9980	-0.7290	-14.7400 = 0
1.0000	+0.8090	+0.3090	-0.9511	-0.5878	+ 8.6800 = 0
1.0000	+0.9048	+0.6374	-0.7705	-0.4258	+ 3.1200 = 0
1.0000	+0.9823	+0.9298	-0.3681	-0.1874	+ 2.8000 = 0
1.0000	+0.9921	+0.9686	+0.2487	+0.1253	+ 0.2800 = 0
1.0000	+0.8443	+0.4258	+0.9048	+0.5358	+31.7900 = 0
1.0000	+0.6845	-0.0628	+0.9980	+0.7290	+32.8100 = 0
1.0000	+0.4818	-0.5358	+0.8443	+0.8763	- 2.7600 = 0

where $x = \delta V_o$

$y = \delta K$

$z = K \cos\omega$

$u = K \sin\omega$

$v = K (t-T_o)$

The normal equations derived are

20.0000x	+0.8132y	+0.5229z	+3.7297u	-1.0698v	+000.0400=0
	+9.7612	+1.1034	-1.7756	-0.3104	- 96.8595=0
		+0.5679	-2.0202	-0.0804	- 36.3256=0
			+11.4518	+1.6321	+215.2699=0
				+10.2905	+ 16.9539=0

the solution of which provided the following corrections:

δV_o = +3.7469 Km/sec

δK = +6.4046 Km/sec

e = 0.16

ω = 260° 20'

To = 0.7825

T = 1.505

Similarly the observation equations used for 4441 are the following:

1.0000x	+0.0628y	−0.9921z	+0.1253u	+0.9980v	− 28.85	= 0
1.0000	−0.4258	−0.6374	+0.7705	+0.9048	+101.04	= 0
1.0000	−0.5358	−0.4258	+0.9048	+0.8443	+ 68.10	= 0
1.0000	−0.7705	+0.1874	−0.9825	+0.6374	+ 33.45	= 0
1.0000	−0.9511	+0.8090	−0.5878	+0.3090	+ 61.76	= 0
1.0000	−0.9980	+0.9921	+0.1253	−0.0628	− 47.78	= 0
1.0000	−0.9298	+0.7290	+0.6845	−0.3681	+ 21.16	= 0
1.0000	−0.5378	−0.4258	+0.9048	−0.8443	− 6.30	= 0
1.0000	−0.4258	−0.6374	+0.7705	−0.9048	+ 50.46	= 0
1.0000	−0.3090	−0.8090	+0.5878	−0.9511	− 15.21	= 0
1.0000	0.0000	0.0000	+1.0000	−1.0000	+ 9.21	= 0
1.0000	+0.2487	−0.8763	−0.4818	−0.9686	− 54.40	= 0
1.0000	+0.6845	−0.0628	−0.9980	−0.7290	− 28.65	= 0
1.0000	+0.8090	+0.3090	−0.9511	−0.5878	− 17.66	= 0
1.0000	+0.9048	+0.6374	−0.7705	−0.4258	− 22.27	= 0
1.0000	+0.9825	+0.9298	−0.3681	−0.1874	+ 16.80	= 0
1.0000	+0.9921	+0.9686	+0.2487	+0.1253	− 19.68	= 0
1.0000	+0.8443	+0.4258	+0.9048	+0.5358	− 50.15	= 0
1.0000	+0.6845	−0.0628	+0.9980	+0.7290	− 34.68	= 0
1.0000	+0.4818	−0.5358	+0.8443	+0.8763	− 43.77	= 0

where x = δ Yo

y = δ Z

z = Kecos ω

u = Kesin ω

v = K (t−To)

The normal equations then are

$$
\begin{array}{rrrrrr}
20.0000x & +0.8132y & +0.5229z & +3.7297u & -1.0698v & -\ 7.420\ =0 \\
 & +9.7612 & +1.1034 & -1.7796 & -0.3104 & -493.3600=0 \\
 & & +8.5679 & -2.9202 & -0.0804 & -\ 35.5400=0 \\
 & & & -11.4318 & +1.6321 & -\ 50.7300=0 \\
 & & & & +10.2385 & +105.\ t\ =0
\end{array}
$$

and the corrections become

$$
\begin{aligned}
\delta V_0 &= -\ 6.50 \text{ Km/sec} \\
\delta K &= +52.94 \text{ Km/sec} \\
e &= 0.1330 \\
\omega &= 78^\circ\ 26' \\
T_0 &= 0.757 \\
T &= 0.975
\end{aligned}
$$

Table V-4 gives the summary of the preliminary and final elements.

In the derivation of a velocity from a measurement of the band at 4552A an arbitrary wavelength of 4552A, was assumed as the mean wavelength of the band and the shifts from this arbitrary value denote the velocities. This is useful for determining the amplitude of the velocity curve and related properties of the Wolf-Rayet orbit. It, however, cannot be utilized for a complete study of the system, unless the γ-axis value is known with certainty.

Table V-4

Wave-length.	Preliminary Elements.	Final Elements.	Lehmann-Filhés Final
4686	Period = 78.50 days	Period = 78.50 days	
	T = 0.79	T0 = 0.783 ± 0.0119	
	e = 0.	e = 0.1744 ± 0.0638	0.16 ± .02
	ω = -	ω = 80° 21' ± 22°55'	96.0 ± 7.7
	γ axis = +62.50 Km/sec	γ axis = +62.56 Km/sec ± 10.11 Km	+ 63.9 ± 2.4
	K = 146.25 Km/sec	K = 159.26 Km/sec ± 11.29 Km	* 163.7 ± 3.5 T = .05 ± .05
4652	Period = 78.50 days	Period = 78.50 days	
	T = 0.78	T = 1.505	T = 1.00 ± .02 P
	e = 0	T0 = 0.7825 ± 0.0039	ω = 87.2° ± 9.3
	ω = -	Ω = 260°20' e = 0.16 ± 0.0543	e = 0.17 ± .03
	γ axis = +57.50 Km/sec	γ axis = +61.24 ± 6.34 Km/sec	γ = 59.9 ± 3.0
	K = 133.75 Km/sec	K = 145.15 ± 8.82 Km/sec	K = 153.5 ± 4.4
4441	Period = 78.50 days	Period = 78.50 days	
	T = 0.757	T0 = 0.757 ± 0.0165	
	e = 0	e = 0.1330 ± 0.0891	
	= -	ω = 78° 26' ± 42° 57'	
	γ axis = -20.00 Km/sec	γ axis = -26.50 ± 11.42 Km/sec	
	K = 143.75 Km/sec	K = 106.69 ± 15.42 Km/sec.	

This is apparent when one scrutinizes the values of ω obtained for the three emission lines. While there is general agreement on the other parameters of the system, the value of ω derived from 4652A is in complete disagreement with that obtained from 4686A and 4441A.

The absorption lines of H γ 4340, HeII 4200 and H δ 4100 have also been used for a study of the spectroscopic orbit. The parameters of the orbit for the absorption line star chiefly depend on the measures of the H γ line. A large scatter of the points from this line together with the relatively smaller amplitude in velocity of the more massive O star made it difficult to carry through a preliminary analysis of the orbit. I, therefore, assumed a value of K best signified by the plotted points of H γ and using Sterne's method carried through a solution for the final elements. The observation equations are the following

1.0000x	−0.0628y	−0.9921z	+0.1253u	−0.0000v	+48.4600	= 0
1.0000	+0.4258	−0.6374	−0.7705	−0.9048	+15.8900	= 0
1.0000	+0.5358	−0.4258	−0.9048	−0.8443	− 3.7300	= 0
1.0000	+0.7705	+0.1874	−0.9825	−0.6374	−20.0400	= 0
1.0000	+0.9686	+0.8763	−0.4818	−0.2487	+60.2000	= 0
1.0000	+0.9980	+0.9921	+0.1253	−0.0628	− 9.4100	= 0
1.0000	+0.9048	+0.6374	+0.7705	+0.4258	+16.2200	= 0
1.0000	+0.5358	−0.4258	+0.9048	+0.8443	−12.0300	= 0
1.0000	+0.4258	−0.6374	+0.7705	+0.9048	−25.4200	= 0
1.0000	+0.3090	−0.8090	+0.5878	+0.9511	−43.2100	= 0
1.0000	−0.0628	−0.9921	−0.1253	+0.9980	−55.8900	= 0
1.0000	−0.2487	−0.8763	−0.4818	+0.9686	+ 3.7900	= 0
1.0000	−0.5358	−0.4258	−0.9048	+0.8443	−53.2900	= 0
1.0000	−0.8090	+0.3090	−0.9511	+0.5878	+ 1.5800	= 0
1.0000	−0.9048	+0.6374	−0.7705	+0.4258	+34.8000	= 0
1.0000	−0.9825	+0.5240	+0.3681	+0.1874	+ 6.4500	= 0
1.0000	−0.9921	+0.9686	+0.2487	−0.1253	+ 1.4300	= 0
1.0000	−0.8443	+0.4258	+0.9048	−0.5358	+11.0600	= 0
1.0000	−0.6845	−0.0628	+0.9980	−0.7290	− 1.0000	= 0
1.0000	−0.4818	−0.5358	+0.8443	−0.8763	+ 1.1800	= 0

where x = δ Vo
y = δ K
z = Kecos ω
u = Kesin ω
v = K (t−To)

which yielded the following normal equations

20.0000x	−0.7348y	−1.2623z	+0.2752u	+1.1759v	+ 13.2400=0
	+9.5714	−0.4791	−0.6107	−0.3558	+ 0.3311=0
		+9.1278	−0.1399	−1.3890	+133.7665=0
			+10.2819	+0.2651	− 19.5961=0
				+10.4281	−192.2746=0

The orbital elements listed in Table V-5 are the final elements derived of the U star.

Table V-5

Final elements of the O star

γ_2 Velorum

P = 78.53 days

γ = −15.07 Km/sec ± 258 Km/sec

K = 42.55 Km/sec ± 0.5 Km.

e = 0.1712

ω = 263°

λ 4340 — L. Filhes elements

γ = −18.0 ± 1.8

K = 43.1 ± 2.6

e = .17

ω = 260°

T = 1.00

The orbital elements obtained for all the three emission lines are remarkably similar. This can be contrasted with CQ Cephei where according to Kappa et al (1966), there is a considerable difference in the orbital characteristics denoted by the velocity curves of CIV 4658 and HeII 4686. A disparity, if it can be called as such, exists only in the values of K with CIV 4441 having the largest value of 196 Km/sec, and the 4652A complex having a value of 145 Km/secs. The large amplitude in the velocity curve of CIV 4441 seem certainly to originate due to the contamination introduced by the absorption line on the long wavelength side.

In the case of HeII 4686, Sahade (1958) has shown that at certain phases a narrow emission is seen superposed on the broad emission feature of 4686. Sahade has interpreted this feature as due to material streaming from the Wolf-Rayet star through the inner Lagrangian point. The presence of this narrow feature is likely to upset within a small limit, the value of the semi-amplitude of the velocity curve. It could also affect the value of the γ-axis, though if it is seen at more phases than a restricted range, it is quite likely that the effect will be nullified. As such I have preferred using the value

of K derived from 4652A, since, it is least likely to be affected by possible distortions that are usually present in the Wolf-Rayet systems. In fact, 4652A may have proved also to be unsuitable for this purpose, were it not for the fact that a violet edge normally seen for 4652A, is totally absent as pointed out first by Smith.

Along with the measures of the Hγ line, I have made measures of the absorption line HeII 4200 as well as Hδ 4100. HeII 4200 is seen weakly in the spectra and hence the helium contribution to the over all absorption of the Balmer series is not likely to be greater than 20-30%. In the reduction of velocity measures of 4340A, I have assumed a value of the wave-length of the absorption line to be that of Hγ, thus ignoring the possible contamination of the corresponding Pickering series. In doing so the results will be affected in the value of the γ-axis and would not change the value of K. The 4200A velocity measures are plotted in Fig.V-4. The lower half of the diagram contains the velocity curve of 4101A. If the velocity curve of 4340A is made to pass through the points of either line and γ-axes derived, then one finds the

γ-axis of 4200A to be about 62 Km more positive than 4340A. This raises the question whether the discrepancy thus observed is due to our neglect of the HeII contribution towards the wavelength of the absorption feature at 4340A. If it were so, and if HeII has contributed appreciably, then the mean wavelength would be shifted more to the violet causing thereby a γ-axis to exist that is more negative than what we have measured. As such this line of reasoning indicates that we are justified in assuming that the wavelength of the absorption feature at 4340A is correctly taken, if one assigns to it the wavelength of the H_γ-line. An explanation of the more positive value of the γ-axis of HeII 4200 is its likely contamination with 4200A emission originating from the Wolf-Rayet atmosphere.

The plots of the velocity measures of the absorption feature at 4101A when fitted with the theoretical curve of 4340A show a γ-axis very much more negative than 4340A. This indicates that the wavelength used for the absorption feature is not correct and the absorption is the sum total of the effect of not only H_δ but also of some other ions that have a transition near about this wavelength. An examination of the spectra

shows that this line is more broad and intense upsetting the decrement of the Balmer series at this particular wavelength. Table V-6 gives the values of $m_p \sin^3 i$ and $m_v \sin^3 i$ based on the mass ratios determined from the H_γ line and each of the other three emission lines used. I have already indicated earlier, reasons for prefering the orbital parameters derived from the emission band at 4652A. The masses of the O and B star derived from 4552A and H_γ are in good agreement with the values of an early O type star. In this connection, an effort was made to derive the spectral type of the O star by using the ultra-violet region high dispersion spectrum taken at Mount Stromlo. No trace of HeII 4481 and OIII 3960 can be seen on the spectra. Also HeI 4387 is very weak, if it exists at all. Hence the spectral type is earlier than O8 and closer to O7. The ratios $\frac{4542}{4471} = 0.4$; $\frac{4542}{H} = 0.2$ and $\frac{3818}{3815} = 0.25$ make it earlier than O8, but later than O7. Hence a spectral type of O7.5 seems best to adopt. The Balmer series are seen on the high dispersion plate until H_{16} with certainty.

There are very few well determined masses of the O stars available in the astronomical literature. The values obtained in this study are in good agreement

Masses calculated 9/8/67

$K_W(4652) = 153.5$ $e = 0.17$
$K_O(4340) = 43.1$ $m_W \sin^3 i = 12.99 \odot$
$m_O \sin^3 i = 46.260$

$K_W(4686) = 163.7$ $e = 0.16$ $m_W \sin^3 i = 14.45$
$K_O(4340) = 43.1$ $m_O \sin^3 i = 54.88$

$K_W(4441) = 196.7$ $e = 0.13$ $m_W \sin^3 i = 19.17$
$K_O(4340) = 43.1$ $m_O \sin^3 i = 59.8$

TABLE V-6

HD 68273	4686A	4652A	4441A
Mass ratio $\frac{M_O}{M_W}$	3.74	3.41	4.62
$M_O \sin^3 i$	50.5 ⊙	40.1 ⊙	91.7 ⊙
$M_W \sin^3 i$	13.5 ⊙	11.7 ⊙	19.8 ⊙

i	$\sin^3 i$	M_W	M_O
60°	.6495	18.0	61.7
65°	.7434	15.7	53.9
70°	.8298	14.1	48.3
75°	.9012	13.0	44.5
80°	.9551	12.2	42.0
85°	.9886	11.8	40.5
90°	1.0000	11.7	40.1

with those listed by Allen (1963) and provide an independent estimate of the mass of an O7.5 star. Assuming the correctness of the estimate, we see that the value for the Wolf-Rayet star is ~~12.2~~ 11.7 $\odot$. Since these values are in close agreement with our estimated values of both the O and W spectral types, it is likely that the $\sin^3 i$ contribution is close to 1. It seems, therefore, very likely, that the system of γ_2-Velorum is an eclipsing binary with a value of orbital inclination close to 90°. This conjecture should be tested as early as possible, for, if γ_2-Velorum turns out to be an eclipsing binary with favourable eclipses, then we are bound to make striking advances in our knowledge of the geometry of the Wolf-Rayet atmosphere by its study.

As indicated early γ_2-Velorum has long been known for its variations in its spectra. The Kodaikanal observations cover over 3 cycles of the star and a feature that is most strikingly seen is the variation in the absorption of HeI 3889. This has been reported earlier by Smith who observed a displaced absorption component of this line a few nights during 1953 and also on a few nights during 1954. Due to the fact that the star has never been subjected to a systematic study

before, it has always been assumed that the occurrence of a displaced HeI 3889 absorption is sporadic in nature. Observations of the system show that the violet edges are seen on two cycles chiefly between phases 2 days and 30 days. This fact seem to suggest that the displaced absorption HeI 3889 originates at certain selected phases in the binary system. However, it needs to be pointed out that in the second cycle observed at Kodaikanal, no displaced absorption was seen even though we had good coverage of the star over a range of phase from 2 days to 35 days. It seems likely that this displaced absorption originates from material flow with a velocity of about -1534.9 Km/sec. in the vicinity of the inner Lagrangian point. The gas streams are visible from phase 2 days to at most 40 days. However, it is not necessary that in every cycle over this phase range, the displaced absorption be present. The streaming of gas about the inner Lagrangian point is also the cause of the narrow emission superposed on the broad emission at 4686A, as reported by Sahade. In this connection, with a period of 78.5 days when one works backward in time, one finds that the phases at which Smith observed displaced 3889A was 18 days during 1953 and 33 days in 1954.

FIGURE V-2

The region around He I 3819 in HD 60213 (Micro photometer tracings from 3800A to 4000A (a) Phase 0.95P (b) Phase 0.1P (c) Phase 0.01P . Notice the enhanced displaced absorption of He I 3819 in (c) indicated by the arrow.

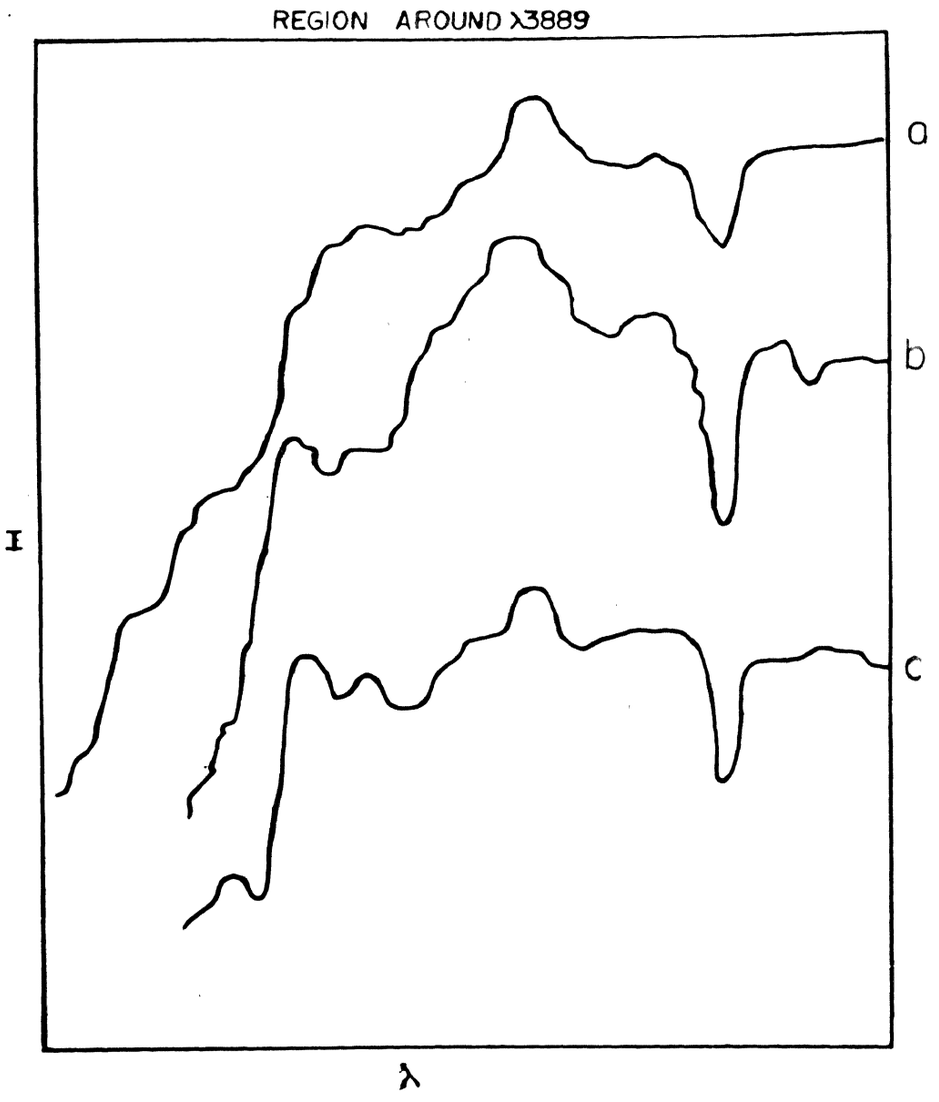
REGION AROUND λ3889
a
b
c
I
λ

Fig.V-5 shows three microphotometer tracings in the region 3839A. It will be seen that the spectrum at phase 0.12 shows the displaced absorption of 3839A.

2.3.HD 193576 (V444 Cygni).

Twentyeight spectra of this binary system obtained with the Mount Wilson, 60-inch telescope with a dispersion of 75A/mm at H γ have been used to study the spectroscopic orbit of the Wolf-Rayet star and the O component. This binary had in the past spectroscopic orbits determined by Wilson, Keeping and Munch. The phases of the observations have been computed with respect to the time of primary minimum from the elements given by Kron and Gordan (1950):

Phase Zero = JD 2426771.379 + 4.212338

The measures of radial velocity were of the emission line HeII 4686 and NIV 4058 along with the absorption lines at H γ, H δ and H β, that originate from the O star. The velocity curve of 4686A indicated a circular orbit and the preliminary elements were obtained on the assumption of circularity. The observations were grouped into 10 normal points. The normal equations are -

The velocity measures of HD 193576

Plate	J.D. of observation.	Phase (in period)	Velocities in Km/Sec.					
			4686e	4603e	4058e	4061a	4340a	4101a
32596	2434144.86	0.64	-183.6	-193.7	-311.8	—	+102.6	+112.3
32597a	144.88	0.64	-248.3	-209.9	-325.1	+107.3	+130.3	+ 43.9
32597b	144.91	0.65	-308.9	-236.4	-338.2	+ 77.2	+103.3	+151.6
32602	145.00	0.91	-24.1	- 73.7	-191.2	—	+124.7	—
32631a	170.76	0.79	-310.8	-229.8	-352.6	+158.6	+ 26.3	+168.2
32631b	170.81	0.80	-270.1	-191.1	-313.7	+ 68.2	+ 96.5	+141.5
32634a	171.77	0.03	+117.0	+ 67.0	- 28.0	—	- 17.1	+ 15.3
32636a	171.95	0.08	+164.6	+ 86.0	+ 36.6	—	- 39.0	+ 50.9
32636b	171.98	0.08	+198.5	+176.7	+ 41.0	-120.6	- 49.8	+ 37.5
32642a	173.88	0.53	+ 35.4	- 36.5	-115.0	- 60.3	+ 36.5	+ 37.4
32642b	173.90	0.54	-121.0	+ 34.3	-201.5	- 60.3	- 6.6	+ 28.5
32649a	174.96	0.80	-318.7	-333.5	-319.0	-165.0	—	—
32649b	175.00	0.80	-298.3	-308.3	-319.0	-113.5	+111.7	+198.5
32654b	175.86	0.00	+ 69.1	+ 79.3	-106.6	+142.7	+ 74.1	+ 23.7
32654c	175.90	0.01	+ 62.2	—	-102.3	—	+122.6	+ 32.4
32654d	175.92	0.02	+ 69.0	+ 38.3	-132.6	+ 7.1	+ 90.2	—
32661a	176.85	0.24	+259.4	+324.5	+359.0	—	- 25.6	- 88.7
32661b	176.87	0.24	+259.3	+238.7	+348.1	-113.4	- 66.4	- 61.8
32669a	177.86	0.50	+ 88.0	+ 85.2	-107.0	- 8.4	+ 30.4	- 3.8
32669b	177.88	0.51	+ 27.7	+ 85.1	-128.8	- 1.0	- 34.9	+ 9.6

The velocity measures of HD 193576 ... Contd.

Plate	J.D. of observation.	Phase (in period)	Velocities in Km/sec.					
			4686e	4633e	4358e	4861a	4343a	4101a
32681a	2434194.71	0.47	+168.0	—	- 23.1	+ 27.0	- 22.4	+ 25.1
32683a	194.87	0.51	- 43.1	- 59.7	- 88.3	-109.2	- 37.3	+ 83.2
32683c	194.98	0.53	- 83.9	- 40.4	- 70.9	-139.3	+ 49.1	+ 20.3
32746b	224.68	0.59	- 97.6	- 66.6	-295.5	+ 42.1	+ 63.8	—

10.0000x	-1.2750y	-3.1850z	-2.3420u	-0.6800v	- 0.3000=0
	+3.5610	+0.5730	-0.4530	-1.3610	+ 54.6830=0
		+5.2640	+1.4340	+0.9160	+135.4640=0
			+4.7570	-1.4920	- 30.0520=0
				+6.4390	+ 40.6960=0

yielding the following corrections

δV_o = 40.3 Km. V_o = +26.5 - 10.3 = +16.2 Km/sec

δK = -14.7 Km K = 297.5 - 14.7 = +282.80 Km/sec

e = 0.1140

ω = 163°.2

To = -0.003 T0 = 0.24 - 0.003 = .237

T = 0.237 + 0.453 = 0.690

Sterne's method was used by virtue of the low eccentricity. A similar attempt with NIV 4058 gave the following normal equations.

10.0000x	-1.3122y	-3.1657z	-1.8510u	+1.3461v	- 0.0300=0
	+3.4171	+0.2590	-0.1685	-0.9259	+ 68.4300=0
		+5.8785	+1.0646	-1.5147	-267.0300=0
			+4.1215	-1.5711	+ 1.5946=0
				+6.5925	+ 3.0169=0

The corrections are the following:

δV_o = +12.1164 Km/sec. V_o = -91.70 Km/sec ± 15.7

δK = -18.0700 Km/sec K = +332.93 Km/sec ± 22.4

e = 0.1615 ± .05

ω = 352° 23' ± 20°10'

T0 = 0.2525 ± .008

T = 1.230

FIGURE V-5a

Velocity measures of $H\beta$, $H\gamma$, $H\delta$ absorption lines in HD 193576.

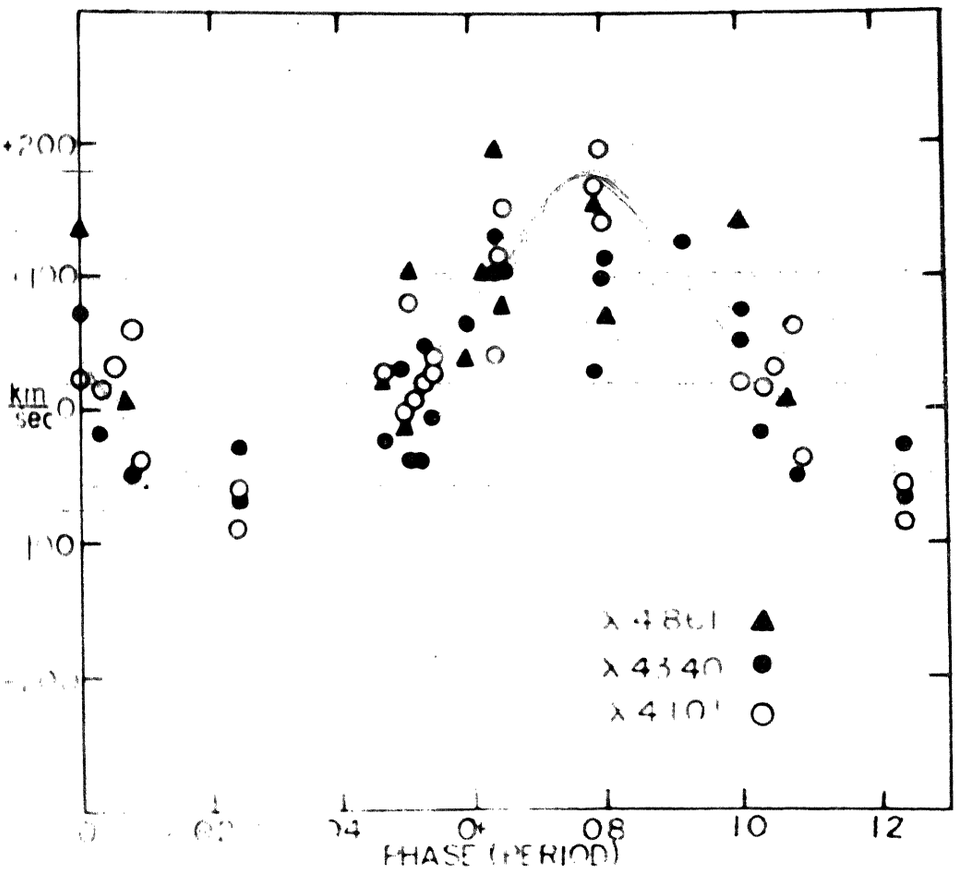
+200
km
sec
λ 4861
λ 4340
λ 4101
08
10
12
PHASE (PERIOD)

FIGURE V-9b

Velocity curve of HD 193576 = BV 4058
The closed circles are normal points.

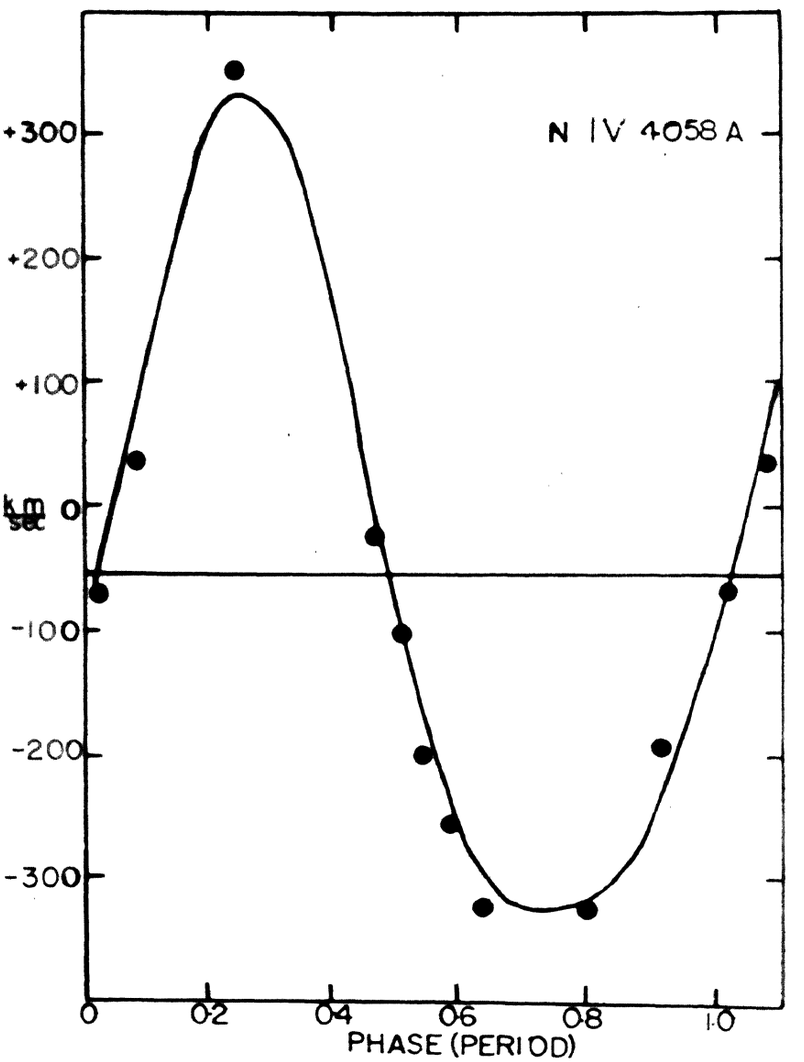
N IV 4058 A
+300
+200
+100
km/sec 0
-100
-200
-300
0
02
04
06
08
1.0
PHASE (PERIOD)

FIGURE V-6a

Velocity curve of HD 193576 = BV 4903
The closed circles are normal points.

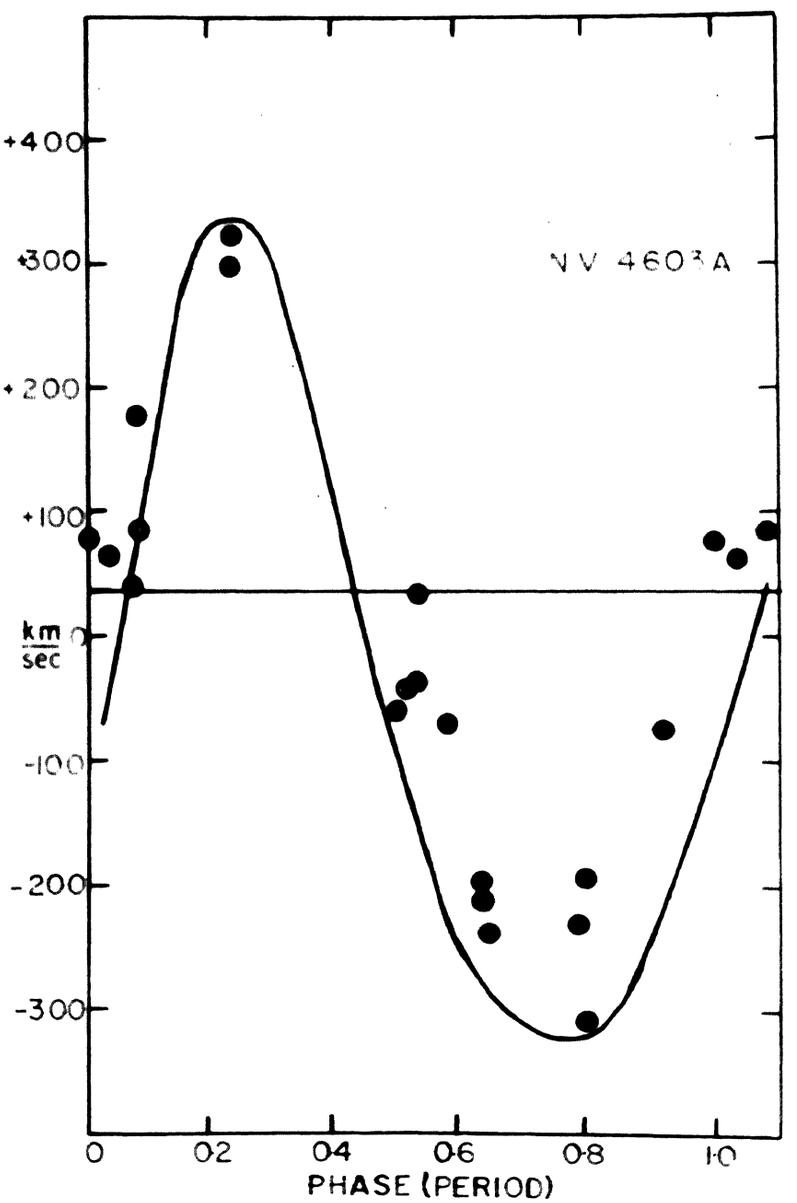
+400
+300
+200
+100
km/sec
0
-100
-200
-300
NV 4603A
0
02
04
06
08
1·0
PHASE (PERIOD)

FIGURE V-64

Velocity curve of HD 193576 = Bell 4636
The closed circles are normal points.

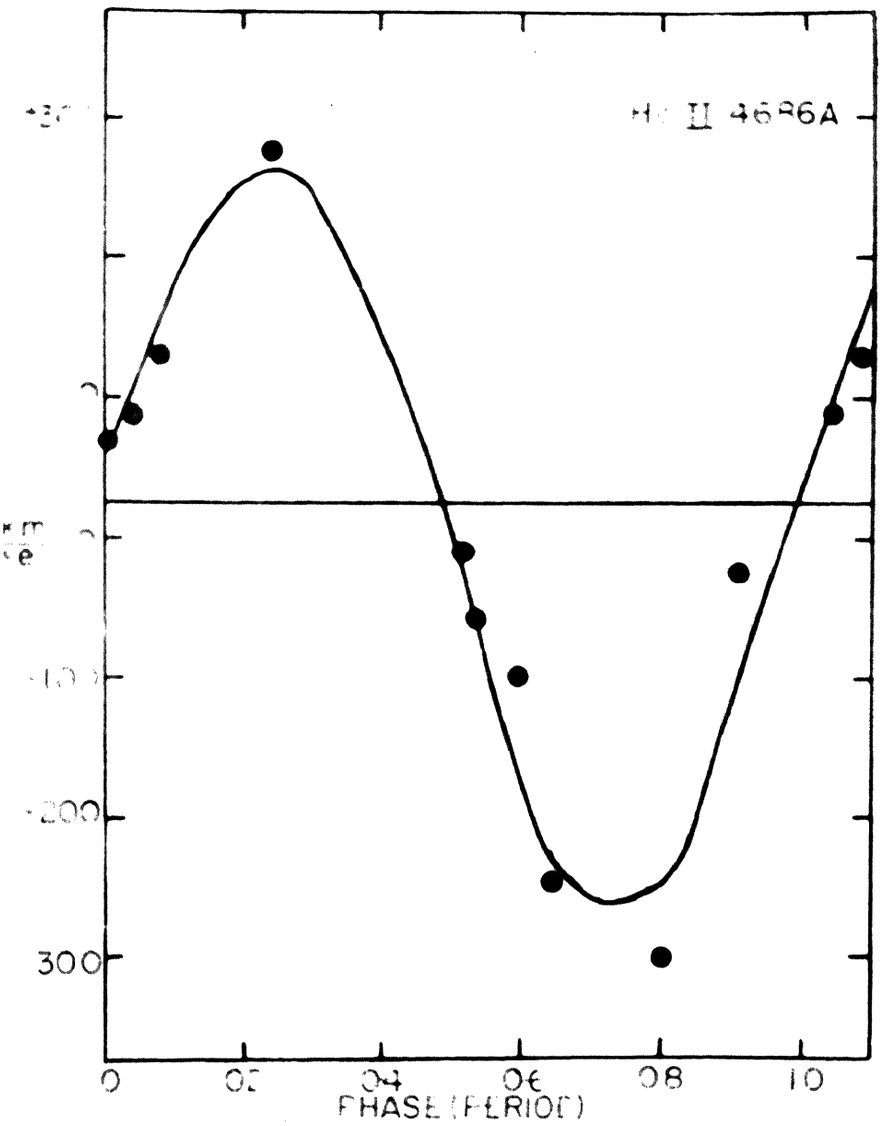
He II 4686A
300
0
02
04
06
08
10
PHASE (PERIOD)

The presence of a certain degree of eccentricity of the orbit has been speculated on for some time. The photoelectric measures of Kron and Gordon show that the secondary minima occur slightly earlier than the mid-point between the primary minima. The longitude of periastron determined from the 4058A and 4686A curves corresponds to 0.25 P and this is in fair agreement with the observed fact that the secondary minima following a primary minimum occurs earlier than it would have, if the orbit were circular. The γ-axis value for 4058A is -52 Km/secs. as against ~~-152~~ +16.2 for 4686A, or a difference of ~~216~~ 68.2 Km/sec. The velocities determined from the absorption lines is plotted in Fig.V-6. They show a certain degree of scatter and indicate a range in location of the γ-axis. This is caused presumably by contamination in the spectrum of the emission lines originating from the Wolf-Rayet star. The velocity measures of H γ have been used to determine the orbit of the O star. A least squares solution was made for orbital elements only with the idea of obtaining the correction of K, which is necessary to determine the mass ratio of the components. The final elements determined from HeII 4686, NIV 4058 are listed in Table V-7 along with the values given by Munch.

Table V-7

HD 193576

Present	Hunter
V_0 = −51.70 ± 15.7 Km/sec (4058A)	−40 Km/sec (4058A)
K = 332.9 ± 22.40 Km/sec	305 Km/sec
ω = 352° 23' ± 3° 10'	—
e = 0.15 ± 0.0475	—
T = 0.2525 ± 0.028	—
f = 1.230	—
$K_0 \sin^3 i$ = 23.1860	24.1
$K_w \sin^3 i$ = 9.7343	9.5
Also K=4138	
P = 4.21230	—
V_0 = + 45 Km/sec	= + 10 Km/sec
K = 123.9 Km/sec	K = 120 Km/sec
e = 0.13	—

Munch has pointed out that the line 4058A experienced changes in profile of marked nature during his period of observation. We shall discuss the changes in profile seen in Mount Wilson plates latter. For the present, it is felt that there were no serious distortions in the profile of NIV 4058, as to warrant a large scatter in the measured radial velocities. A comparison of Munch's values with ours shows fair agreement between the γ-axis derived by him and in this study. It should be recorded that Munch's values are preliminary elements not corrected by a least squares solution. He has also assumed that the orbital eccentricity is zero. The value of γ-axis given by Munch falls within the range of my determination -51 ± 5 Km/sec. Munch obtains a value of K = 300 Km while the value derived here is 333 ± 22 Km/sec. Since the masses of the stars are very sensitive to the value of K, it is worthwhile to point out that the discrepancy in the values of $M_0 \sin^3 i$ and $M_H \sin^3 i$ between Munch's and present work originates to large extent in the difference between the two K values. The masses determined from 4686A, while close to the values that we know are valid in the case of Wolf-Rayet stars, are still not to be preferred because we know that 4686A in a binary system is liable to have complications by virtue of gas streaming

near the inner Lagrangian point. As such, especially for binary systems of small period, and hence of small separation of the components, it would be necessary to view these masses derived from 4686A, with a little degree of caution. We, therefore, are limited to using 4026A and the absorption lines. The masses derived then are 28.1 $M_\odot$ for the O star and 9.7 $M_\odot$ for the Wolf-Rayet star. The Wolf-Rayet star's value is in close agreement with Hunch's value. However, the mass of the O star is significantly different from that derived by Hunch. This is essentially because of the fact that the mass ratio as derived here is significantly different from that obtained by Hunch. It should be noted, however, that that the K value of the absorption line is in agreement with that of Hunch.

There are very few mass determinations of the O stars available in the literature. However, the spectral type of O8 which Hunch assigns and which I confirm on the high dispersion tracings available calls for a mass much more than the value given by Hunch. We, therefore, feel justified in using the mass determination of the O star with confidence. One needs to carry through a least squares solution to see whether a better representation

of the orbital elements could be obtained from Kuiper's data. For the present, we shall consider the values of the Wolf-Rayet and O star as equivalent to 10.360 and 30.000 on the basis of Kron's value i = 78°.

It is well known that the Wolf-Rayet spectrum of 193576 shows very striking changes in the line contours of its various emission lines at various phases. A study of these contours help us in building a picture of the binary system as a whole. With this in mind, I have illustrated in Figs.V-7, V-8, V-9, the variations experienced at various phases by HIV 4058, HeII 4686, HeII 4061 as measured from low dispersion spectra. In the case of HeII 4686, we find that at the conjunctions a narrow hump appears at about the peak of the profile and this hump which is on the red side at phases close to the primary minimum, moves over to the violet side at phases, close to the secondary minimum when the Wolf-Rayet is eclipsed. This variation in 4686A was first pointed out by Wilson in 1942. Fig.V-8 gives details of the profile at eight selected phases. In general, the overall widths of the lines are essentially the same. But in the vicinity of the conjunctions, the second hump caused by the superposed narrow emission seems to be primarily responsible

FIGURE V-7

Line profile variations with phase as derived for NIV 4059 from low dispersion spectra of HD 193576.

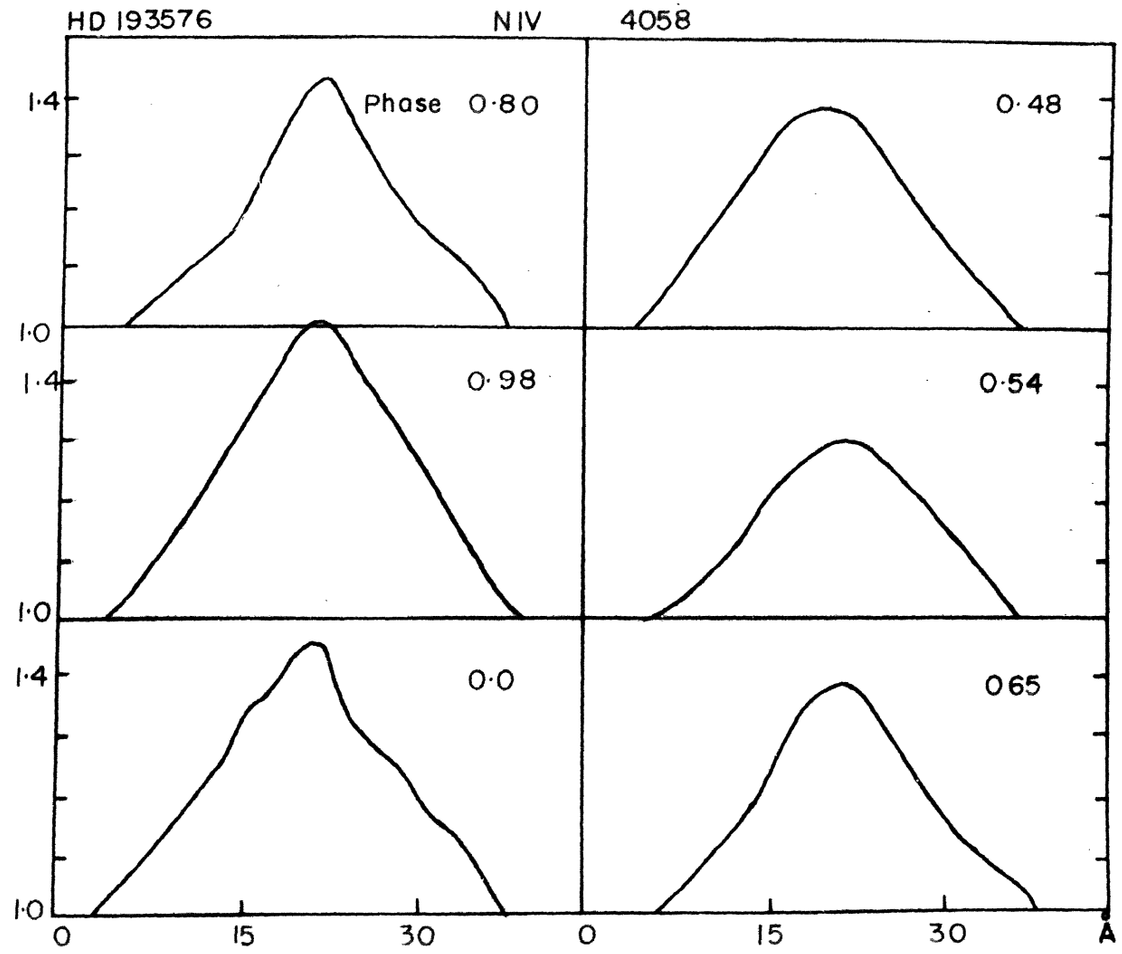
HD 193576
NIV 4058
Phase 0·80
0·48
0·98
0·54
0·0
065
1·4
1·0
0
15
30
Å

PLATE V-8

Line profile variations with phase in HD 193576 - He I 4686

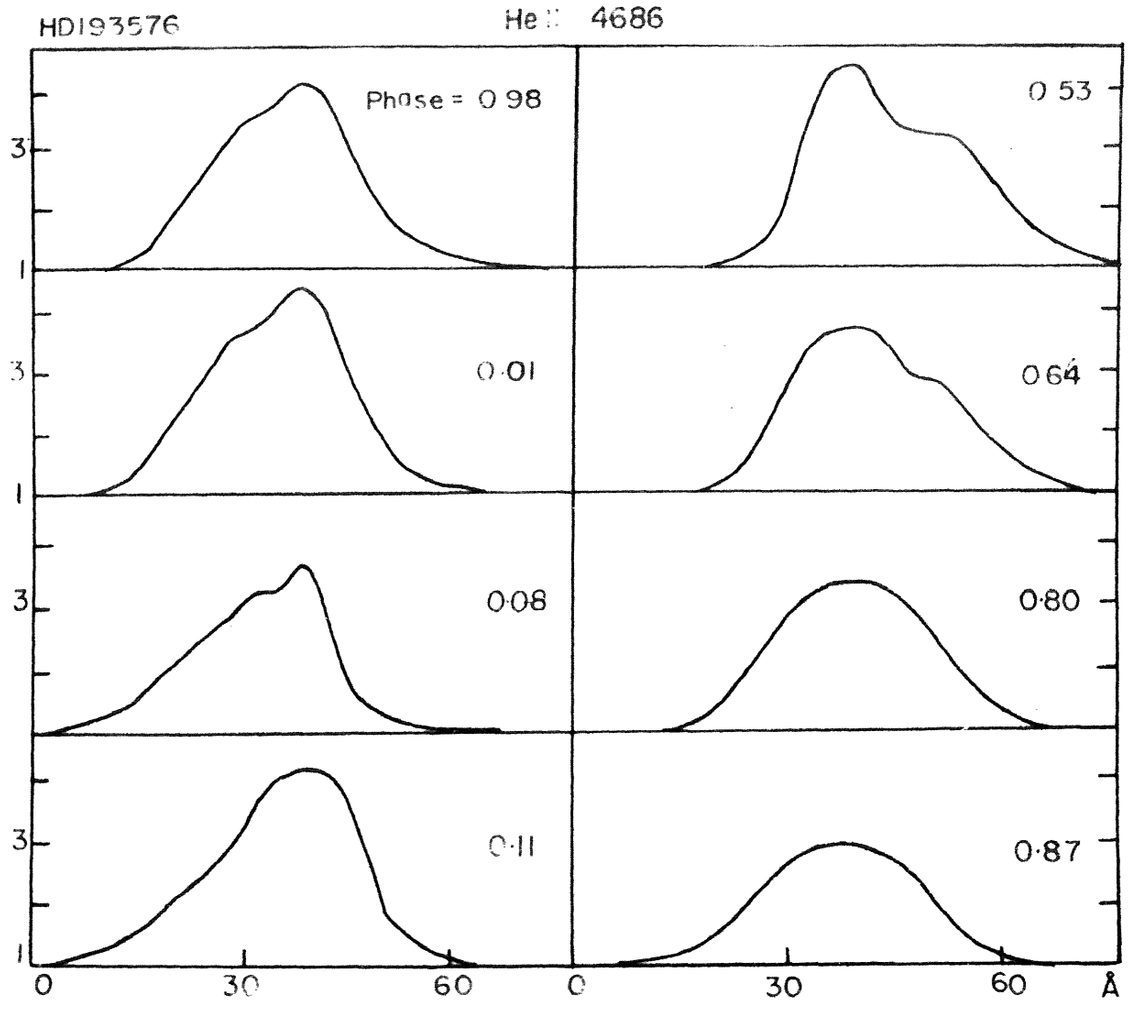
HD193576
He II 4686
Phase = 0 98
0 53
0·01
0·64
0·08
0·80
0·11
0·87
3
1
0
30
60
Å

FIGURE V-2

Line profile variations with phase in
HD 193576 - He I 4026

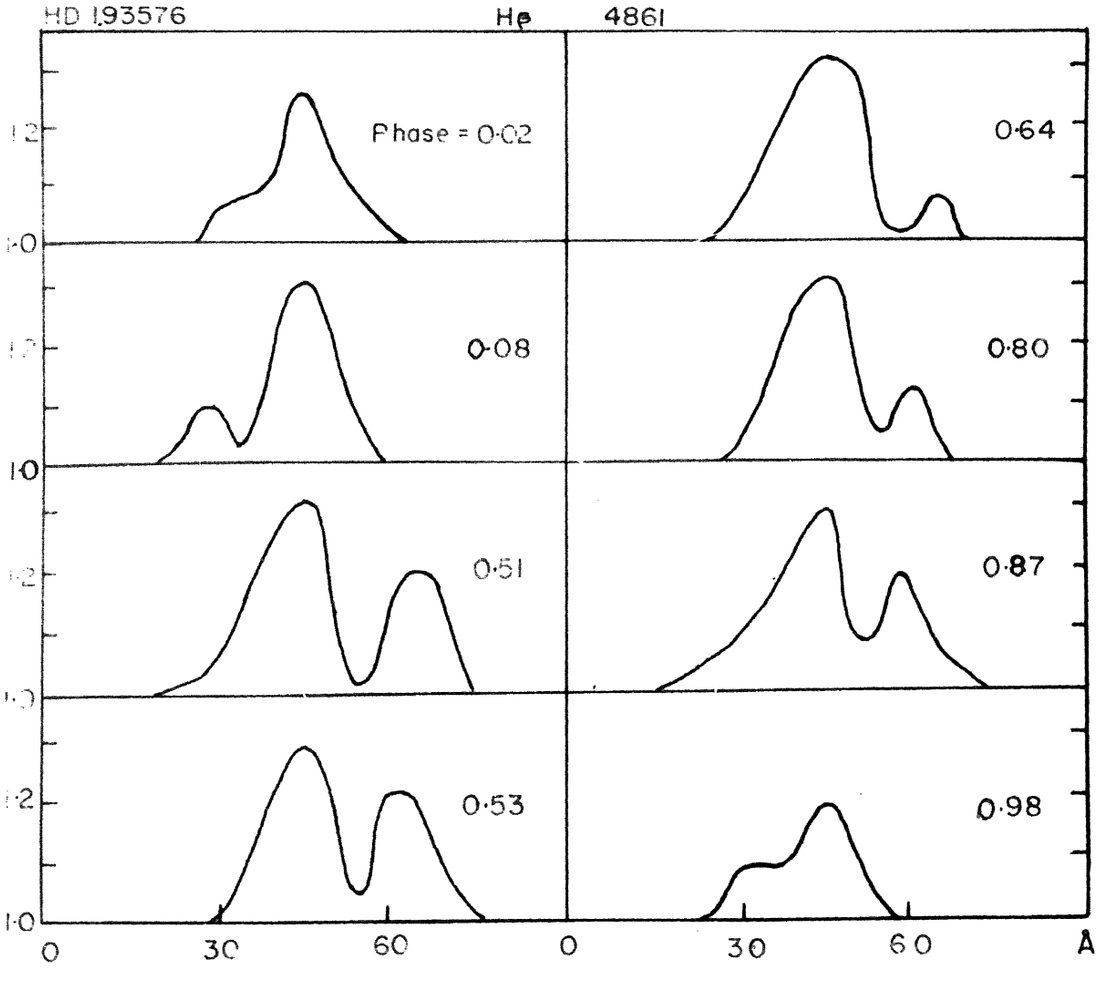
HD 193576
He 4861
Phase = 0·02
0·64
0·08
0·80
0·51
0·87
0·53
0·98
1·2
1·0
0
30
60
Å

for the changes in the profile. Sahade has shown that this narrow emission originates at the inner Lagrangian point and the observations reported here substantiate his point of view.

The profile of HeII 4686 essentially portrays the variations in location of the Hβ absorption line of the O star and the consequent effects that it has on the appearance of the overall structure. However, the total emission width seems to be greater near secondary minimum than it is at primary minimum. The profile at phase 0.02 has the absorption component on the violet side caused by an approaching O star but the narrowness of the overall emission cannot just be explained by a heavy cultilation of the emission line by the Hβ profile of the O star. It, therefore, seems that the emission line itself has a difference in width near about primary and secondary minima, or in other words the emission line is narrower when the Wolf-Rayet star is closest to the observer than it is when it is farthest away.

The profiles of 4059A are displayed in Fig.V-7. I have given six of these profiles to indicate the fact that no serious changes in the structure have been

observed during the period when these plates were obtained and hence we can adopt the values obtained of radial velocity measures from this line with a good degree of confidence. However, a few minor changes in the appearance of the profile need further mention. The profile close to primary minimum is wide and fairly sharp peaked, while that near secondary minimum is broad. It appears that the profile is intrinsically broader near primary than at second minimum. This behaviour seems to be opposite to that experienced by the HeII emission line at 4860A.

High dispersion spectra obtained at phases 0.02, 0.48, 0.71 and 0.95(P) have been available, to study with better resolution, some of these characteristic changes. These spectra obtained at 10A/mm. with the 100-inch coude spectrograph extend in the ultra-violet to about 3300A. In fact, these plates at selected phases, more especially at conjunctions, were exposed to study the profiles of the higher members of the Balmer series and how these have been affected by the electron scattering envelope around the Wolf-Rayet star.

Fig.V-10 shows the profile of the $3s^3S - 3p^3P$ multiplet of NIV at 3479A, 3483A and 3485A. The Kinematic

FIGURE V-10

The profile of HV 3437 at phase 0.0 and 0.48 in HD 193576.

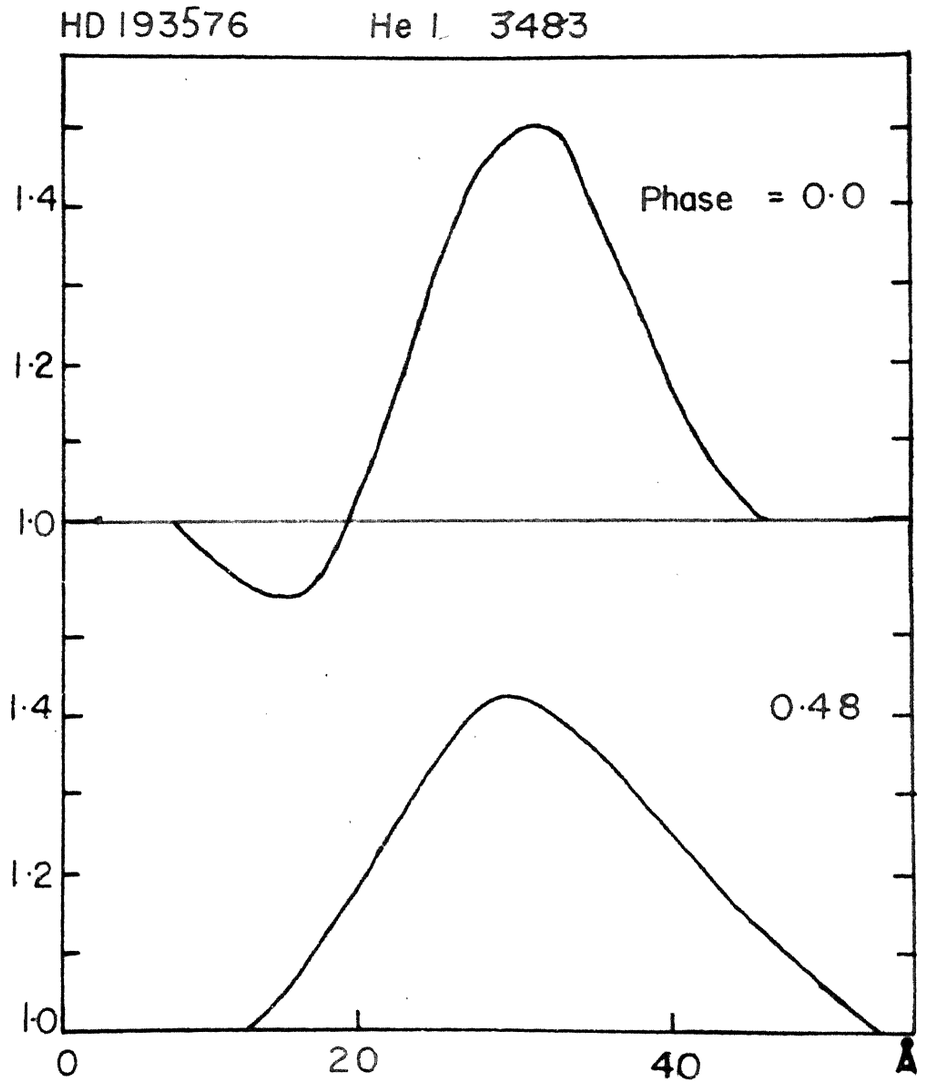
HD 193576
He I 3483
Phase = 0·0
0·48
1·4
1·2
1·0
1·4
1·2
1·0
0
20
40
Å

conditions in the Wolf-Rayet envelope are such as to broaden the individual transitions considerably, so that we see them unresolved separately. The main characteristic, that is of interest, is the presence of a violet absorption edge displaced with respect to the centre of the emission 3492A by 1160 Km/sec. This feature is seen only at primary minimum when the Wolf-Rayet star eclipses the O component. The surprising fact is that at this phase the Wolf-Rayet spectrum should have the normal characteristics of a WN5 star. The appearance of a violet absorption edge for HD 3433 is not seen on any of the high dispersion spectra of HD 192163, HD 191765 or HD 193577. It, therefore, seems to be a characteristic stimulated by the component of the binary system. The multiplet $3p^1P - 3d^1D$ at 4058 does not show the absorption feature as can be seen in Figure V-11 where the profiles of this line derived from high dispersion spectra are shown. However, these profiles show that there are subtle differences among them at conjunction phases and at elongation.

Fig.V-12 illustrates the variations seen on the high dispersion spectra of the emission complex at 4100. The role of the spectrum of the O component in causing a distorted emission profile is obvious.

FIGURE V-11

The profiles of HeV 4053 in HD 193576 derived from high dispersion spectra taken at phases 0.0, 0.40, 0.71 and 0.95 (P).

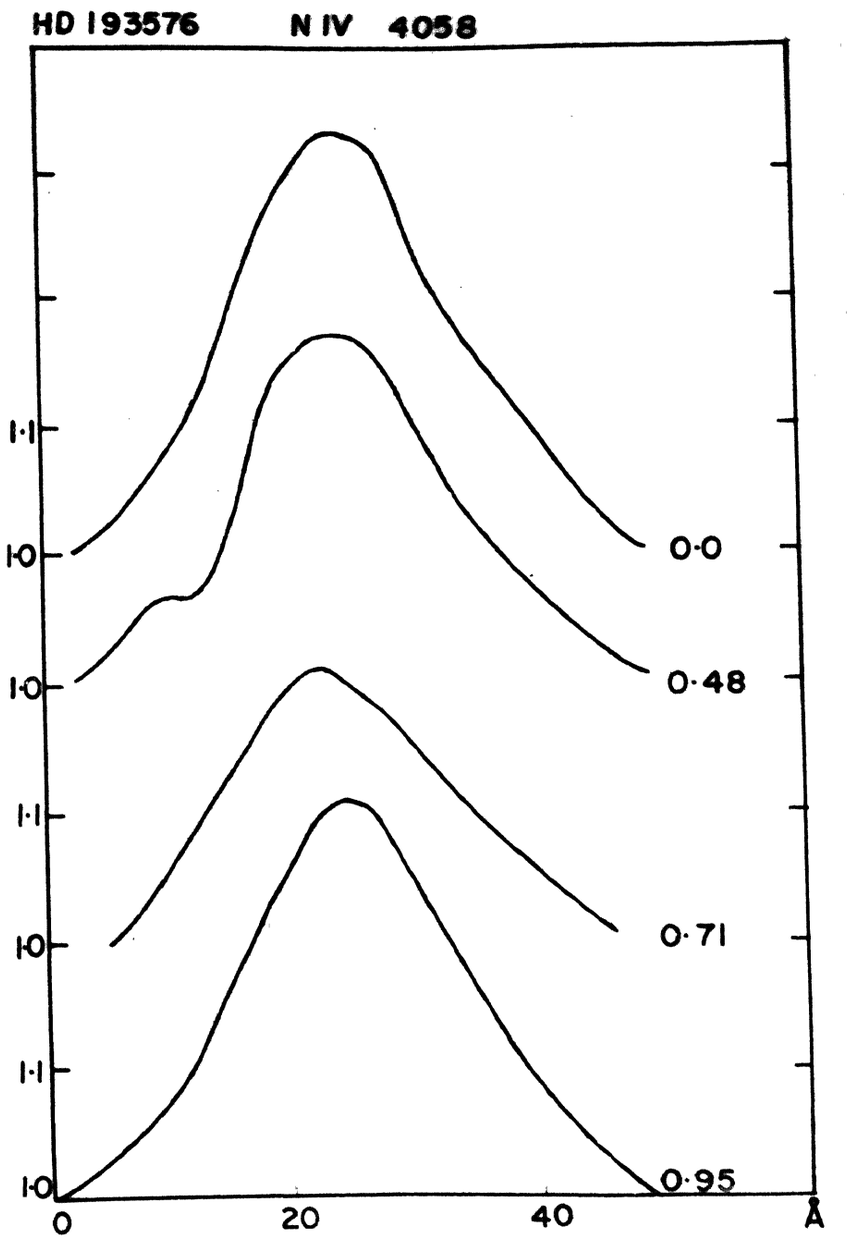
HD 193576 N IV 4058
1·1
1·0
0·0
1·0
0·48
1·1
1·0
0·71
1·1
1·0
0·95
0
20
40
Å

PLATE V-12

The profiles of 4100A in HD 193576 obtained at phases 0.0, 0.43, 0.71 and 0.95(?)

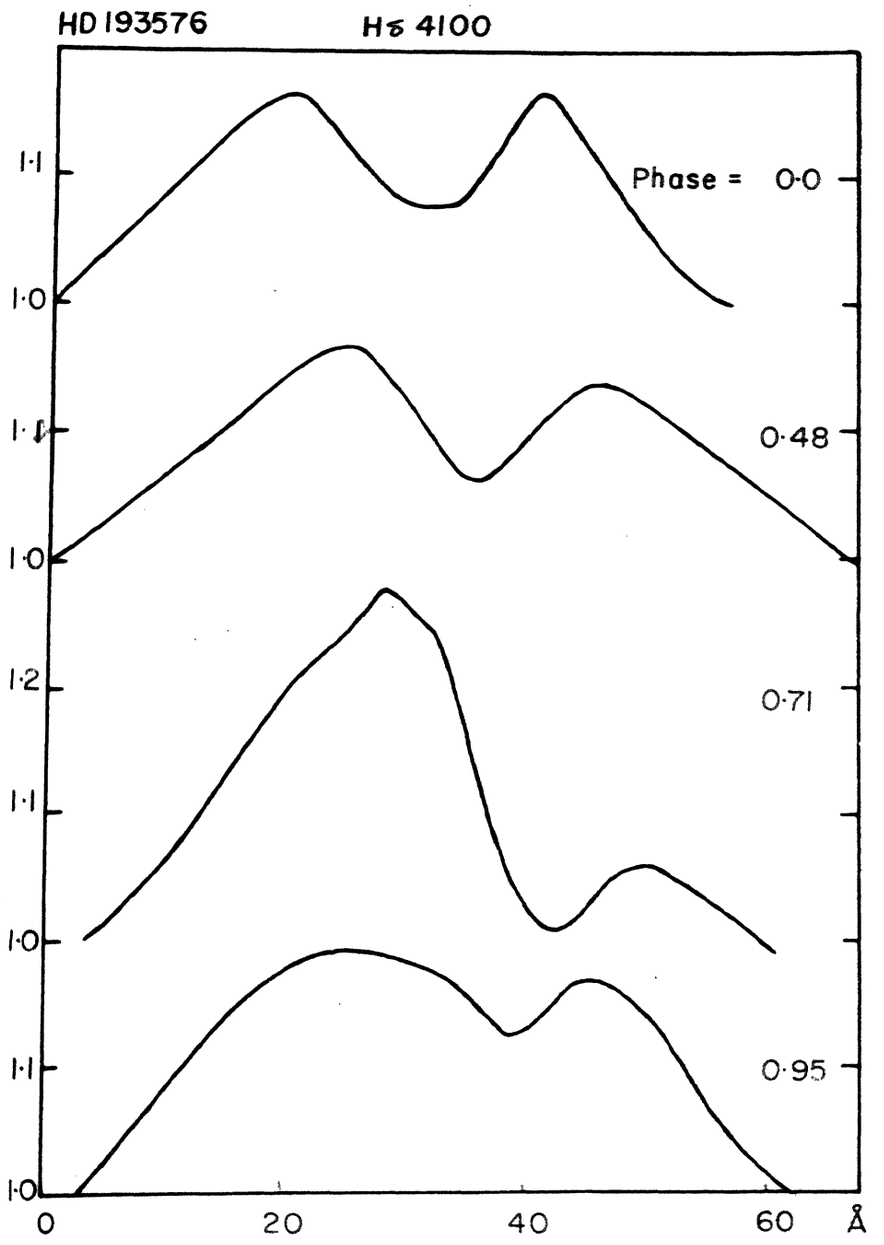
HD 193576
Hδ 4100
Phase = 0·0
0·48
0·71
0·95
1·1
1·0
1·1
1·0
1·2
1·1
1·0
1·1
1·0
0
20
40
60
Å

Figure V-12b

The profiles of 4340Å in HD 193576 obtained at phases 0.0, 0.48, 0.71 and 0.95 (D)

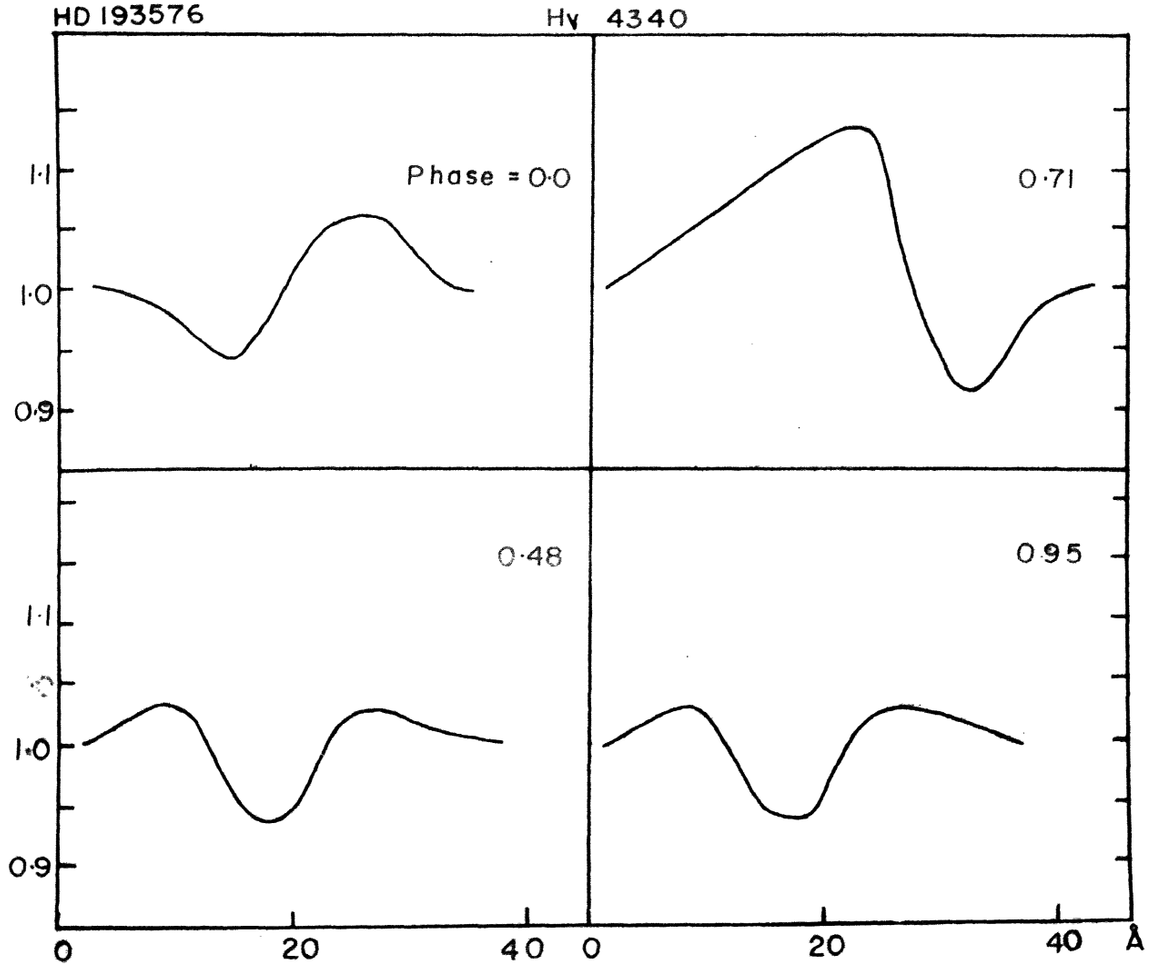
HD 193576
Hγ 4340
Phase = 0·0
0·71
0·48
0·95
1·1
1·0
0·9
0
20
40
Å

FIGURE V-13

The higher members of the Balmer series in absorption of HD 193576 obtained at primary and secondary minima.

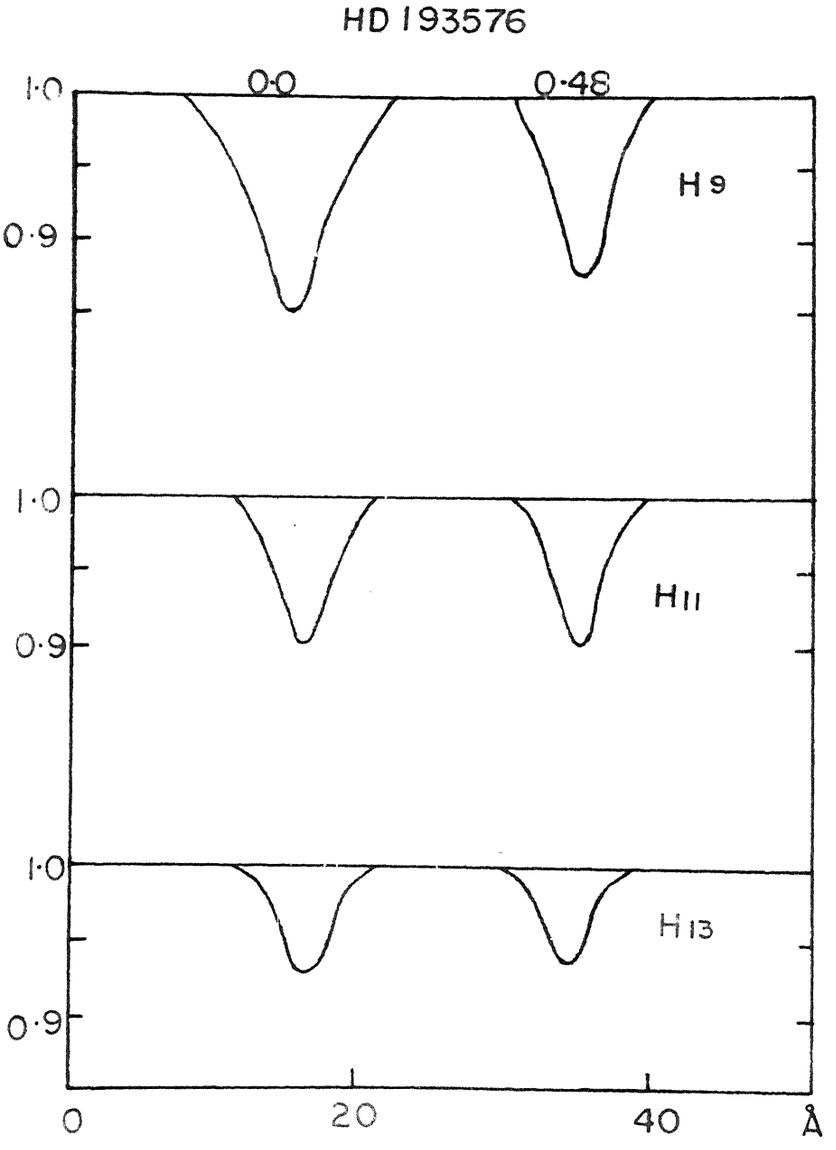
HD 193576
0·0
0·48
1·0
0·9
H 9
1·0
0·9
H 11
1·0
0·9
H 13
0
20
40
Å

The higher members of the Balmer series that originate in the O star atmosphere are widened at primary minima when the O star shines through the electron scattering envelope of the Wolf-Rayet star. Fig.V-13 indicates the differences in profile for H9, H11 and H13 for the two phases representing primary and secondary minima. The increase in widths is obvious, confirming our speculations regarding the electron scattering envelope. However, the intensities of the hydrogen lines increase by a small amount at this phase. Unless more quantitative information is available, it may be premature at present to consider this as definite evidence of enhanced hydrogen absorption in the Wolf-Rayet atmosphere, even though such a process is normally feasible.

5.4. HD 193928.

This faint Wolf-Rayet star has a spectral type on the Beals classification between WN5 and WN6. On the Hiltner scheme it is categorized as WN6-B. The emission lines are broad and quite intense and hence are easier to measure than in any other Wolf-Rayet binary of the WN sequence. The only existing orbit of the star is given by Hiltner in which he has given the velocity measures of 4686A and 4603A. Hiltner has pointed out that

Table V-8

The velocity measures of HD 193928

Plate.	J.D. of Observation.	Phase	Velocities in Km/Sec.		
			4058o	4603o	4635o
32598	2434144.97	0.60	-150.5	+62.5	+221.4
32601a	145.95	0.56	-173.1	- 53.5	+ 98.1
32601b	145.98	0.56	-186.2	- 92.4	+132.2
32605	146.90	0.51	-147.1	- 98.7	+ 91.3
32632	170.92	0.40	-270.0	-195.3	- 4.6
32635	171.88	0.36	-265.8	-288.0	- 97.0
32643	173.95	0.26	-261.0	—	- 61.2
32655	175.97	0.17	-265.5	-228.7	-53.0
32660	176.83	0.13	-295.7	-337.6	- 80.0
32668	177.95	0.08	-152.5	-172.4	- 19.2
32684	194.94	0.29	-265.7	-266.1	- 90.5
32688	195.91	0.25	—	-276.0	- 47.0
32724	200.98	0.00	- 80.9	-274.1	+ 37.2
32728	201.91	0.97	- 29.0	-222.5	+ 23.6
32732	202.96	0.92	- 29.4	-119.4	+ 70.8
32747	224.73	0.92	—	- 85.9	+ 27.2
32754	225.85	0.87	- 39.7	- 67.5	+ 76.5
32762	227.93	0.77	- 28.2	+ 61.6	+137.4

4058A experiences severe changes in line profile, and at the same time, and there are numerous occasion when the displaced absorptions of 3933A and 4471A exist.

My determination of the orbit of the star rests on 18 spectrograms obtained at Mount Wilson. The lines 4686A, 4058A and 4603A have been measured for this binary star. Because of the faintness of the star, the spectra could not be exposed well enough to make the absorption lines visible in the binary. They were primarily obtained for the purpose of spectrophotometry of the emission lines. The velocities measures of this star are given in Table V-8. The normal equations

10.0000x	-1.2529y	-1.3792z	-1.6839a	-1.3969v	-11.5[illegible]=0
	+4.3106	-0.5104	-0.7341	-0.8419	-14.2093=0
		+4.1671	-0.1123	+0.6627	-28.6698=0
			+5.8530	-0.7423	-68.6964=0
				+3.3713	+37.5176=0

yield the following final elements

P = 21.64 days
e = 0.122 ± 0.0168
V_0 = +59.80 ± 7.642 Km/sec
K = +147.00 ± 9.1474 Km/sec
ω = 51° 28' ± 20° 51'
T0 = 0.343 ± 0.0034

A comparison of these elements with those of Hiltner's is of some interest. I have assumed the period

given by Hiltner as 21.64 days and the preliminary phase zero is JD 2434179.77. The preliminary orbit was assumed to be circular and using Sterne's method an eccentricity of 0.12 is derived. The γ-axis of the 4686A velocity curve has a value of 59.8 Km/sec., in exact agreement with the value derived by Hiltner. However, the value of K differs by about 17 Km/sec. I have not carried through an analysis of the elements using 4058A. Fig.V-14 shows the velocity curve of 4686A in the upper half of the diagram and the 4058A points are shown in the lower half. The points defining 4058A indicate an arbitrary shift in phase. The solid curve is the computed velocity curve of 4686A, the dashed curve is the velocity curve displaced by 0.1P.

It is difficult to explain the nature of this phase shift as seen in 4058A. It is quiet likely that over the duration of the observations, there has been violent activity on the star causing such a displacement.

Fig.V-15 is a plot of the emission line HV 4603 with the solid curve representing the variation of 4686A. It is seen that the curve fits the points well but for the displacement in the γ-axis by 185 Km/sec. The mass function derived is 4.6215 solar masses.

FIGURE V-14

The velocity measures of HD 193928
Upper diagram - HeII 4686
Lower diagram - points are of HEV 4351. The
solid curve is the theoretical curve of 4686A.
The dashed curve is this 4686A Curve displaced
in phase.

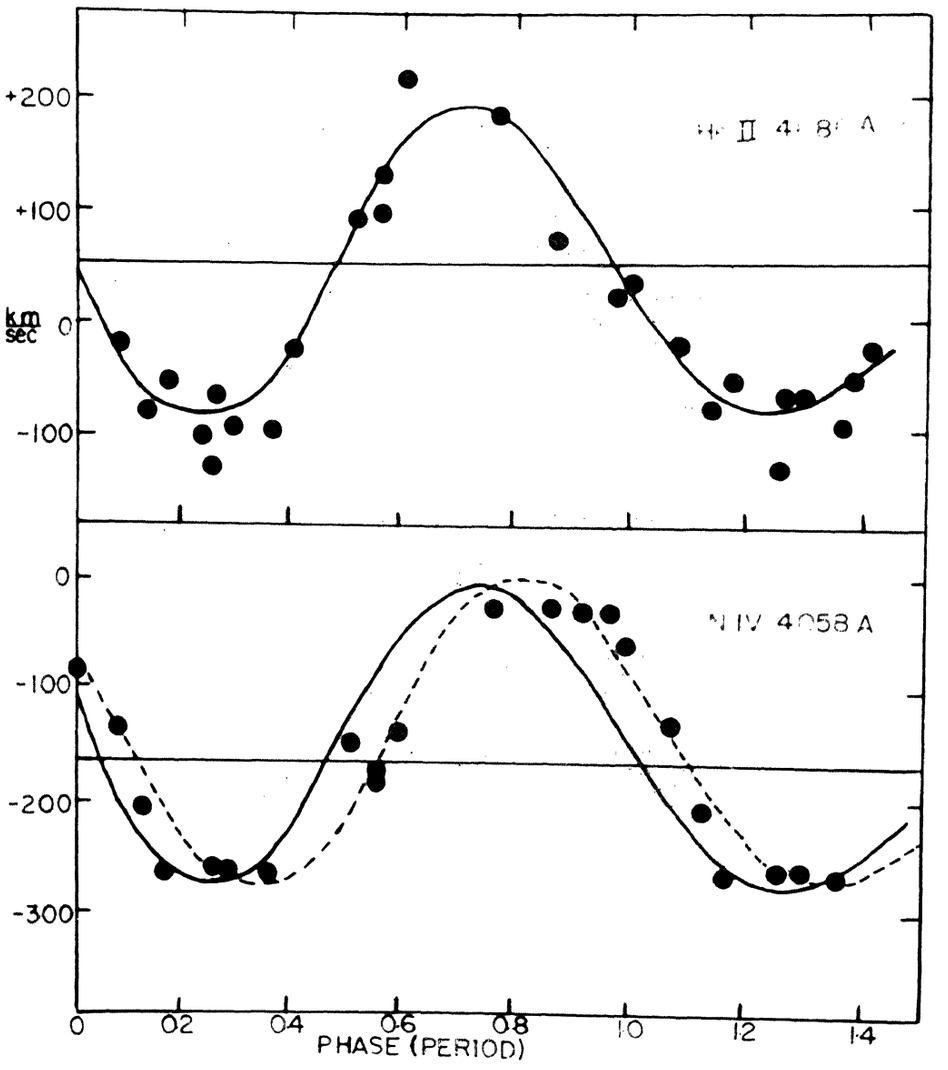
+200
+100
km sec 0
-100
0
-100
-200
-300
N IV 4058 A
0
02
04
06
08
10
12
14
PHASE (PERIOD)

Figure V-15

The velocity measures of HV 4633 in NGC 1903[3]
The curve is the theoretical curve of 4616.

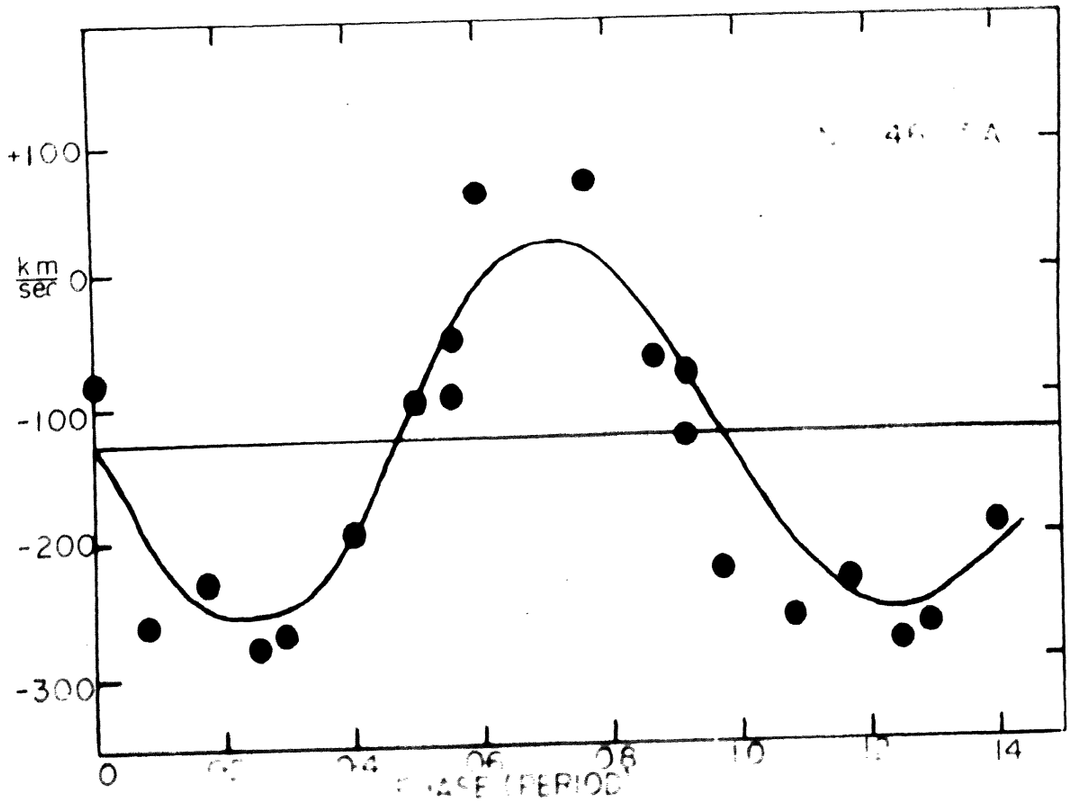
+100
km/sec 0
-100
-200
-300
0
14

The study of the profiles in a system of this kind is obviously of considerable interest. Fig.V-16 shows the variations experienced by HeII 4686 at four different phases. At phase zero, the Wolf-Rayet star is farthest from the observer. At this phase, the profile of 4686A is narrow with a slight hump on the longward side. At a phase when the Wolf-Rayet star is closest to the observer, which happens to be at phase 0.5, the profile is almost symmetrical and narrow. The profile is broad at ph ases 0.77 and 0.60 and the hump seen near phase zero continues to prevail. Fig.V-17 and V-18 give the profiles of 4200A and HeII 4860. In both the sets, it is seen that the lines are narrow at phase zero. On the other hand, the profiles at elongations are wider than at phase zero and on some occasions as seen in 4200A, there are suggestions of displaced humps in the structure. The profile of 4200A, at phase 0.51, has a hump on the shorter wavelength side. However, the reliability of the presence of this hump cannot be stated with any degree of certainty because there has been no additional plate taken on the same day to confirm it.

The variations experienced by 4058A have been striking during the period of observation by Hiltner.

Plate V-16

Line profiles of HeII 4686 in HD 193928 for different phases.

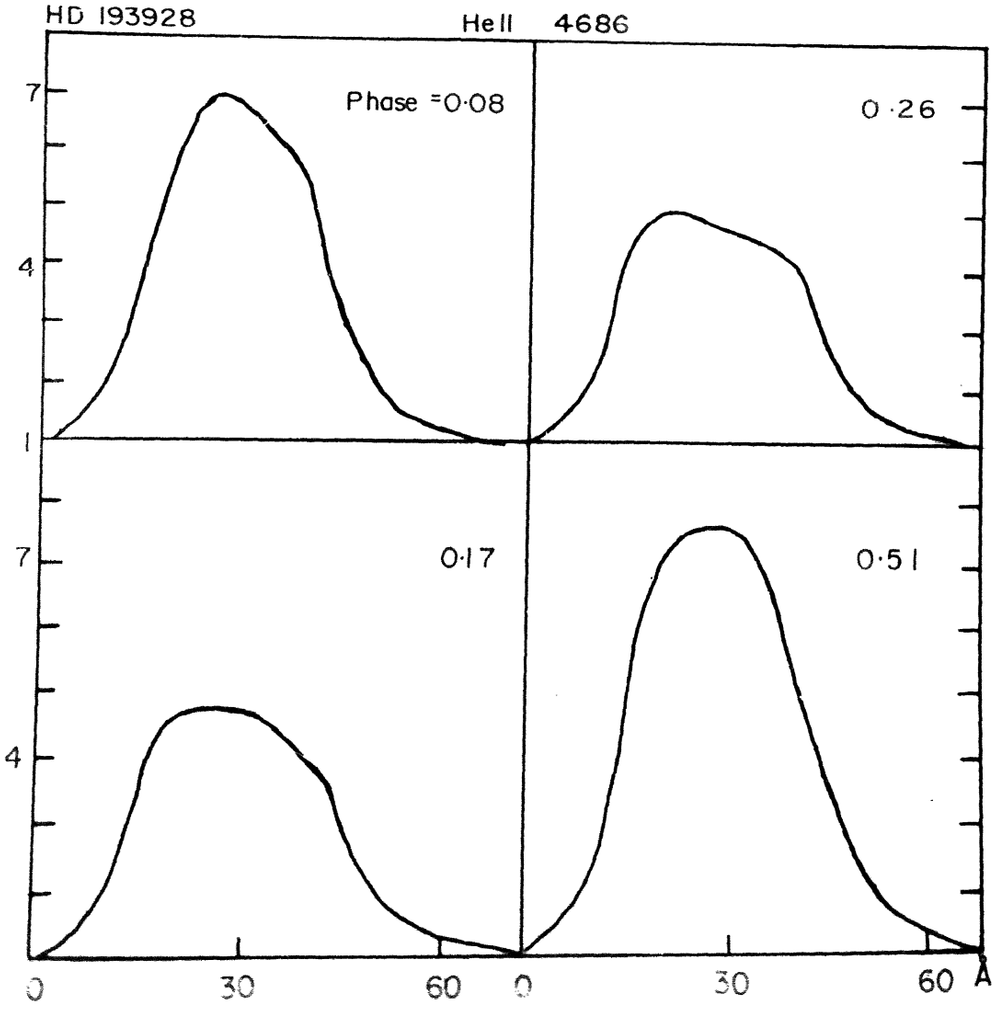
HD 193928
HeII 4686
Phase =0·08
0·26
0·17
0·51
7
4
1
7
4
0
30
60
0
30
60
Å

FIGURE V-17

Line profiles of HeII 4200 in HD 193928
for different phases.

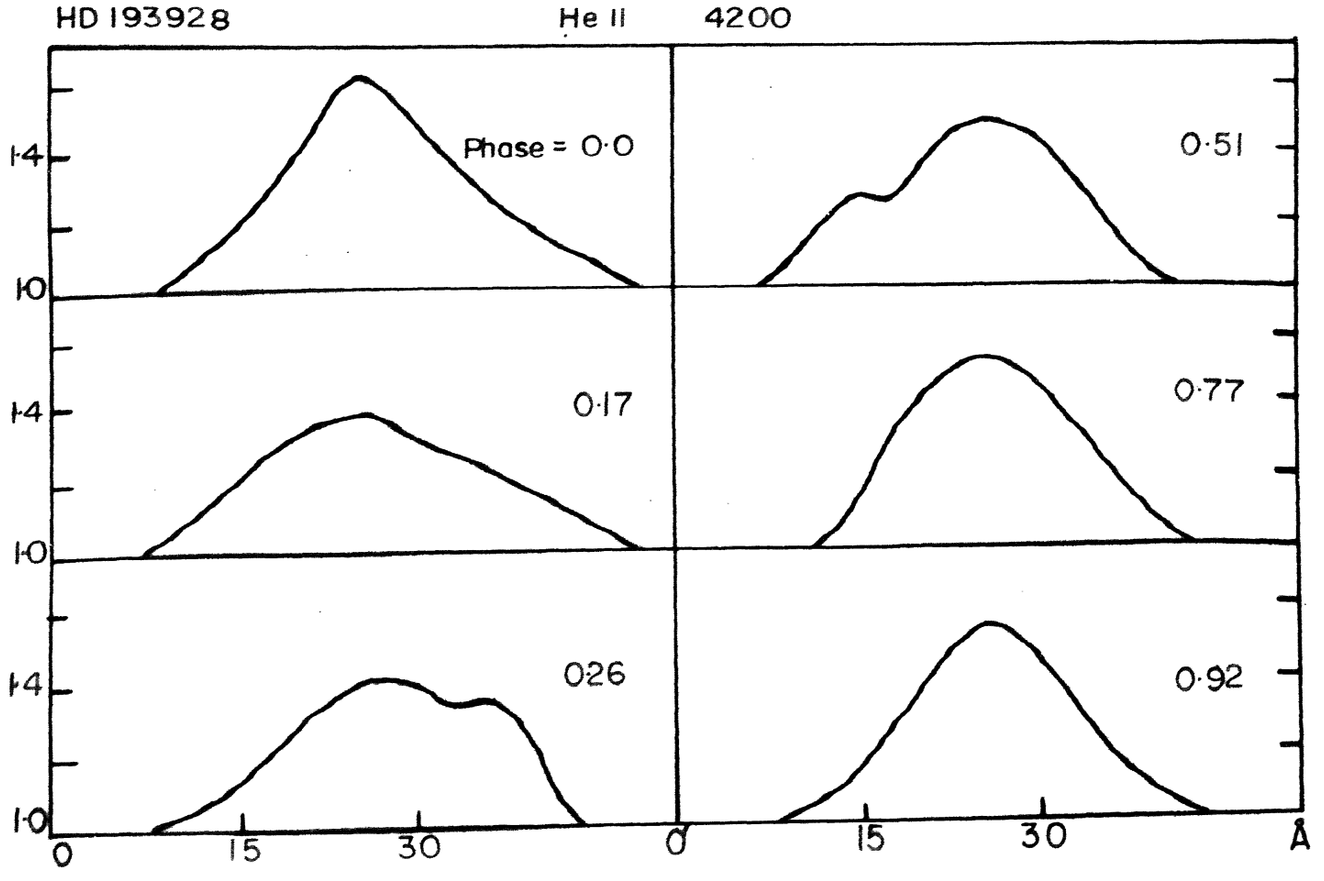
HD 193928
He II 4200
Phase = 0·0
0·51
0·17
0·77
026
0·92
1·4
1·0
0
15
30
Å

FIGURE V-III

Line profiles of 4861Å in HD 193283 for different phases

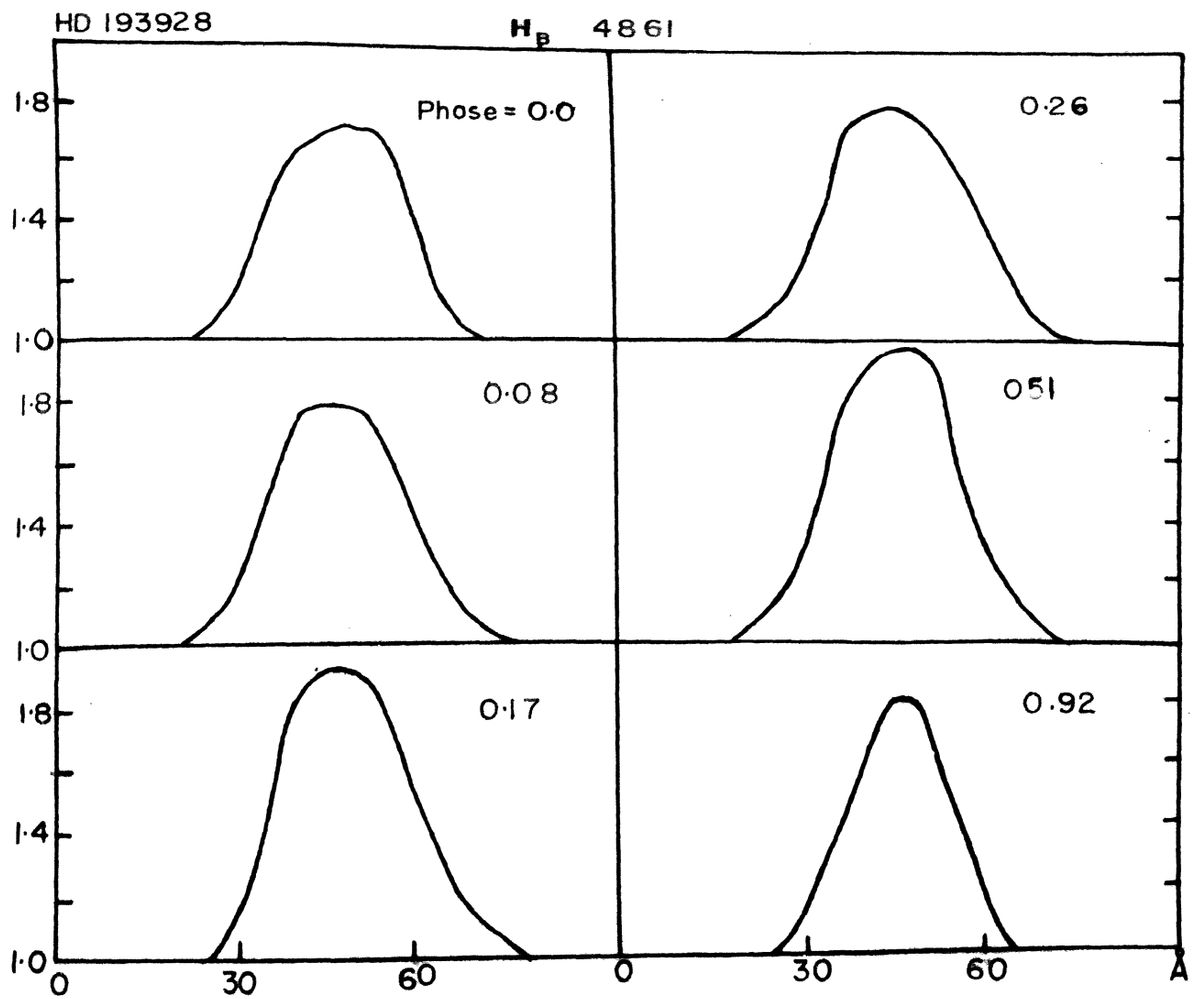
HD 193928
H_β 4861
Phose = 0·0
0·26
0·08
051
0·17
0·92
1·8
1·4
1·0
0
30
60
Å

Plate V-12

Line profiles of HV 4058 in HD 193928 for
different phases.

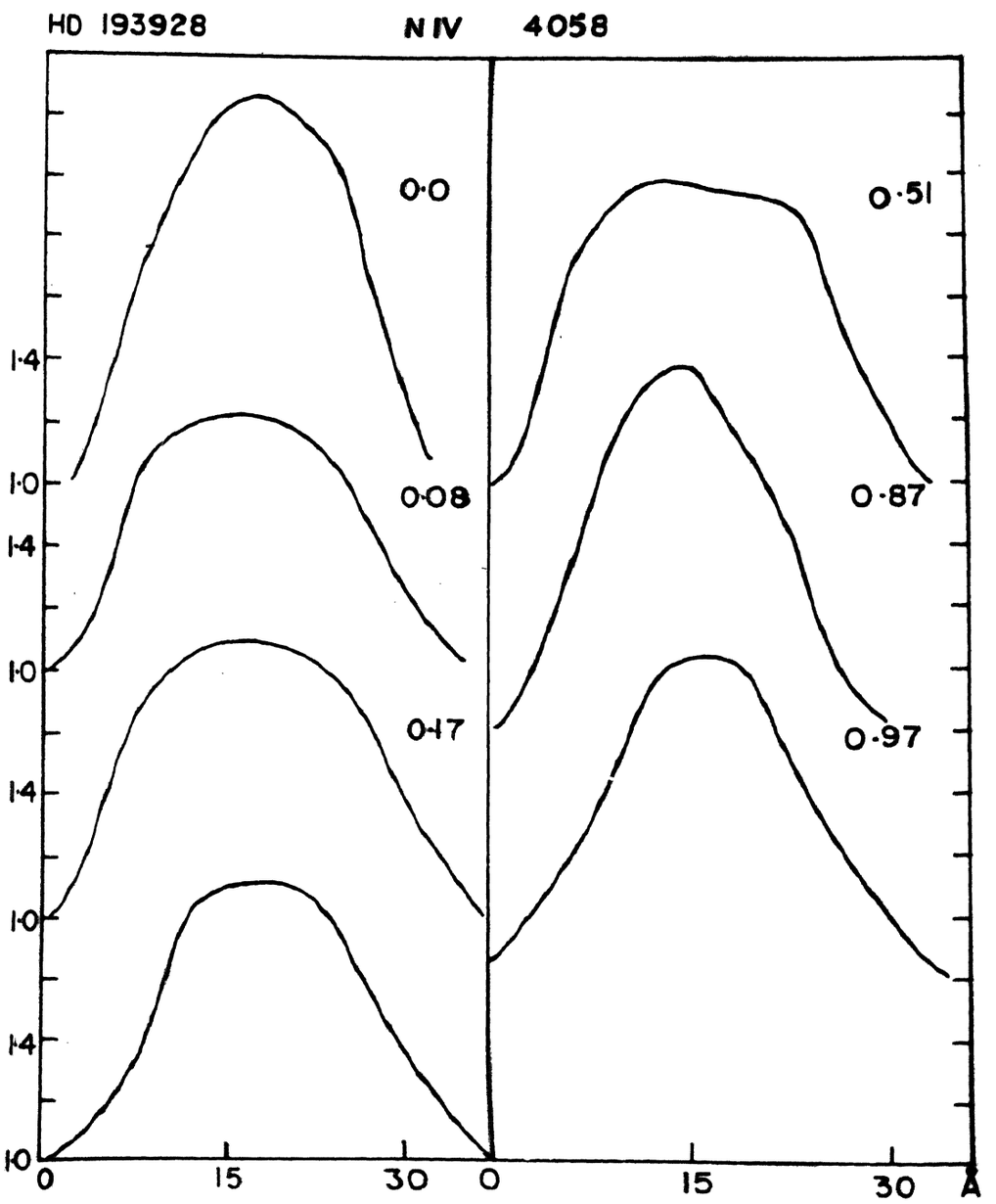
HD 193928
N IV 4058
0·0
0·08
0·17
0·51
0·87
0·97
1·4
1·0
1·4
1·0
1·4
1·0
1·4
1·0
0
15
30
0
15
30
Å

Our observations make it a certainty (Fig.V-19) that there are changes in the profile of this emission line. The line is more narrow near phase zero and similar to the pattern set by the others. It is more broad at the elongations. However, the profile at phase 0.51 is quite wide and indicates a rather intense hump on the longward side. This perhaps, is the kind of variation noted by Hiltner and it is the presence of this distortion in the profile that prevented me from carrying through an analysis of the orbit.

The system of HD 193928 is, therefore, one which seems to have striking spectral variations. One is reminded of the variations seen in HD 50896, which of course is not an established binary system. The amplitude of velocity variation is appreciable and it is quite likely that this star will turnout to be an eclipsing variable. If it is so it would have only grazing eclipses. A comparison of the mass functions with that of CQ Cephei (f(m) = 4.449) is of interest. The values are quite large and it does seem possible that HD 193928 can be a good candidate in any search programs of eclipsing binaries among Wolf-Rayet stars.

5.5. HD 186943.

The spectrum of this star on the Beals classification is WN5. On Hiltner's scheme it is WN5-A. The emission lines seen on the blue plate are HeII 4686 the two nitrogen V lines at 4619A and 4603A together with NIV 4058. The Pickering series of HeII in emission are present, but are quiet faint for accurate measurement. The NV lines do not seem to have violet absorption edges. There are some absorption features seen in the spectrum. The spectra available for my study were obtained with a glass prism and hence it was not possible to observe the higher Balmer series. According to Hiltner (1945) these absorption features are extremely weak.

The only orbit of the star available until today is the one derived by Hiltner. This study yielded a period of 9.55 days on the basis of velocity measures of 4686A, the NV lines and NIV 4058. The elements were determined essentially from the curve of HeII 4686. Hiltner reported a phase shift between the velocity curves of 4686A and 4603A. Hiltner also derived a velocity curve from the hydrogen absorption lines.

In this study, I had available, only 10 spectra

Table V-9

The velocity measures of HD 186943

Plate	J.D. of Observation.	Phase.	Velocities in Km/Sec.		
			4686e	4603e	4058e
32653	2434175.75	0.78	-122.4	-116.2	-212.2
32659	176.78	0.89	- 6.8	- 32.3	-212.2
32667	177.87	0.01	+149.6	- 38.8	- 43.3
32686	195.79	0.88	+102.0	-180.8	-324.8
32720	200.74	0.39	+136.0	+103.3	-120.9
32725	201.71	0.50	- 27.2	- 58.1	-160.3
32730	202.84	0.61	-102.0	- 90.4	-316.1
32748	224.80	0.91	+ 20.4	- 6.5	-295.9
32761	237.86	0.25	+232.4	+219.6	-199.3
32766	228.90	0.33	+170.0	+ 38.8	+ 4.3

covering the entire cycle. The plates were exposed for spectrophotometry of NIV 4058, since Miltner has indicated an anomalous behaviour of the 4058A emission feature. Preliminary orbits were obtained for 4058A, 4686A, and 4603A. The γ -axes derived from these show that there is fair agreement between the values derived from NIV 4058 (75 Km) and NV 4603 (40 Km). On the other hand, HeII 4686 has a γ -axis value of 105 Km. The fact, that the NV 4603 line has a systemic velocity equivalent to that of NIV 4058, indicates that the NV lines have little or no violet absorption edges. The observations reported here were combined with those of Miltner to yield a revised value of period of 9.5594 days. The phases were computed with the formula

Phase zero = JD 2431253.041 + 9.5594E

The Miltner observations of 4686A were combined with the 4686A measures reported in this study and used for an improved determination of the orbital elements.

The normal equations

10.0000x	-0.1792y	-0.3050z	-1.4827u	-1.7203v	- 0.0100=0
	+2.5804	-0.6818	-0.6698	-0.7375	-17.3586=0
		+3.1132	-0.3018	+1.0337	-45.8361=0
			+3.8364	+0.5016	-17.2323=0
				+4.2390	+74.4057=0

Table V-10

HD 186943

4509Å	4753Å	4673Å
P = 9.5534 days	P = 9.5534 days	P = 9.5534 days
e = 0.0361 ± 0.0214	e = 0	e = 0.0162
ω = 153° 54' ± 6° 54'	ω = 150°	ω = 149°
K = 211.5 ± 12.3 Km/sec	K = 165 Km/sec	K = 162.5 Km/sec
V_0 = 136.74 ± 6.71 Km/sec	V_0 = +170 Km/sec	V_0 = +[illegible] Km/sec
f = 0.235 ± 0.0172		
i = 0.654		
	$M_p \sin^3 i$ = 21.0	
	$M_w \sin^3 i$ = 5.8	

FIGURE V-20

The Hoff 4086 velocity curve of HD 196943

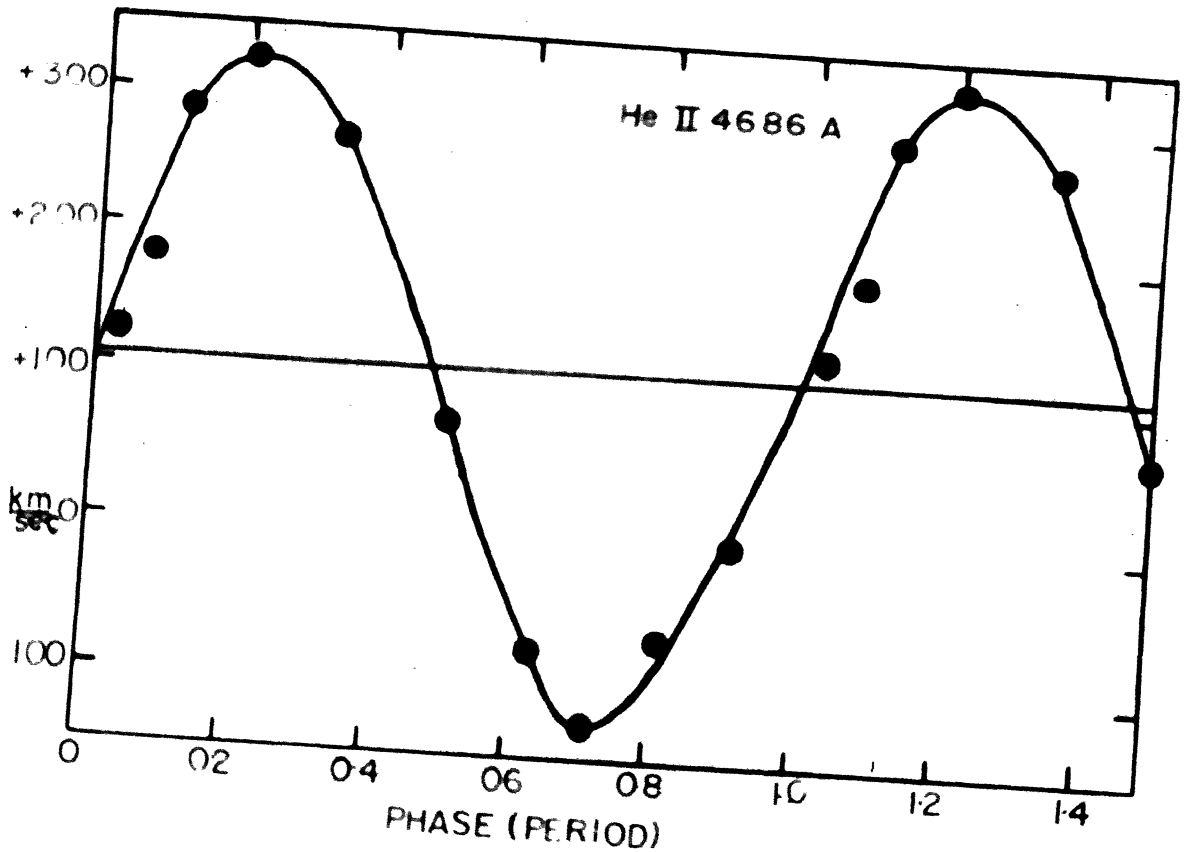
He II 4686 A
+300
+200
+100
0
100
km/sec
0
0·2
0·4
0·6
0·8
1·0
1·2
1·4
PHASE (PERIOD)

PLATE V-21

The velocity curves of HD 146043
Upper diagram HV 4958
Lower diagram HV 4993

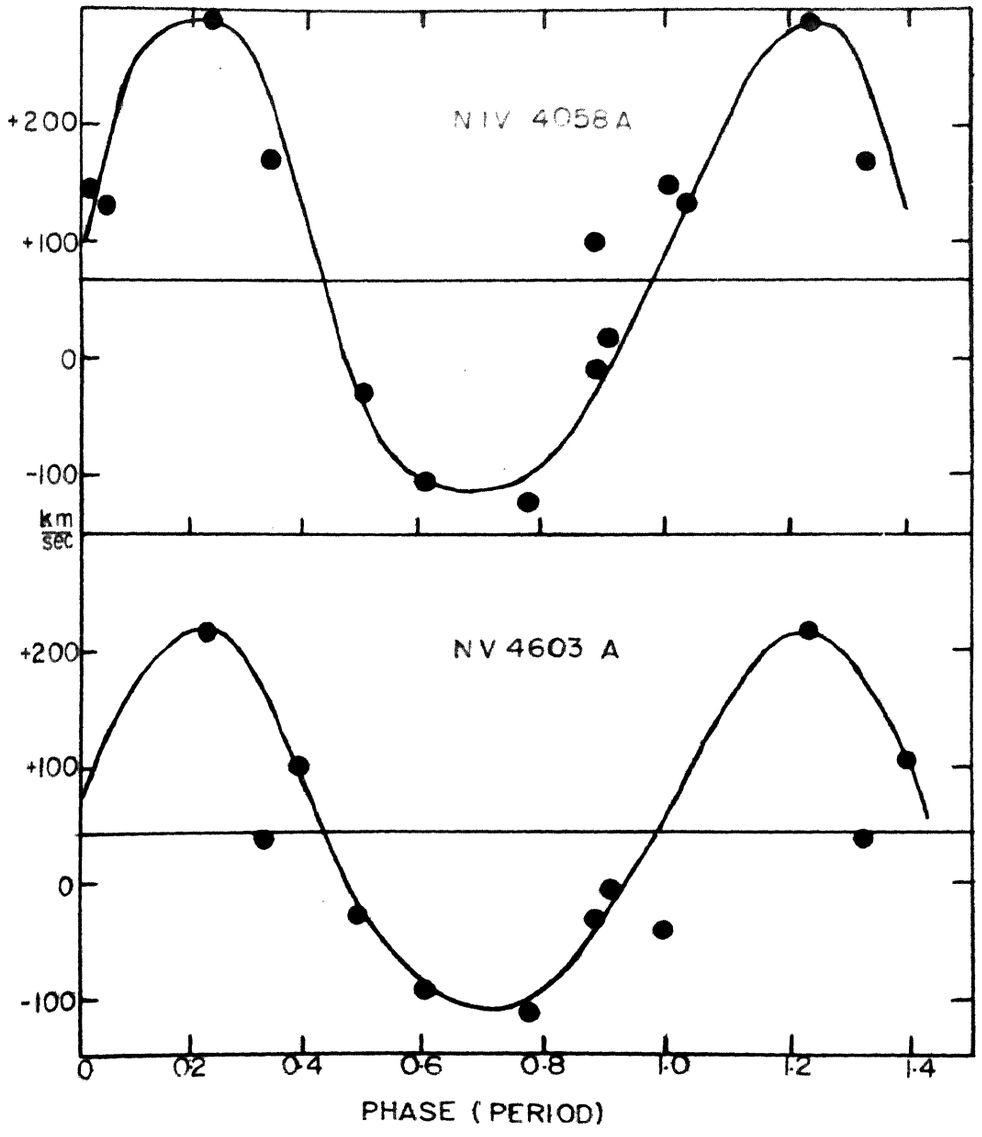
N IV 4058 A
+200
+100
0
-100
km/sec
N V 4603 A
+200
+100
0
-100
0
0·2
0·4
0·6
0·8
1·0
1·2
1·4
PHASE (PERIOD)

FIGURE X-22

Line profiles of HV 4358 in SS 136543

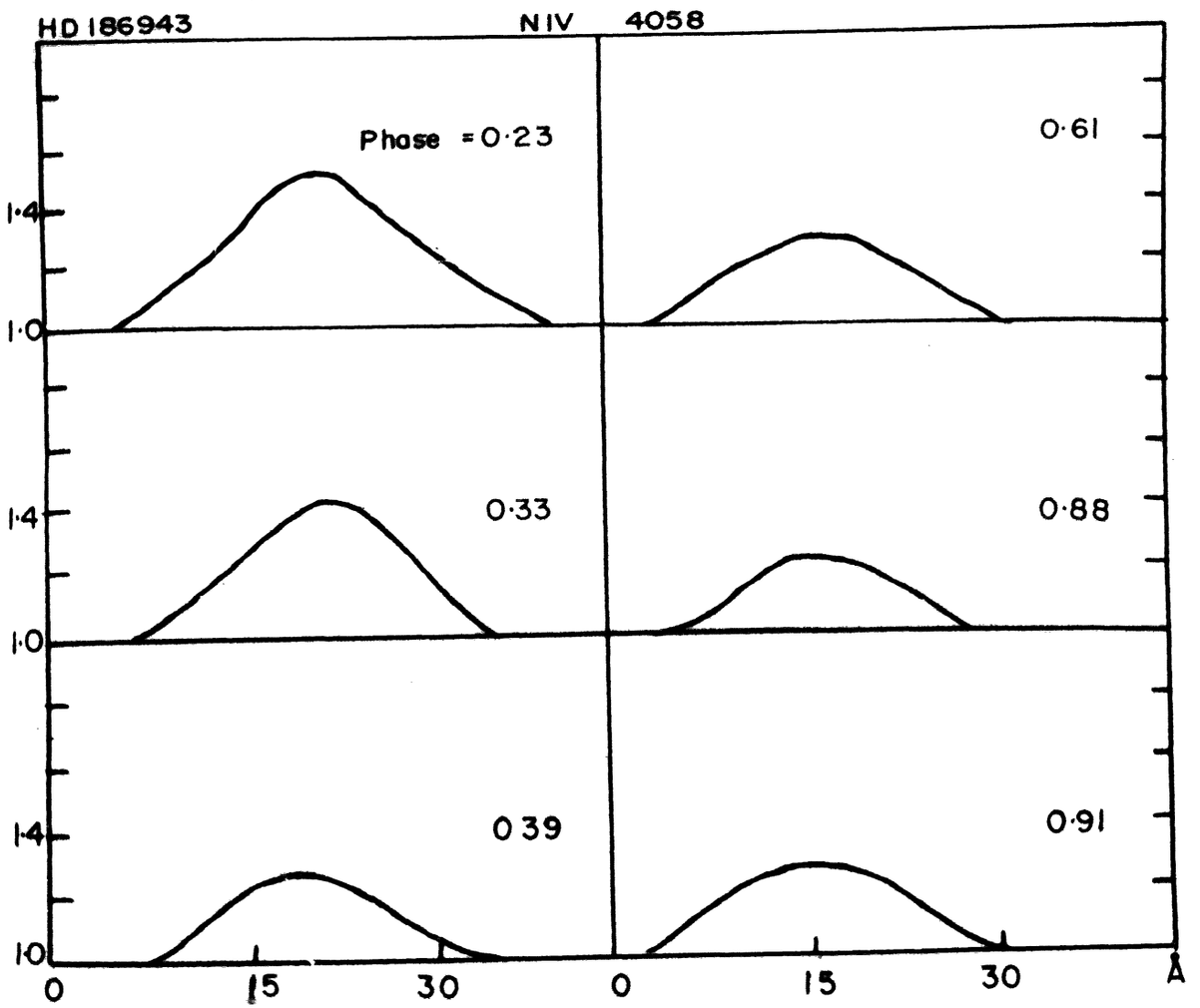
HD 186943
N IV 4058
Phase =0·23
0·61
0·33
0·88
0 39
0·91
1·4
1·0
1·4
1·0
1·4
10
0
15
30
0
15
30
Å

gave the following final elements:

P = 9.5594 days
e = 0.0361 ± 0.0211
ω = 150° 54' ± 6° 54'
K = 211.58 ± 12.9325 Km/sec
V_o = 106.74 ± 6.715 Km/sec
$f(M)$ = 0.235 ± 0.072
T = 0.654

The preliminary orbits obtained for 4058A and 4603A are given in Table V-10 for comparison with the values obtained for 4686A. Figs.V-20 and V-21 show the velocity curves obtained in 4686A, 4603A and 4058A.

The 4058A emission line is extremely weak in this star. In order to obtain this with the correct density, it was necessary to over-expose the 4686A region. As such, we have no line profiles of 4686 for this star. The 4058 line at the time of observation does not seem to exhibit the striking changes reported on by Hiltner. At a phase close to zero in Fig.V-22, the line is sharper than at other phases. It is quite possible that by a coincidence, the plates obtained at Mount Wilson happened to fall during one of the quiescent spells of this system. An interesting feature reported by Hiltner was that there is a phase difference between the velocity curves of 4686A

and 4603 NV. Essentially from our observations, we fail to find such a phase shift. This is also an added confirmation of the fact that the spectra available for this study were taken at a quiet phase.

5.6. HD 211853.

The spectral type of this star is WN6. Hiltner classifies it as WN6.5-A. The predominant line is HeII 4686. The rest of the emission lines are fairly weak. Absorption lines at H_β, H_γ and H_δ are present. The velocities of these indicate that they originate from the companion. Occasionally a violet shifted 4411A is seen. Hiltner (1945) has given an orbit for the star utilising the velocity measures of 4686A, 4058A and 4603A. His measures of the H lines were not such as to give a confident measure of the velocity curve of the companion. Recently Hiellaing and Hiltner (1963) has reported on the light variation of this star. The obvious characteristic of the light curve is the intrinsic variability of the system shown by a lack of repeatability from cycle to cycle. An improved period of the binary has also been derived by Hiltner. This is one of the stars in which Hiltner (1950) has measured the emission line intensities photoelectrically and found that when the Wolf-Rayet star was eclipsed by the companion the emission intensity was

the greatest. The observations of light variations by Hiltner through UBV filters indicate that an eclipse of the system does take place but the intrinsic variation in the Wolf-Rayet star is such as to prevent easy study of this light curve by conventional methods.

I have only 10 spectra, primarily obtained for spectrophotometry, available for velocity measures. However, these have been utilized for measuring the velocities of 4686A, NIV 4058, NV 4603 and the hydrogen lines of H γ and H δ of the companion. These measures are given in Table V-11. Only preliminary elements have been derived on the basis of the three emission lines (Fig.V-23). These indicate that the system is one of small eccentricity. The mass function values derived are given in Table V-12. There is close agreement between the mass functions derived from HeII 4686 and NV 4603 while that derived from 4058A, deviates considerably from the other two emission lines. This is in agreement with the findings of Hiltner that NIV 4058 lacks repeatability.

The velocity measures of the hydrogen lines plotted are seen in Fig.V-24, one sees a general scatter of the points but the trend of velocity is similar to what has been seen by Hiltner many years ago. It is rather

Table 11

HD 211853

Phase	Velocities		
	4686A	4603A	4[illegible]3A
0.06	+ 15	-145	-105
0.09	0	-	-160
0.20	+ 95	- 80	0
0.34	+180	+125	+ 20
0.48	+250	+280	+ 65
0.58	+ 40	+125	-160
0.64	+ 30	+120	-145
0.92	-225	-200	-290
0.93	-140	-270	-225

Table V-12

HD 211853

4536A	4358A	4023A
K = 220.00 Km/sec	K = 135.[illegible] Km/sec	K = 235.0[illegible] Km/sec
V_o = +15.70 Km/sec	V_o = [illegible] Km/sec	V_o = -5.0 Km/sec
e = 0.1256	e = 0.20[illegible]	e = 0.240[illegible]
ω = 78° 54'	ω = 63° 43'	ω = 315°
$a \sin i = 2.010 \times 10^7$ (km)	$a \sin i = 1.391 \times 10^7$ (km); $a \sin i = 2.033 \times 10^7$	
Mass function (f/m) = 7.240	Mass function (f/m) = 2.40[illegible]	f(m): 8.23[illegible]

FIGURE 23(a)

Velocity curve of HD 211853 - HeI 4686

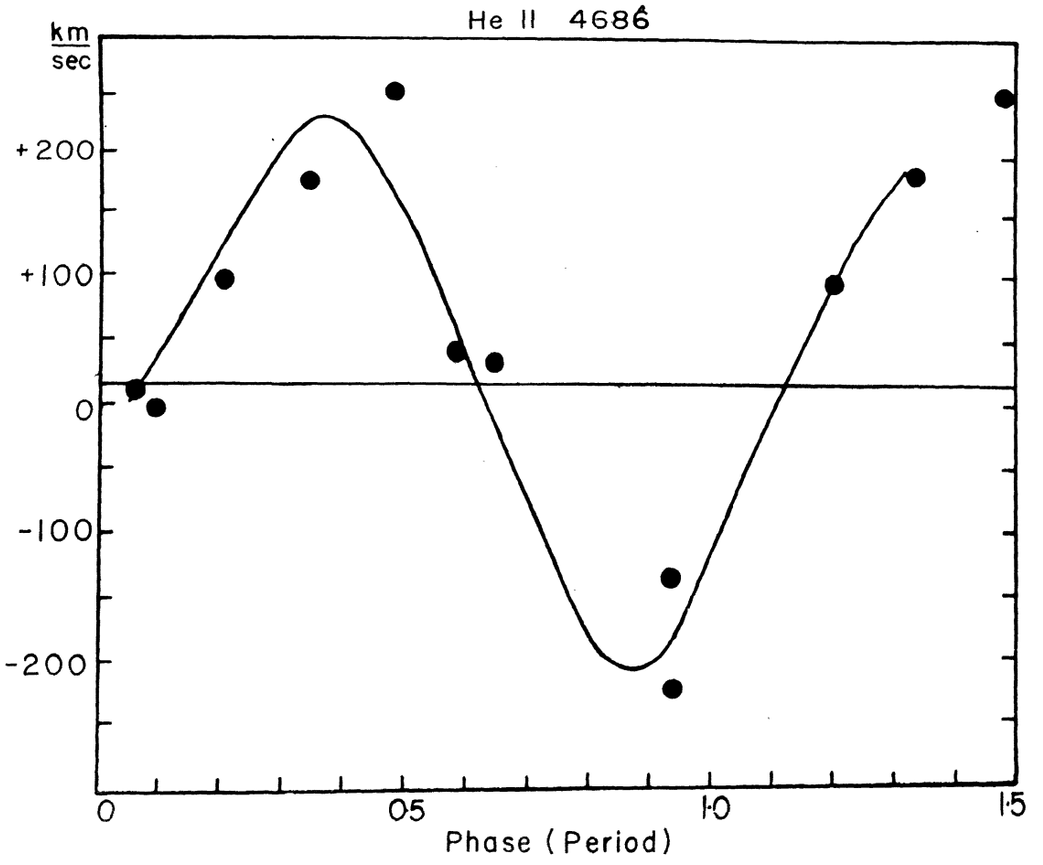
He II 4686
km
sec
+200
+100
0
-100
-200
0
05
1·0
1·5
Phase (Period)

FIGURE V-23(b)

Velocity curve of HD 211853 - HIV 4059

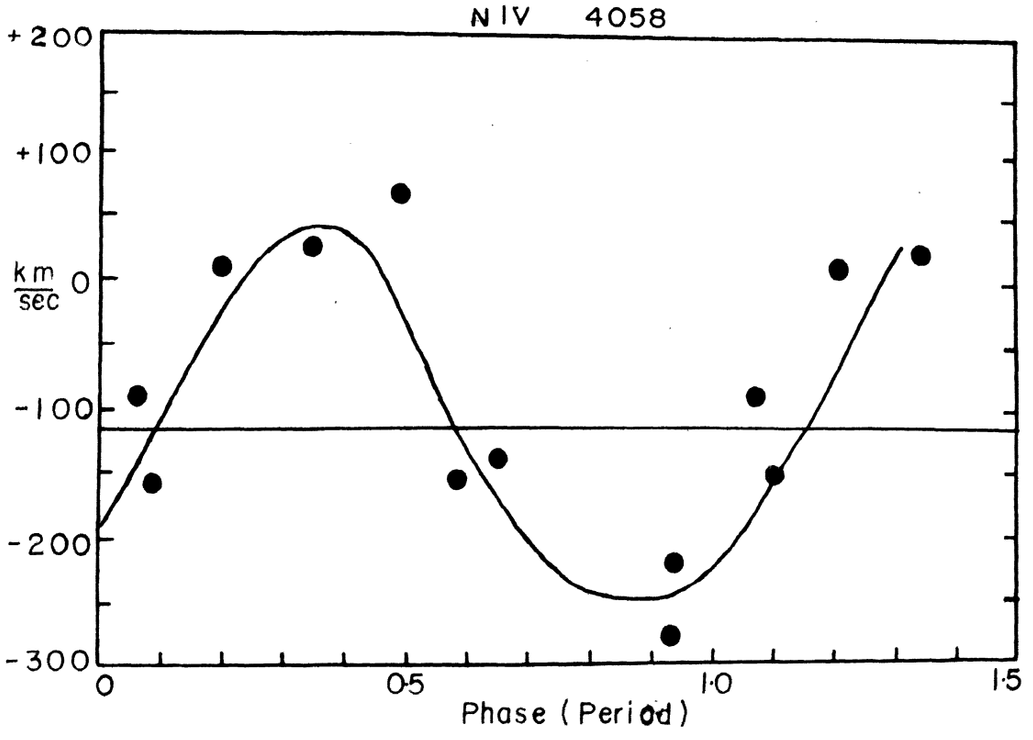
N IV 4058
+200
+100
km/sec 0
-100
-200
-300
0
0·5
1·0
1·5
Phase (Period)

FIGURE V-23(e)

Velocity curve of HD 211853 - BV 4603

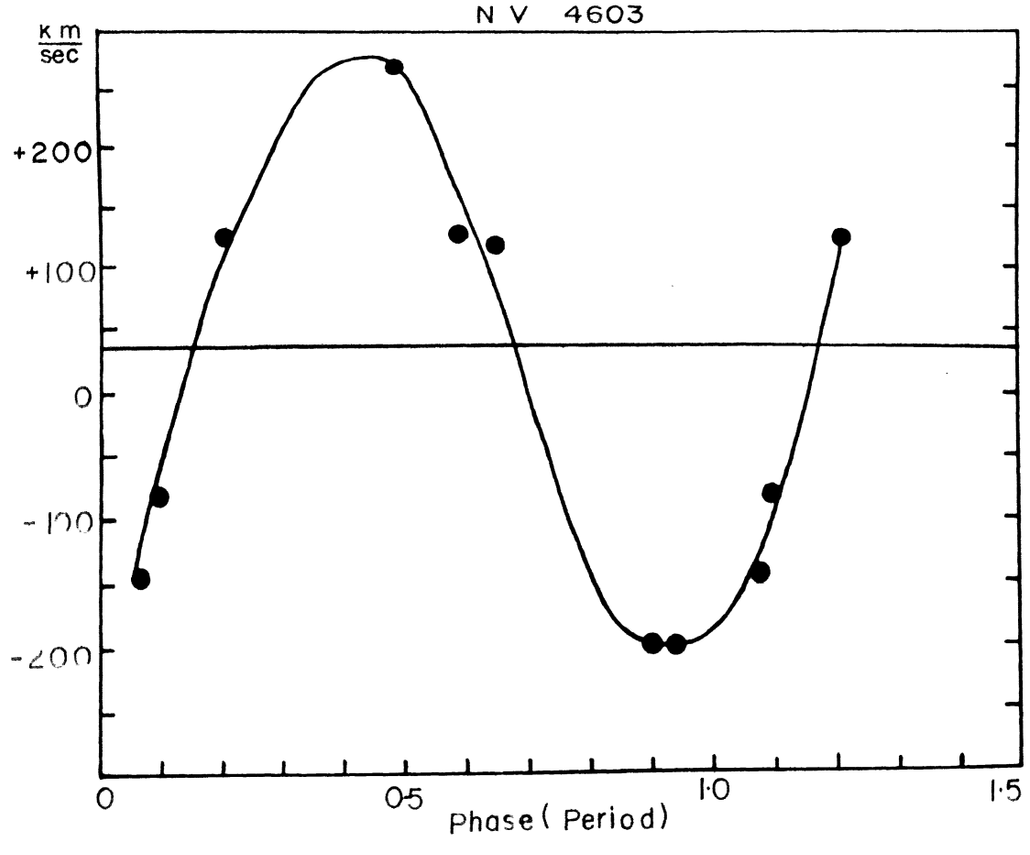
N V 4603
km/sec
+200
+100
0
-100
-200
0
0·5
1·0
1·5
Phase (Period)

FIGURE V-24

Velocity measures of the hydrogen lines
in HD 211853

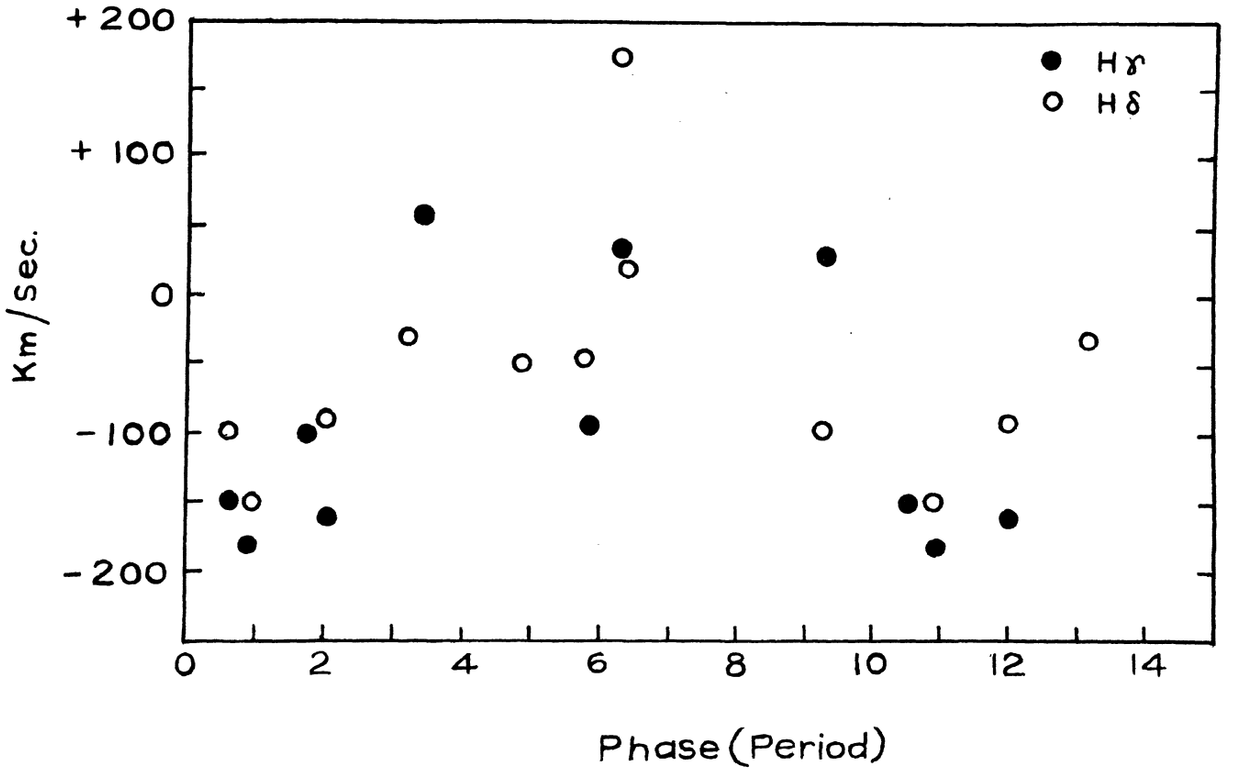
+200
+100
0
-100
-200
Km/Sec.
Hγ
Hδ
0
2
4
6
8
10
12
14
Phase (Period)

difficult to fit a velocity curve of the companion, through the points that are available, and therefore, I have made no attempt to estimate the mass of the companion.

I have derived line profiles for this system for 4686A, 4058A and 4861A (Figs.V-25, V-26 and V-27). The variations seen in HeII 4686 are reminiscent of those seen in V444 Cygni. At phase close to zero corresponding to the position, when the Wolf-Rayet star is closest to the observer, the profile is narrower than when the Wolf-Rayet star is farthest from the observer. At phase 0.47, there is a double hump structure in 4686A. This double hump is seen even at phases 0.60 and 0.61 and one can speculate on its existence even at phase 0.09. However, the fact that at phase 0.31 the profile is symmetrical indicates that this change of profile is more due to the intrinsic variations in the system than one caused by the variation of phase. The 4058A profiles show in general that in the vicinity of phase zero, the profile is narrower than it is elsewhere. The intensity of 4058A is extremely weak in this star and hence it is not easy to derive a reliable profile of this emission line. The profile of the emission line at 4860A is affected considerably by the presence of

FIGURE V-23

Line profiles of Hell 4686 in HD 211853

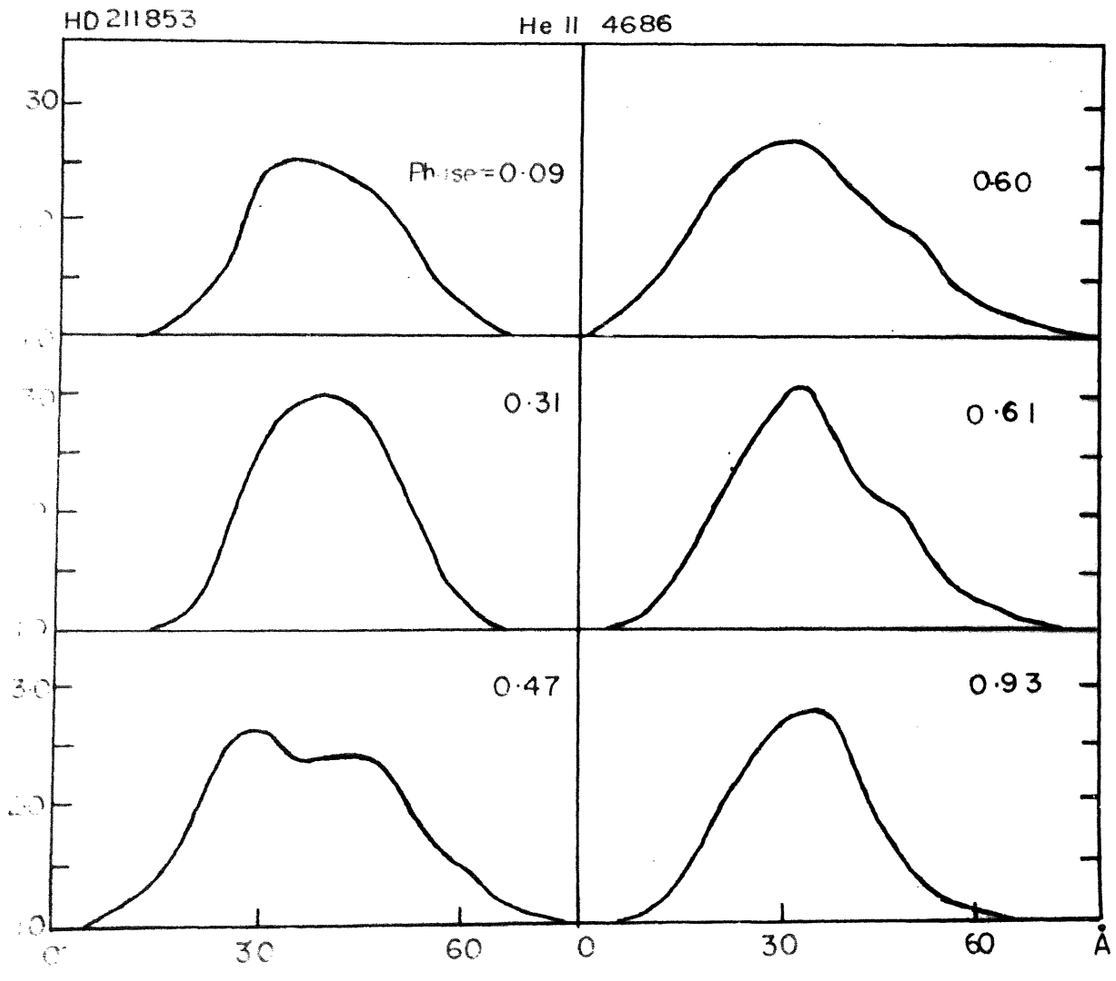
HD 211853
He II 4686
Phase=0·09
0·60
0·31
0·61
0·47
0·93
30
30
30
0
30
60
0
30
60
Å

Fig. V-26

Line profiles at different phases of V
4758 in HD 211853.

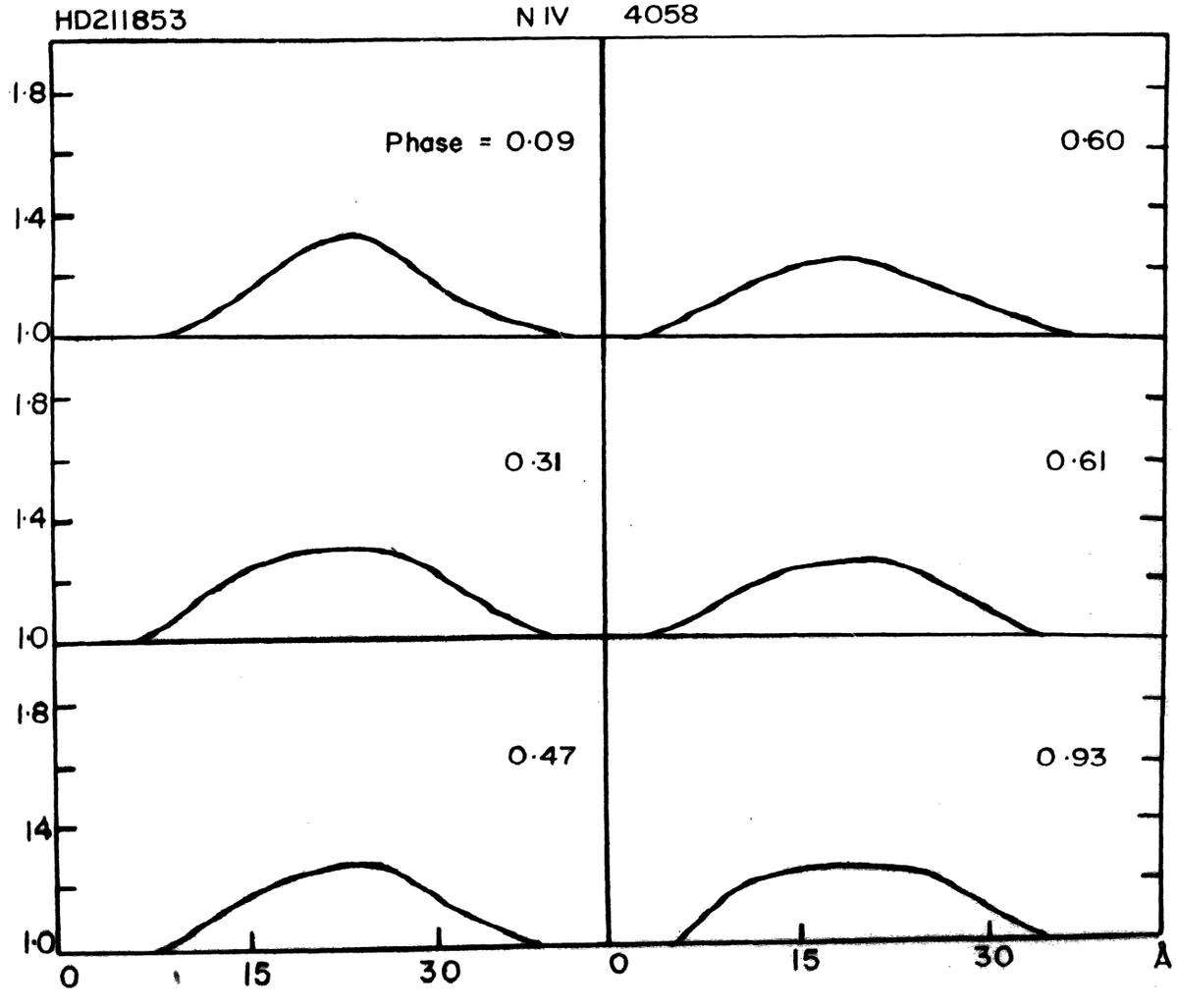
HD211853
N IV 4058
Phase = 0·09
0·60
0·31
0·61
0·47
0·93
1·8
1·4
1·0
0
15
30
Å

FIGURE V-27

Line profiles of 4686A at different phases in HD 21853

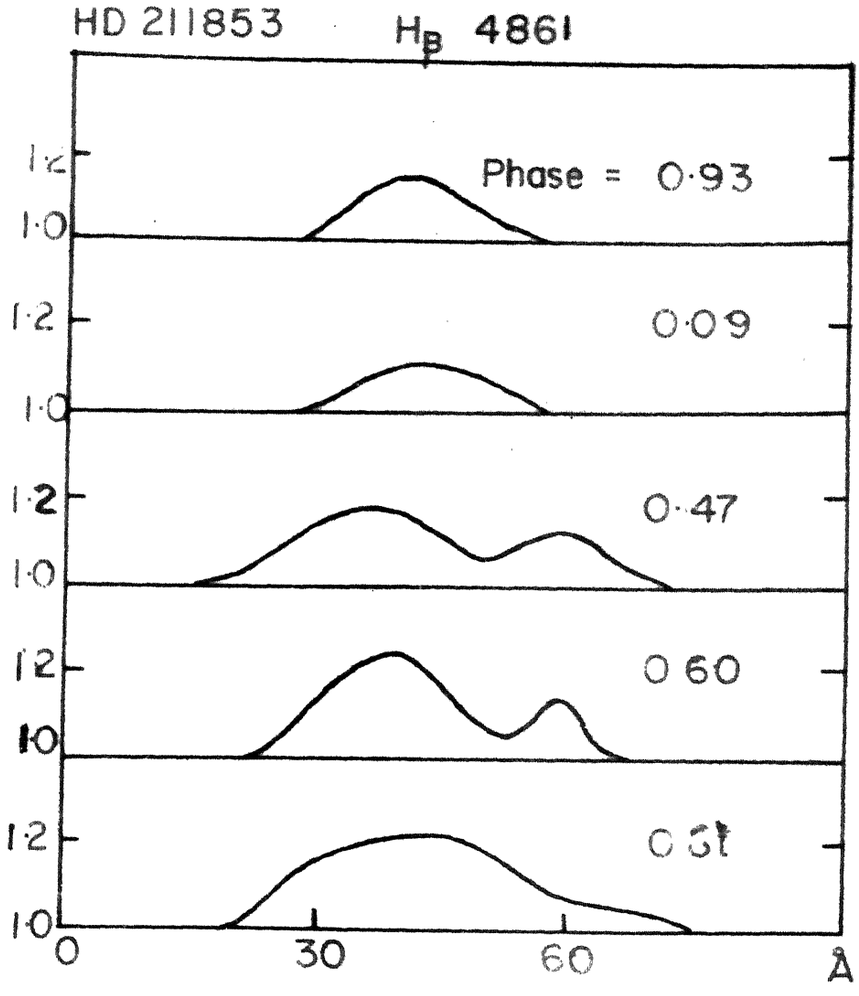
HD 211853
Hβ 4861
Phase = 0·93
0·09
0·47
0 60
0 81
1·2
1·0
0
30
60
Å

the H_β line of the companion. In general, the emission intensity of ionised He, in the vicinity of phase zero seems to be much less than what it is in the vicinity of phase 0.50 to 0.60. The double hump structure at 0.6 is typical of what one would expect of a receeding O star and an approaching Wolf-Rayet star, with the absorption line of H_β of the O star mutilating the smooth structure of the emission line originating from the Wolf-Rayet star.

5.7. Discussion.

The observations of five binary systems detailed above provide us with a set of information which can be usefully examined to get at a picture of the Wolf-Rayet atmosphere. I have attempted to derive orbital elements for the different systems using different lines. While these orbital elements are liable to be affected by mass motionsin the binary system, the availability of line profile data simultaneously, enables a judicious selection of the orbital elements to be made. Four of the systems have orbital elements with a least square fitting ~~into~~ to the observations. The system of V444 Cygni is the only one that has a well established light curve. It, therefore, provides the best mass estimate for the Wolf-Rayet star as well as the companion O star. The values obtained for

γ_2-Velorum satisfactorily agree with the present day concepts of masses of the Wolf-Rayet stars. It remains to be seen whether γ_2-Velorum is an eclipsing binary.

A striking feature observed in most of the binary systems examined is that there are large-scale changes in the line profiles caused either by intrinsic variability in the atmosphere of the Wolf-Rayet star or a phase dependent variation depending on the geometry of the situation. Many of these systems have a structure in HeII 4686, at phases of conjunction, that are typical of material flow through the inner Lagrangian point. It is present even in such a well separated system like γ_2-Velorum. Hence, we may conclude that in almost all cases of Wolf-Rayet binary systems, gas flow through this point is likely to be present. Many of the systems examined show large scale changes in intensity of emission. These are apparent in the He lines of the Pickering series in V444 Cygni, in HD 193928, and also in HD 211853. This is suggestive of the fact that it is likely that in a Wolf-Rayet atmosphere, specially of a Wolf-Rayet star that is a member of a binary system with an early type component, the longitudinal distribution of emission is by no means uniform. We have ample justification for this presumption.

not only from the data given here but also from the study of CQ Cephei. In general, there seems to be more emission present near the conjunctions than at elongations. The question of course is whether such a peculiar longitude distribution of emission intensity is stimulated by the presence of the companion. It is difficult to answer this question with any degree of certainty with the present state of observation.

The red-shift experienced by HeII 4686 seems more or less a certainty for the systems examined. γ_2-Velorum with its large separation of components and a period of 78.5 days also shows the phenomenon. This puzzling aspect of the enhanced systemic velocity determined from HeII 4686 is likely to be a vital clue in any explanation of the origin of the emission of HeII 4686. Could it be due to fluorescence as a result of which selective excitation is possible only when the gases that give rise to 4686A emission have a certain velocity of recession with respect to the exciting source ? This is a problem that needs careful consideration. For the present, the reality of the phenomenon is established beyond doubt.

The binary system have been an automatic choice for examination of several of the hypotheses advanced

earlier concerning the nature of the Wolf-Rayet atmosphere. HD 193576 stimulated Wilson to show that a "transit time effect" would be present if the old Beals hypothesis was valid. The Beals picture of a simple expanding shell suffers from various defects. Alternative models postulated have there own difficulties. Many years ago, Beppu (1951) showed that rotational instability could explain the large widths in the emission line in the stars. He also showed that this would call for an excitation gradient of the Wolf-Rayet atmosphere in such a way that the widest lines have the highest excitation. Quite independently, Limber (1964) has postulated that the wide emission in the Wolf-Rayet star can be explained in terms of forced rotational instability consequent to the continual gravitational contraction in a post main-sequence stage. Limber has examined this hypothesis quantitatively and he has shown that it is very attractive when compared to the old Beal's hypothesis. A significant aspect of this theory is that the narrow lines originate farther away from the stellar surface than the lines which have enhanced widths. Limber also pointed out that there is a surprising coincidence between the volume occupied by the electron scattering envelope of HD 193576 and that formed by the inner Lagrangian lobe about this component.

Velocity measures of HoII 4696 (individual measures) of the binary system HD 63273, HD 193576 and HD 186943.

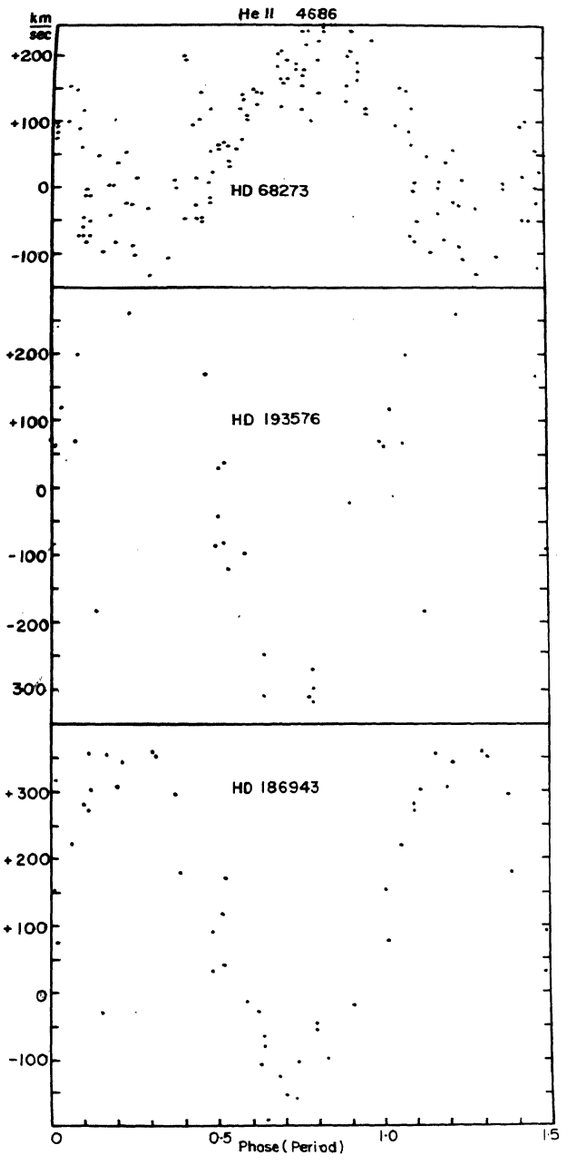
He II 4686
km/sec
+200
+100
0
-100
HD 68273
+200
+100
0
-100
-200
300
HD 193576
+300
+200
+100
0
-100
HD 186943
0
0·5
1·0
1·5
Phase (Period)

While the rotational instability hypothesis has many attractive features which indicate a situation closer to reality than any achieved so far, nevertheless, several difficulties exist that need explanation. In Fig.V-23, I have plotted the individual velocities of 4686A for four binary systems. If rotation is an important feature, then for the eclipsing system V444 Cygni or even for the other systems it would be necessary to observe the Rossiter effect, caused by rotation. It will be seen that an examination of these curves shows that Rossiter effect cannot be detected. Limber of course postulates that the absence of a Rossiter effect is not likely to invalidate the hypothesis, since several mechanisms could mask the feature. The broadest emission lines in the system of γ_2-Velorum are identical to those seen in V444 Cygni. The observations listed above on the broadening of the higher members of the Balmer series at the phase when the O is eclipsed by the Wolf-Rayet star clearly indicate the definite manifestation of electron scattering. Therefore, one can postulate with sufficient degree of confidence, the fact that such an electron scattering envelope exists in every Wolf-Rayet atmosphere. Several of the binary systems studied have different values of K. It is very likely that

some of them may be systems with the higher orbital inclination and some with a small value of sini. In general, it seems as though there is very little difference in the line widths of 4686A for the various systems. On the basis of the rotational instability hypothesis, it is necessary to find a change with the inclination. However, the lack of decrease in the emission widths is likely to be offset, by the postulate of electron scattering envelopes of differing properties in such a way that the electron scattering more than offsets the narrowness of the emission lines.

It seems that a profitable avenue for study of the Wolf-Rayet phenomenon, is as has been speculated on earlier, the binary systems. We need to detect many more binary systems than we have so far, in order to find among these systems that have favourable inclinations for an eclipse, systems that can provide reliable information on the masses of the stars and also those that can be usefully utilized in enabling the easy conjecture of a model of the Wolf-Rayet atmosphere.

CHAPTER VI

ZETA PUPPIS

6.1. Introduction.

The presence of bright lines in the spectra of Wolf-Rayet stars and P Cygni stars have been known for over a century. These stars are classified as peculiar since they differ widely from normal stellar spectra. Former investigators in this field were unable to fix these peculiar stars on the evolutionary diagrams due to lack of sequence from the normal spectral class. Wright and Lamkott (1918) observed that the O star 9 Sagittae, BD + 35° 3993, 29 Canis Majoris and the nucleus of the planetary nebula NGC 2392 exhibit selective emission at HeII 4686, NIII 4634-42. It is strange that of the four NIII lines at 4097A, 4103A, 4634A and 4640A only the lines at 4634A and 4640A should appear in emission while the other two are pure absorption lines. Payne examined several southern O stars and reported the presence of emission lines 4632-42 in their spectra.

The star 9 Sagittae is a typical O star showing the vestiges of Wolf-Rayet character. This star has been studied carefully by Swings and Struve and recently by

Underhill (1959). The interesting feature of its spectrum is the greater intensity of 4686Å compared to the NIII lines. Wyse has shown that HeII 3203 is a strong absorption line. It is obvious, therefore, that HeII 4686 must also be a strong absorption line with superimposed faint emission formed in the outer shell of the star.

The emission features possess great widths as observed for Wolf-Rayet stars and probably indicate a common mechanism of emission. Hence, it is regarded that the source of emission bands is as an embryonic Wolf-Rayet atmosphere.

Mumblet and Mannino (1958) have advanced the proposition that fluorescence mechanism is responsible for the presence of emission lines of HeII and NIII and that the slow variations of emission lines is due to the occasional nitrogen flaring taking place at a reduced rate. On the other hand, Swings and Struve (1940) believe that the helium atoms after absorbing Lyman-alpha radiation from $2s^2 {}^3S$ level are brought to quantum number 4 from where they cascade down to n = 3 emitting the 4686Å line.

The excitation of CIII 5696 is quite different from that of the NIII lines 4634-42. In the case of the

NIII lines, the upper levels are reached directly from the ground level by an absorption of one quantum of radiation whereas in the case of carbon atoms, the ground state of C^{++} cannot be excited to the upper state by absorption of a quantum of radiation. Hence, it was suggested by Underhill (1957) that the appearance of CIII 5696 in emission is a result of the formation of C^{++} ions in the $1s^2 2s 3d\,^1D_2$ level selectively by the ionization of C^+ ions from the $1s^2 2s^2 3d^2D$ levels by HeII 304 quanta.

The emission lines show a positive luminosity progression in the stars and use has been made of the strength of the line NIII 4634-42 as a luminosity criterion in the early O stars.

These emission lines have extensive wings having a range upto 60Å. The profiles of these emission lines appear to be composite having a central narrow core in addition to the overlying emission. This effect is particularly seen in the profile of the line CIII 5696 and to a lesser extent in NIII 4634-42.

Zeta Puppis is well known in spectroscopic literature, for the receding series of ionized helium

were first seen in the spectrum of this star. Zeta Puppis is a bright star in the southern sky having a visual magnitude of 2.3. Its spectrum has been classified as Of. It is suspected to belong to the Vela group of early stars and is in league with γ_2-Velorum in exciting the Gum nebula.

Two high dispersion spectra of this star, one in blue and the other in red obtained at Mount Stromlo were available for a study of the spectrum. As the spectra were well exposed for photometry, I though it worth-while to study comparatively the 3n and 5n series of HeII lines. Microphotometer tracings were made from the plates and the tracings were reduced to intensities. The equivalent widths of the 3n and 5n series of He are tabulated in Table VI-a.

6.2. The number of absorbing atoms.

The number of atoms active in forming the Balmer, Pickering and the 5n series of HeII lines can be estimated by the method given by Unsold (1941)

$$(N_2)\ N_1 = \frac{W \times 10^{20}}{0.886 f \lambda^2}$$

where λ is the wavelength in Angstroms, f is the oscillator strength and (N2) N is the number of atoms above 1 cm^2 of the photosphere. This approximation fails for the earlier members of the series and becomes valid, the higher the principle quantum number. Hence, one can plot for each value of the n, the principle quantum number, the corresponding value of N$_2$ N and extrapolate to get an asymptotic value. A similar procedure is adopted for the 4n and 5n series of Helium and the relevant data are summarised in Table VI-1. In this way we obtain the number of atoms N_{rn} above each cm^2 of the photosphere in the sth excitation level of the neutral stage of ionization. A similar procedure is adopted for the Pickering series of HeII.

6.3. Electron Density.

The electron density in the atmosphere may be found from the Saha Eggia Keller formula

$$\log n = 23.26 - 7.5 \log n_a$$

where n_a is the number of the last resolvable Balmer line and n is the positive ion density related to the electron

Table VI-1

Determination of N_2H

n	Wavelength	W(A)	f	Log N_2H
3	6562.82	1.23	6.41 x 10^{-1}	14.39
4	4861.33	2.28	1.19 x 10^{-1}	14.96
5	4340.47	2.08	0.45 x 10^{-1}	15.44
6	4101.74	1.57	0.22 x 10^{-1}	15.68
7	3970.07	1.45	0.13 x 10^{-1}	15.91
8	3889.05	1.36	0.80 x 10^{-2}	16.11
9	3835.39	1.35	0.54 x 10^{-2}	16.29
10	3797.90	1.51	0.38 x 10^{-2}	16.53
11	3770.63	1.37	0.28 x 10^{-2}	16.59
12	3750.15	0.89	0.21 x 10^{-2}	16.53
			Extrapolated value—	16.55

Determination of H_4 HeII

n	Wavelength	W(A)	f	Log H_4 HeII
9	4541.59	0.9976	1.872×10^{-2}	14.46
11	4199.83	0.5408	8.185×10^{-3}	14.63
13	4025.60	0.4151	4.360×10^{-3}	14.82
15	3923.48	0.3040	3.039×10^{-3}	15.13
17	3858.07	0.3357	2.431×10^{-3}	15.02
19	3813.50	0.4828	1.647×10^{-3}	15.36
21	3781.68	1.0772	1.166×10^{-3}	15.86
			Extrapolated value =	15.43

Determination of d_5 Ref1

n	Wavelength	W (A)	f	log
13	6683.20	1.9755	5.874×10^{-3}	14.08
15	6406.30	0.9015	3.401×10^{-3}	14.76
16	6310.80	2.2461	2.674×10^{-3}	15.32
17	6233.80	1.9862	2.154×10^{-3}	15.38
18	6170.60	3.0879	1.756×10^{-3}	15.77
19	6118.20	2.2000	1.459×10^{-3}	15.61
20	6074.10	0.9862	1.231×10^{-3}	15.34
21	6036.70	0.6271	1.033×10^{-3}	15.22

Extrapolated value 15.59

density by the relation

$$n_e = 1.1n$$

Using the above equation, the value of $\log n_e$ turns out to be equal to 14.56, which is in good agreement with Aller's (1954) value for a typical of star.

6.4. Relationship with the Wolf-Rayet stars.

It is difficult to speculate at this stage the evolutionary relationship between the of stars and the WR stars, if any such is possible. The emission at 4686A, 4640A and 5696A are essentially the only points of similarity. It may not be even necessary to postulate a similarity between the of and the WR stars, provided one seeks selective excitation effects to cause the emission. In fact, it is possible that the selective excitation is also operative in the WR stars, since conditions may be prevalent in both atmospheres for such stimulation. The similarity may end at this stage. The WR stars may be hydrogen deficient as shown in Chapter IV. On the other hand the of stars are not, as can be seen from the study reported herein. Hence, one may consider that the of stars are a restricted class of e stars, with shells, that may have little in common with the WR stars.

REFERENCES

Allen, C.W.,	1963	Astrophysical Quantities, 203.
Aller, L.H.,	1943	Ap.J., 97, 135
Aller, L.H. and Faulkner,	1964	Ap.J., 140, 166
Andrillat, Y.,	1957	Ann. de Astr. Supp. No.2
Bappu, M.K.V.,	1951	Harvard Thesis
Bappu, M.K.V.,	1957	Bull. Int. Inst. Sci. India, No.9, 155
Bappu, M.K.V.,	1958	Mem. Soc. R. Sc. Liege, tome XX, 40
Bappu, M.K.V.,	1966	(In press)
Bappu, M.K.V., and Menzel, D.H.	1954	Ap.J., 119, 508
Bappu, M.K.V., and Sinvhal S.D.	1955	A.J., 60, 152
Bappu, M.K.V., and Sinvhal S.D.	1959	Observatory, 79, 140
Bappu, M.K.V., Vaintarajan and Viswanadham	1966	(In press)
Beals, C.S.,	1929	M.N., 90, 202
Beals, C.S.,	1930	Pub. Dom. Ap.Obs. 4,271
Beals, C.S.,	1934	Pub. Dom. Ap.Obs. 5,125
Boelmsten, K.,	1955	Arkiv f. Fysik, 9,457
Boelmsten, K.,	1956	Arkiv f. Fysik, 10,567

Cannon, A.J.,	1901	H.A., 28, 148
Chamberlain, J.W.,	1953,	Ap.J., 117, 397
Chandrasekhar, S.,	1934	M.N., 94, 522
Edlen, B.,	1956	Vistas in Astronomy, Volume II, 1946
Gaposchkin, S.,	1941	Ap.J., 93, 202
Gaposchkin, S.,	1958	A.J. 63
Glad, S.,	1953	Arkiv f. Fysik, 7, 7
Graham, J.A.,		Observatory, 85, 196
Hallin, R.,	1966	Arkiv f. Fysik, 31, 511
Hjellming and Hiltner, W.A	1963	Ap.J., 137, 1080
Hiltner, W.A.,	1945	Ap.J., 121, 356
Hiltner, W.A.,	1950	Ap.J., 112, 477
Humblet and Swings	1958	Mem.Soc. R.Sc. Liege, tome XX, 98
Kopal, Z., and Shapley, L.B.,	1946	Ap.J., 104, 160
Kron, G.E., and Gordon, K.C.,	1950	Ap.J., 111, 454
Kuhi, L.V.,	1966	Ap.J., 143, 753
Kuhi, L.V.,	1965	A.A.S. abstracts.
Limber, D.N.,	1964	Ap.J., 140, 1331
Mennel, D.H.,	1929	P.A.S.P., 41, 344
Munch, G.,	1950	Ap.J., 112, 266
Oke, J.B.,	1954	Ap.J., 120, 22
Perrine, C.D.,	1918	Ap.J., 47, 52
Petrie, W.,	1947	Pub. Dom.Ap. Obs., 7, 353

Plaskett, J.S.,	1922	Pub. Dom. Ap. Obs. 1, 325
Roberts, M.S.,	1962	A.J., 67, 79
Rottenberg, J.A.	1952	M.N., 112, 125
Sahade, J.,	1956	A.S.P., 67, 348
Sahade, J.,	1958	Mem.Soc. R.Sc.Liege., tome XX, 434
Schleisinger, F., and Jenkins, L.F.	1940	Yale Bright Star Catalogue.
Smith, M.J.	1955	Harvard Thesis
Sobolev, V.V.,	1947	Moving envelopes of Stars, Leningrad State University, Chap.III
Stecher and Milligan,	1962	Ap.J., 136, 1
Struve, O.	1944	Ap.J., 100, 189
Swings, P., and Jose, P.S.	1950	Ap.J., 111, 513
Swings, P., and Struve, O.	1940	Proc. Nat. Acad.Sci., 26, 540
Swings, P., and Struve, O.	1940	Ap.J., 91, 546
Thomas, R.N.,	1949	Ap.J., 109, 900
Thomas, R.N.,	1949b	Ap.J., 109, 480
Underhill, A.B.,	1957	Ap.J., 126, 28
Underhill, A.B.,	1959	Pub. Dom. Ap. Obs.XI,209

Unsöld, A.,	1941	Zs. f. Ap., 21, 1
Vorontsov-Velyaminov, B.,	1945	Russ. A.J., 22, [illegible]
[illegible]non, [illegible].,	1950	B.A.N., [illegible], 165
Westerlund, Bengt [illegible] [illegible].,	1964	M.N., 128, 311
Wilson, O.C.,	1939	Pub.A.S.P., 51, 55
Wilson, O.C.,	1940	Ap.J., 91, 379
Wilson, O.C.,	1942	Ap.J., 95, 402
Worssell, W.H.,	1916	M.N., 76, 418